



DESC glove

Prototyping a novel wearable
device for post-stroke
hand rehabilitation
Rebecca Baldi

DESC glove

Prototyping a novel wearable
device for post-stroke
hand rehabilitation

by

Rebecca Baldi

to obtain the degree of Master of Science
at the Delft University of Technology,
to be defended publicly on Tuesday August 5, 2020 at 14:30 PM.

Student number: 4924282
Project duration: January 10, 2020 – August 5, 2020
Thesis committee: Prof. G. Smit, TU Delft, Supervisor
Prof. D. Plettemburg, TU Delft, Head of chair
Dr. F. Trauzettel, TU Delft

This thesis is confidential and cannot be made public until August 5, 2021.

An electronic version of this thesis is available at <http://repository.tudelft.nl/>.

Preface

The basis for this research, and the reason why I was immediately fascinated by the possibility to work on this project, is my evergreen passion for sensory restitution in people with severe sensory deficits. Since I was younger, in the process of choosing my bachelor field of study, I became enthusiastic of the bionics subjects while spending a week at Scuola Superiore Sant'Anna for an orientation event. The representative teachers of the department presented the Biomedical Engineering course they offered (Bionics) by exhibiting a bionic hand which included sensory feedback, their team had just developed. At that time I had no idea of how biopotential could be used to control robotic arms but I promised myself that one day I would be able to take part in this challenging research field in order to provide a normal life to people that have an amputated limb.

One can only imagine my happiness when I realized I had the opportunity to work on a thesis project for sensory feedback delivery in post-stroke patients in the beloved Artificial Hands Area in the Institute of Biorobotics of Sant' Anna. The best part of the project is that it would have been completely in my hands both ideally and practically, and I couldn't be more excited to challenge my limits and knowledge once more.

It was thanks to all the people around me always willing to help that I overcame those difficult challenges I set for myself. I would have not made it without the support of my supervisor Leonardo Cappello who kept pushing my limits, telling me to believe I would have made it with my own strength. A special thanks goes to my mentor in electronics, the PhD student Valerio Ianniciello, who answered to all my doubts with extraordinary competence and kindness.

I sincerely believe that the position I find myself in today is all a consequence of my mother's teachings and dedication. She gave me the opportunity to see beyond the limits imposed by space and time as we know them, and to acquire the necessary curiosity which pushed me to travel and undergo a personal growth. The support given from my family during my whole career was extraordinary, and I would like to thank my mother Alessandra, my dad Luca, my sisters Rubina and Allegra and my cousin and best friend Vittoria. I would also like to thank my cousin Alberto for being my role model and inspiring me since day one with his great intelligence, to my eyes (and not) he will always be the best electronic engineer working for Apple.

I express gratitude to everyone who, in a way or another, contributed to the development of this work. A sincere thanks to my TuDelft supervisor, Gerwin Smit, who supported me during the whole project and year abroad.

Rebecca Baldi
Delft, August 2020

Abstract

The human brain integrates tactile sensory information from the fingertips to efficiently manipulate objects. Sensory impairments due to neurological disorders, e.g. stroke, largely reduce hand dexterity and the ability to perform daily living activities. Several feedback augmentation techniques have been investigated for rehabilitative purposes with promising outcomes. However, they often require the use of unpractical, expensive, or complex devices. In this work we propose the delivery of vibrotactile feedback based on the Discrete Event-driven Sensory feedback Control (DESC) to promote motor learning in post stroke rehabilitation. For this purpose, we prototyped a novel wearable device, namely the DESC glove. It consisted of a soft glove instrumented with PolyVinylidene Fluoride (PVDF) sensors at the fingertips and eccentric-mass vibration actuators to be worn on the forearm. We proceeded with the characterization of the device, which resulted in promising outcomes.

The DESC glove was tested with ten healthy participants subsequently in a pick and lift timed task. The effects of augmented vibrotactile feedback were assessed comparing it to a baseline, consisting of wearing the device unpowered. The results of this pilot study showed a decrease in the time necessary to perform the task, a reduction in the time delay from load force to grip force activation and a diminishing of the grip force applied on the object, which led to a lower breakage rate in the intervention condition. These promising outcomes encourage further experiments with stroke survivors to validate the effectiveness of the device to improve hand dexterity and promote stroke rehabilitation.

Key words: *Stroke, Hand, Rehabilitation, Sensory, Vibrotactile, Feedback, Glove, Wearable.*

Contents

1	Introduction	1
1.1	Introduction: Sensory information in hand motor performance	1
1.1.1	Upper limb impairment	1
1.1.2	Sensorimotor control of the upper limb	2
1.1.3	Sensory input for optimal movement	2
1.1.4	Augmented feedback to stimulate neural plasticity	4
1.2	Current rehabilitation protocols	4
1.2.1	Approach to rehabilitation	4
1.2.2	Constraint-Induced Movement Therapy (CIMT)	5
1.2.3	Mirror therapy and robot-assisted therapy	5
1.3	Augmented sensory feedback in rehabilitation	6
1.3.1	Aspects of feedback	6
1.3.2	Feedback modalities	6
1.3.3	Strategies for robot-assisted error feedback	6
1.3.4	Developing a reliance on extrinsic feedback	7
1.3.5	The sensory side of rehabilitation is an open question	7
1.4	Auditory Feedback	7
1.4.1	Types of augmented auditory feedback	7
1.4.2	Auditory feedback devices	7
1.4.3	Conclusions on sensory feedback	8
1.5	Visual Feedback	8
1.5.1	Benefits of Virtual Reality rehabilitation	8
1.5.2	General features of a Virtual Reality setup	9
1.5.3	Studies in Virtual Reality for rehabilitation purposes	10
1.5.4	Other visual feedback delivery methods.	10
1.5.5	Conclusions on visual feedback	10
1.6	Haptic Feedback	11
1.6.1	Movement-based (implicit) and sensory-based (explicit) haptic feedback.	11
1.6.2	Feedback for kinesthetic illusion	12
1.6.3	Devices for haptics	12
1.6.4	Conclusions on haptic feedback	13
1.7	Multimodal Feedback.	13
1.7.1	Virtual reality and haptic feedback.	14
1.7.2	Robotic rehabilitation: visual and haptic feedback	14
1.7.3	Visual and auditory feedback	15
1.7.4	Visual, haptic and auditory feedback	15
1.7.5	Conclusions on multimodal feedback	15
1.8	Sensory information enhancement	16
1.8.1	Vagus-nerve stimulation	16
1.8.2	Stochastic resonance	16
1.8.3	Conclusions on sensory enhancement	18
1.9	Future directions for augmented feedback	18
1.10	Goals of the project.	20
1.11	Idea: DESC glove	20

2	PVDF sensors prototyping and manufacturing	23
2.1	Hardware prototyping outline	23
2.2	Sensors design	23
2.3	PVDF sheet laser cutting	25
2.4	Offset cleaning for short circuit prevention	25
2.5	Cables connection	27
2.6	Silicone layers around sensors	27
2.7	Sensors placing on the glove	29
3	Sensors characterization	33
3.1	Set up: 3D moving platform, load cell and sensors	33
3.2	Experimental procedure parameters	35
3.3	Sensor characterization results	35
3.3.1	Sensor response behavior	35
3.3.2	Sensors response to velocity	36
3.3.3	Sensors response to force	37
3.3.4	Sensor response delay	38
3.4	Feasibility for DESC feedback	39
4	Design of the Printed Circuit Board	41
4.1	Electronic board prerequisites	41
4.2	Acquisition and amplification circuits	41
4.3	PIC Microcontroller	42
4.4	Final design of the board	42
4.5	List of components	44
4.6	Hardware block diagram	44
4.7	Board 1 manufacturing	45
5	Firmware description	47
5.1	Board 1: Sensors signal acquisition	47
5.1.1	Analog to digital conversion	47
5.1.2	Touch event detection	48
5.1.3	Serial port communication	49
5.2	Board 2: Vibration Actuators	50
6	Experiments on healthy subjects	53
6.1	Participants	53
6.2	Setup for the experiment	53
6.2.1	Pick and lift task setup	53
6.2.2	Augmented vibrotactile feedback setup	55
6.3	Experimental procedure	57
6.4	Data acquisition and analysis	59
6.4.1	Motor performance analysis	59
6.4.2	Characterization of the device	60
6.4.3	Statistical Analysis	61
7	Results and Discussion	63
7.1	Results	63
7.1.1	Grip force and Number of breaks	63
7.1.2	Coordination plots	65
7.1.3	Grip force to load force delay	65
7.1.4	Duration of the task	68
7.1.5	Characterization of the device results	69
7.2	Discussion	70
7.2.1	Grip Force and Number of breaks	70
7.2.2	Coordination plots	70
7.2.3	Grip force to load force delay	71
7.2.4	Duration of the task	71
7.2.5	Performance of the device analysis	71

8	Conclusions and Further Outlooks	73
8.1	Conclusions	73
8.2	Study limitations and possible improvements	73
8.3	Societal and ethical impact.	74
	Appendices	75
A	Consent Form and Study Information Sheet	77
	Bibliography	83

Introduction

To be published as: *"Non-invasive Augmented Sensory Feedback in Post-stroke Hand Rehabilitation Approaches"*,
Leonardo Cappello and Rebecca Baldi, Leonard Engels, Christian Cipriani,
in the book *"Somatosensory Feedback for Neuroprosthetics"*, ELSEVIER.

1.1. Introduction: Sensory information in hand motor performance

Stroke is like a heart attack for the brain: a disruption of the blood supply leads to tissue damage and disruption of normal brain function. Approximately 80 million people worldwide have experienced stroke and over 13 million new strokes occur every year [68]. Stroke is one of the major causes of disability worldwide [56], and can have long lasting consequences for the affected. Impairments in portions of the body contralateral to the affected side of the brain can generate loss of hand motor function which poses a dramatic limitation in performing everyday life activities and reduces the patient's independence. As a consequence of brain damage, tactile sensitivity is often compromised, and, the lack of information on mechanical contact states reduces the synergy in movements and the ability of manipulating objects [8].

Depending on the location and extent of the damage that the stroke caused in the brain, the consequences vary strongly. The common obstruction of the medial cerebral artery, for example, can lead to muscle weakness, hemianesthesia, hemianopsia, hemineglect, apraxia, and disturbed spatial perception, to name just a few. Damage to pons, cerebellum or midbrain can lead to hemiataxia, (partial) loss of pain and temperature sensation in face and body, hemiparesis, hemiplegia, and tetraplegia. At a lower level of processing, damage leads to primary sensory deficits, such as anopsia or tactile impairments, whereas higher level damage, at a later stage of processing, leads to more cognitive defects, such as neglect or agnosia [114].

1.1.1. Upper limb impairment

In the majority of stroke survivors, the upper limb is affected [115], with more than 80% experiencing acute hemiparesis of the contralesional limb, and more than 40% experiencing it chronically [29]. Sensory deficits, such as impairments of touch, mechanical, temperature, and pain sensations, two-point discrimination, and proprioception, are also common in the contralesional arm [11, 22, 29, 95]. Yet, in some, grasping with the ipsilesional upper limb is affected as well [93, 94], in part because some corticospinal fibers do not decussate in the medulla, meaning that both cerebral hemispheres are needed for optimal function of either limb [22]. Rehabilitation after stroke mostly focuses on motor rehabilitation, but it is well-known that primary and secondary motor areas in the brain also respond to sensory stimulation [10]. Indeed, impairments of grasp force control, prehension patterns, and fine motor manipulation have been associated with sensory impairments [10, 22, 29]. Chronic loss of tactile sensitivity and proprioception decreases awareness of limb, shoulder, and trunk position and movement, which is essential for spontaneous use of the whole limb [10, 29, 117]. Conversely, lesions to the primary motor cortex have also been reported to lead to tactile agnosia, which is typically associated

with primary sensory cortex lesions, and severe motor lesions lead to changes in connectivity of all sensory areas [10]. Motor and sensory properties are tightly intertwined and need to be integrated for optimal motor behavior [10, 27, 114].

1.1.2. Sensorimotor control of the upper limb

Any movement necessarily starts *open-loop*, that is, without sensory feedback, since afferent information from eyes, tactile receptors, and proprioception are always processed with some delay [52] [119]. This is made possible by “internal models” of movements: the “inverse model” produces motor commands by estimating how a limb needs to be moved to grasp an object, for example, based on its position, length and weight [57, 104, 119]. Figure 1.1 shows a schematic representation of the interaction with the environment during movements, and how the brain processes information to generate motor commands. An “efference copy” of the motor commands is used by the “forward model” to predict the sensory consequences of the movement. For example, efficient grasping of an object is “separated” by the central nervous system (CNS) at “sensorimotor control points” into a series of simpler subtasks [49], as is shown in detail in Figure 1.2. Discrepancies between predicted and actual sensory information, so-called sensory prediction errors, become evident at these control points and allow the intact CNS to correct movements, rendering them “closed-loop”, and to improve the internal models [49, 119].

As the part of the CNS that is mainly responsible for smooth movements, these internal models, too, are likely based in the cerebellum, so damage would directly affect the ability to use and maintain internal models [46, 58, 88, 91]. However, as would be expected, there is strong interplay directly related to the formation and refinement of internal models also with other regions of the CNS, such as the primary motor and sensory cortices [47, 72, 88]. Lesions in parietal or premotor areas, for example, may also negatively affect the ability to integrate sensory feedback during movements, likely affecting efficient movement planning and execution [10].

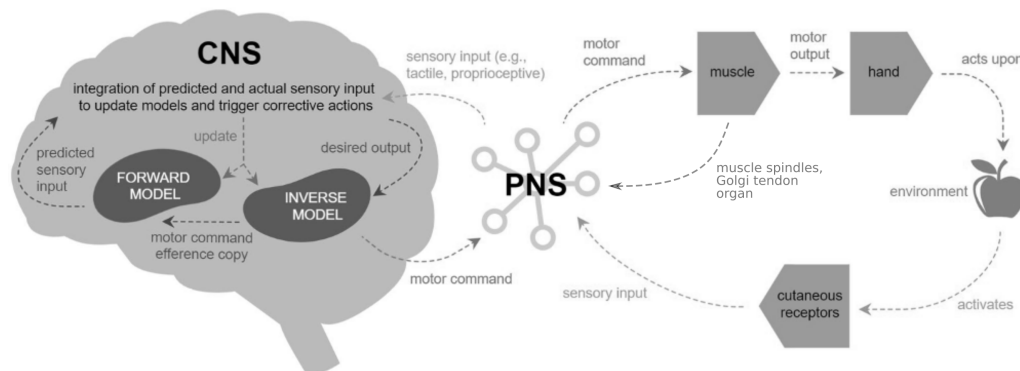


Figure 1.1: Schematic of sensorimotor control. To grasp an object, the desired output is translated into motor commands by the inverse model in the central nervous system (CNS). These motor commands are sent to the peripheral nervous system (PNS) to activate the muscles that move the hand to the desired position. Feedback on length, velocity and force of the muscle is sent back to the central nervous system. Activation of sensory afferents, for example through contact with an object, are sent back to the CNS where these sensory events are compared to the predicted sensory events that the forward model created based on the efference copy of the motor commands. In the case of a mismatch between prediction and actual event, the internal models are updated for future repetitions of the same task, and, if necessary, corrective motor actions are initiated.

1.1.3. Sensory input for optimal movement

For efficient grasping, sensory feedback depends crucially on mechanotactile receptors in the skin of the hand, particularly the discrete sensory events upon contacting, lifting, replacing, and releasing an object [49, 51, 53], but surface friction recognition, too, is important for accurate force scaling (e.g. [9]). Visual information and proprioception are particularly important during the reaching phase towards an object to accurately shape arm and hand [95]. Chronic impairment of any of these sensory properties after stroke leads to motor impairment in part due to inaccurate internal models that cannot be updated properly [10, 95]. The inability to detect mismatches of predicted and actual sensory information can cause anosognosia, leading to significantly poorer recovery [10] (As shown in Fig. 1.2).

Vision and even auditory stimulation also activate mirror neurons which play an important role in learning and mimicking movement [10]. This may serve as a means to stimulate the motor system after stroke even if other pathways are damaged [10].

Patients who have impaired sensorimotor or visual capabilities are more dependent on caregivers than those with motor impairments alone [27] and have difficulties exploring and relating to their environment, making them less independent and affecting long-term participation [29]. In addition, affected temperature or pain sensation, balance, or proprioception affect the safety of the stroke survivor even if there is adequate motor recovery [29].

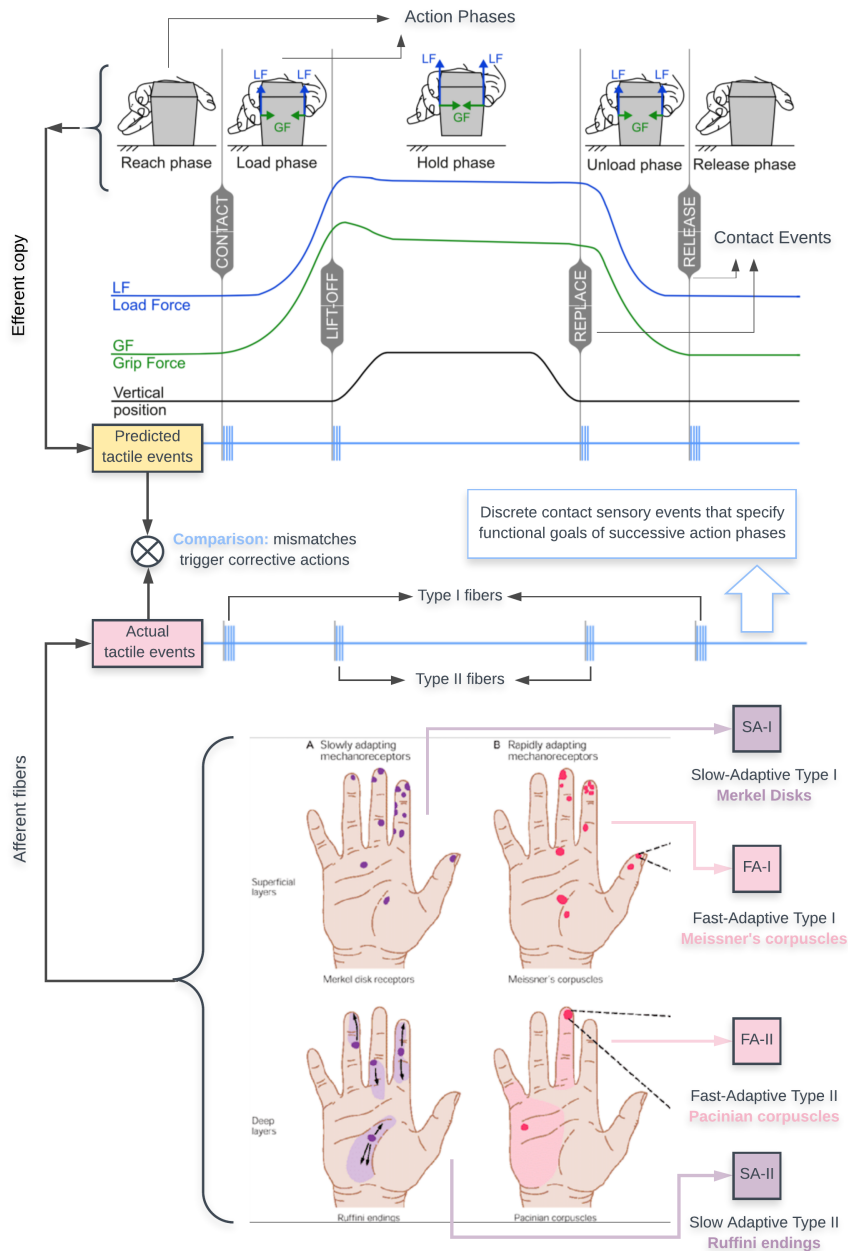


Figure 1.2: Sensory information role in an object manipulation task. Figure adapted from [21] (up) and [38] (down). The task phases related to subgoals are shown on the top, with the corresponding levels of load force (LF) and grip force (GF) during the grasping task. The mechanoreceptors and different types of afferent fibers, shown in the bottom part of the figure, activate in correspondence of discrete contact events. The actual tactile events are compared with the predicted tactile events generated from an efferent copy of the motor command by the internal models. The mismatches between predicted and actual tactile events are used to implement corrective actions on the motor commands.

1.1.4. Augmented feedback to stimulate neural plasticity

Therapy intended to recover lost sensation may aid in re-learning and compensating for lost motor abilities, particularly for the upper limb [10]. Short-term effects may result from compensation, but long-term effects will come about from restoration of sensory function due to plasticity, by strengthening existing connections and the recruitment of new ones [114]. Plasticity in intact areas of the brain is related to the damage to intracortical connections [50]. It is important to enhance ipsilesional recovery during therapy, as increased activity in the contralesional hemisphere relates to poorer recovery [50]. Based on this knowledge, it can easily be argued that, restoring sensory functions will directly and indirectly aid in recovery of motor functions [10]. However, although it is generally agreed upon that augmented feedback is beneficial for motor learning, the way to most effectively provide it is still debated [109]. Approaches could include focusing specifically on task-inherent feedback, but patients with cognitive or more severe perceptual impairments may not be able to make use of intrinsic feedback [115]. In those cases, “augmented” or “task-external” feedback, such as that delivered from a therapist, a timer, or some other device, could provide the sensory input that is missing to improve performance of a given task.

In the following, we will provide an overview of current rehabilitation protocols, followed by an in-depth review of the various approaches to providing augmented sensory feedback for upper limb rehabilitation after stroke, partitioned by sensory channels. A number of studies have found positive effects of augmented sensory feedback, but it is as yet too early to provide a final verdict on its usefulness, or even on how best to implement this form of feedback. Thus, this book chapter will end with a section providing an outlook on and suggestions for future research and developments.

1.2. Current rehabilitation protocols

Several upper limb rehabilitation techniques have been developed to promote the recovery of the impaired extremity function after stroke, with the ultimate goal of restoring independence and quality of life of those affected. Rehabilitation exercises aim at reactivating the neural pathways involved in the completion of a task and provoking neural plasticity and motor learning [28]. Motor learning mechanisms are fundamental for a rehabilitative process: it is necessary that the functional gains of the training sessions persist in time and that their effects can be generalized to untrained motor actions [61]. It cannot be assumed that, whenever the performance increases during training, the gains in motor and sensory assessment scales are retained over time.

1.2.1. Approach to rehabilitation

General guidelines on the criteria that rehabilitation protocols should meet in order to be maximally effective for motor learning are present in literature [44]. An important aspect to take into consideration is the orientation of the training programs: they should be patient-tailored and goal-tailored, taking into consideration the level of individual cognitive impairments. Other important characteristics of rehabilitative training are that they should resemble real-life contexts as much as possible and be motivating for the patient. Motivation is increased by designing exercises relevant to the activities of daily living [27]. An appropriate level of involvement and challenge too is fundamental to promote motivation during training. Difficulty and intensity of the exercises should increase over time. Another important characteristic of rehabilitative training is to resemble the real-life context as much as possible and be motivating for the patient, and the task variability should be largely taken into consideration. It is important to introduce rest periods and variability among exercises, even during massed practice, i.e. when a single task is performed repeatedly. This could result in a performance decrease during the acquisition session but it ultimately leads to improvements in the long term, which can be seen in retention tests. Variability among training exercises will also facilitate generalization of motor learning to untrained movement [61].

In the first stage of the rehabilitation sessions, in case the patient shows severe motor impairments, it is common practice to passively stimulate the sensorimotor system through massages, passive joint or soft tissue mobilization techniques or assisted movements [45]. In the second stage, sensory training is often addressed more explicitly, for example with sensory recognition exercises, which train to reconnect stimulation of mechanoreceptors and proprioceptors with conscious percepts [98]. The unmasking of already present afferent sensory pathways can promote neuroplasticity and increase hand sensitivity [89]. The importance of sensory stimulation is often underestimated in rehabilitation proce-

dures which usually focus mainly on motor function recovery [10]. In the following, we describe the most common rehabilitation procedures used today.

1.2.2. Constraint-Induced Movement Therapy (CIMT)

Constraint-Induced Movement Therapy (CIMT) is a technique that consists in the restraint of the unaffected arm while training the impaired limb. The restriction can be done for the greater part of the waking hours while the patient is performing daily life activities (usually 90%), and can also be included during the massed practice sessions, preferably for at least 6h a day for two weeks [27, 28, 61]. After an injury, patients tend to neglect the use of the affected extremity because of the consequent/resulting pain and fatigue. Using the unaffected arm for most of the daily tasks results in a lower effort and better timing for achieving a goal. Hence, the concept of CIMT is to force the use of the impaired limb to perform standard tasks such as reaching, grasping and pinching. However, this practice has strict requirements: patients involved in CIMT protocols must have at least 10 degrees of active wrist, thumb and any other two fingers extension on the affected hand. These requirements are necessary in order for the therapy to be beneficial, and 90% of the patients do not satisfy these eligibility criteria [27].

1.2.3. Mirror therapy and robot-assisted therapy

CIMT stands in theoretical contrast to mirror therapy, where synchronized movements are performed with both arms to increase coordination. Bimanual training techniques have been proven to promote motor learning by generating a mirror-induced movement in the paretic limb that reduces the inhibition of the damaged cerebral hemisphere [37]. Although mirror-therapy resulted in fewer improvements compared to the unilateral practice [73] but is still widely used combined with functional repetitive training, robotic therapy and other rehabilitation techniques.

Robot-assisted therapies have gained attention in the last decades as they allow to perform highly repetitive, intensive and adaptive physical training. Robotic devices can be either exoskeletons, which match the kinematics of the impaired limb's joints, or end-effector robots acting only on the distal part of the arm. Robotic trainers are sometimes used in virtual reality (VR) settings, combined with visual, auditory and haptic feedback to promote involvement in the task. These robotic technologies can operate in active assist mode, guiding the hemiparetic limb with assist-as-needed principle [30, 81]. In this modality, many repetitions of the same action are performed, reducing robot assistance over the course of training, to stimulate an increase in the patient's active participation. In contrast, passive mode robotic training enhances post-stroke recovery by providing proprioceptive feedback only [86, 112]. Finally, both the impaired and the sound limb can be involved in the therapy, as for example in bimanual mode robotic training which exploits the mirror-therapy concept previously mentioned.

A great advantage of robot-assisted therapies is the potential they offer to quantitatively monitor the recovery through accurate kinematic recordings. In fact, they allow therapists to assess the smoothness and correctness of the movements at the end of each training session. Moreover, task variability can be easily introduced in several ways when using a robot for rehabilitation purposes, e.g., by introducing a force-field in the exercise to challenge the patients and induce them to adapt their internal models to a varying environment [61]. A further advantage of robotic therapy is the increase in motivation due to the gamification of the exercises, which can be designed to challenge the patients with short-term goals. This can ultimately lead them to voluntarily increase the dose of the treatment.

The main issues behind the use of robotic rehabilitative techniques are their high costs and their poor practicality in a home setting. The use of these therapies requires technical assistance and a medical center setting. Moreover, no significant advantage is seen unless a high number of repetitions in the same session are performed (at least 100, usually 300) [17]. The risk with such intensive training sessions, patients and therapists feel exhausted and are unable to participate effectively into the rest of the daily activities, with the risk of hindering the beneficial effects of the global therapeutic treatment. On the other hand, this increased intensity and motivation may be the key for improving the outcomes of the rehabilitation therapy and reducing the therapist's workload [81]. Importantly, robotic training might allow one therapist to treat several patients at the same time. The therapist can provide assistance and explanation as needed while the repetitive training itself is performed by the patients independently. This could lead to an overall increase of the hours each patient can spend training under the supervision of a therapist and thus to an increase of quality rehabilitation.

1.3. Augmented sensory feedback in rehabilitation

Beyond practice, feedback is generally considered to be a fundamental factor in motor (re-)learning. With the term feedback indicates the influx of sensory information related to the performed movement or task. Broadly, we can differentiate two types of feedback according to the source that generates it: “inherent feedback” is information that is naturally perceived during a given motion or task, for example coming from proprioception, vision, hearing, and mechanoreception at the hand. The second is artificially added or enhanced via an external source; it is therefore named “augmented feedback” (often referred as explicit, extrinsic, or artificial). It can be produced either by a human or an artificial device [115].

1.3.1. Aspects of feedback

Augmented sensory feedback can be delivered according to different strategies, which, according to Molier et al. [84], can be described by their *aspect* and *modality*. We define aspect as the way the sensory feedback is delivered, i.e., its *nature* and *timing*. The nature of the feedback concerns its content, which can either be about the action, commonly referred as *knowledge of performance*, or about the outcome of the action itself, referred as *knowledge of results* [84, 115]. Timing is the second fundamental aspect of feedback, which defines the moment in which feedback is provided and its duration. The stimulus could be delivered during the execution of the motor task (concurrent feedback) or after its conclusion (terminal feedback) [109]. As for the duration, the stimulus can be either delivered as instantaneous information (discrete feedback) or in a prolonged fashion (continuous feedback). *Biofeedback* is a particular type of feedback that delivers information about the users own actions (e.g., finger movement, muscle activation, heart rate); it is concurrent with the task and continuous (*real-time*) [39].

1.3.2. Feedback modalities

Conversely, modalities are subtypes of sensory experience that the augmented stimulus elicits and depend on the type of the receptor activated. Augmented feedback can be delivered through the following modalities: i) auditory, which comprises all the stimuli that can be captured by the hearing system such as the sound of a metronome or verbal signals, ii) visual, which includes all the cues made available through vision, such as virtual reality displays, signaling lights, gestures, etc., and iii) haptic, which refers to the sense of touch and can be further be split into skin pressure, vibration, skin stretch, etc. In addition, different feedback modalities can be combined to provide multimodal feedback. If the modality of the augmented feedback is identical to the natural one, the feedback is *modality-matched* (e.g., when grasping force is augmented with pressure feedback) [3]. If, instead, the sensory information is provided through a different modality (e.g., an increasing contact force represented as a sound with increasing volume), the feedback is *modality-mismatched*. The means by which feedback is provided is often called *display*, but it is not confined to the visual domain. In fact, a computer screen can be a display as much as a vibration motor or a speaker [109].

1.3.3. Strategies for robot-assisted error feedback

A possible approach for delivering augmented sensory feedback consists of manipulating it with the aim of tuning its effects on motor learning and rehabilitation. Especially in the field of robotic rehabilitation, two opposite paradigms of feedback modulation have been extensively studied, namely *Error Reduction* (ER) - also referred to as haptic guidance – and *Error Augmentation* (EA) - also known as motor amplification. The ER paradigm advocates for a reduction of the performance errors of participants while performing a motor task, which normally occurs by means of a robotic tool that guides the participant’s limbs in accomplishing the task, to restore motor function after stroke [81]. Since the motor system has been demonstrated to behave as a “greedy” optimizer that rapidly incorporates the robot’s assistive forces to reduce the degree of voluntary control and muscle activation [32], it was suggested that the assistance should be provided “as needed”, i.e., with the minimal amount of external assistance [75, 97]. Conversely, EA paradigms tend to amplify the movement error by means of disturbing force fields, since motor learning is in fact driven by error [32]. However, it was demonstrated that skilled subjects benefit more from learning with EA than less skilled subjects [83, 109], which ultimately translates to the recommendation of tuning the modulation based on the specific skill level of each patient.

1.3.4. Developing a reliance on extrinsic feedback

When providing augmented feedback, there may be a risk of training the patient to rely on it more than intended. The guidance hypothesis speculates that the salience of concurrent extrinsic feedback may lead the patient to depend on this extrinsic feedback, ignoring any intrinsic feedback. Improvements that are shown during the performance of the task with extrinsic feedback delivery are therefore lost in retention tests [109]. In other experiments, however, concurrent feedback seemed beneficial during the performance of more complex tasks [10].

Several studies on this issue have shown that intermittent trials without feedback allowed the participants to integrate external and internal feedback rather than coming to depend exclusively on the external feedback. In those studies, the participants could replicate the learned movements in retention tests without external feedback, probably because the augmented feedback had allowed them to refine the internal model of the task [6, 24, 106, 118].

1.3.5. The sensory side of rehabilitation is an open question

Many authors argue that, as yet, there is insufficient literature evidence to support (or refute) the effectiveness of interventions specifically focused on the sensory aspect of stroke rehabilitation [10, 11, 29, 69, 115]. Nonetheless, the absence of evidence does not imply the evidence of absence, and several recent studies encourage further investigation of this topic, as supported by emerging technologies and rehabilitation techniques [19, 62]. Indeed, it has recently been suggested that combined sensorimotor training outperforms conventional motor-oriented therapies [19]. In the following, several approaches are described that use different sensory channels to provide specific sensory training. Notably, according to our current knowledge of sensory cortical processing, the different sensory channels strongly interact with each other in the CNS and they cannot be treated as separate moduli [4, 92, 108], therefore it is theoretically impossible to aim at targeting *only* one channel but rather *mainly* one channel.

1.4. Auditory Feedback

Verbal encouragements are the most common forms of auditory stimuli delivered by physical therapists in clinical practice [84]. Due to the variable nature of this form of feedback, it has been difficult to evaluate its effectiveness in sensorimotor rehabilitation. However, it is known that auditory stimuli play an important role in motor learning [109], and induce brain plasticity, as further exemplified by the fact that trained musicians show anatomical differences in their motor and premotor cortex, and cerebellum compared to non-musicians [10]. Playing a musical instrument is in fact a complex task that requires fine motor coordination and the association of different sensory stimuli with motor actions. Based on this potential interaction between motor coordination and music, it has been suggested that music can be leveraged to provoke neuroplasticity to facilitate rehabilitation of stroke patients.

1.4.1. Types of augmented auditory feedback

A common way of providing auditory feedback in rehabilitation therapies is through rhythmic stimulation, which can improve motor function and proved particularly beneficial for gait training [10, 19], possibly due to the rhythmic nature of the gait. However, music-based interventions produced beneficial effects also in interventions targeting the upper limb [10, 19, 87], suggesting that music (and rhythm in particular), can guide motor timing and improve motor control. Beyond music therapy and rhythmic stimulation, three possible ways of displaying auditory feedback have been identified by Sigrist et al. [109]: i) auditory alarms, ii) sonification of movement variables, and iii) sonification of movement error. While the first type of auditory feedback implies the delivery of auditory stimuli without any form of modulation to signal that some variable exceeded a threshold, the other two involve the use of data values to change the parameters of the auditory stimuli. These data can be, respectively, kinematic and dynamic variables of the body (e.g., limb velocity, grasp force, body position, etc.) or deviations of these variables from a desired value.

1.4.2. Auditory feedback devices

It is worth noting that auditory feedback is very often displayed in combination with other sensory modalities, which hinders the possibility of drawing general conclusions regarding the impact of this sensory modality in the improvement of sensorimotor performance [84, 87, 114, 117]. In the remainder of this section, we report a number of studies that attempted at providing evidence of the efficacy of auditory

feedback for neurorehabilitation.

In a study by Malucci and Eckhouse, concurrent auditory feedback was displayed to a group of stroke patients to guide their reaching trajectory of the upper limb, while the rest of the patients received physical training alone. Modifications of the trajectory were seen both in the group undergoing practice alone and the one with auditory feedback, however, the auditory feedback group obtained better path performance [79]. Another approach that has been tested consists in using musical instruments to practice music-supported motor rehabilitation, in which the patients learn to play simple songs on a piano or rhythms on a drum. The effect on motor performance of auditory feedback delivered while playing an instrument was attributed to error-based learning [96, 120]. Van Vugt and colleagues [116] aimed to test the error-based learning hypothesis by providing Music-Supported Therapy (MST) with and without delayed auditory feedback. Surprisingly, the group receiving delayed feedback outperformed the one receiving real-time concurrent feedback in the well-known 9-Hole Pegboard Test. The authors argued that auditory-motor integration may be impaired in stroke patients so that concurrent audio feedback led to over-correction of non-existing errors.

Another application of auditory feedback to improve upper limb motor performance was presented by Thielman [113]. Auditory feedback on trunk position aimed to reduce trunk compensation movements during reaching in post-stroke patients. The feedback was faded over time in accordance with the guidance hypothesis. Both the feedback group and a control group of subjects restrained to a chair improved their performance, but the feedback group improved significantly more than the restrained group. This result suggests that extrinsic feedback can increase sensory awareness during the performance of a motor task, which could ultimately favor motor learning.

1.4.3. Conclusions on sensory feedback

The scarcity of evidences on the effectiveness of auditory feedback in sensorimotor rehabilitation and the lack of a standardized procedure prevent us from drawing a satisfactory conclusion on this method. On the other hand, promising results have been obtained in improving both motor control and sensory awareness, which confirm the high potential of auditory feedback and encourage further studies in this direction. Notably, auditory feedback is often multimodally combined with other types of augmented feedback [59, 67, 77], which will be described in the next paragraphs.

1.5. Visual Feedback

Vision is considered the most important sense for the interaction with the environment in activities of daily life. The fundamental importance of vision for motor learning and the performance of complex motor tasks is widely acknowledged [109]. Visual information can be leveraged to provide augmented feedback related to motor performance or movement-related parameters with rehabilitative purposes. In motor learning, the effectiveness of visual feedback largely depends on task complexity and skill level [109], and optimal visual feedback should therefore be tailored to the specific user's needs to avoid cognitive overload. It is suggested that adding visual stimuli to rehabilitation therapy promotes the learning process [84] and increases motivation during the training [86]. Beyond mirror therapy, which has shown beneficial effects in stroke rehabilitation and is regarded by some authors as a form of augmented feedback [10, 29, 86, 87], visual feedback is effectively delivered in the form of *Virtual Reality* (VR) [36, 66, 86, 87, 117]. This type of rehabilitation involves the use of simulated realistic environments that are displayed through different devices, such as virtual reality headsets, projectors or monitors [66]. The virtual environments are characterized by different levels of *presence* and *immersion* [10, 66]. While the former is a subjective measure of how much the person experiences actively being in the virtual environment, the latter objectively factors how much the virtual system is intended to capture the user's attention [66]. A variety of devices can be used to interact with virtual environments, ranging from the computer mouse to state-of-the-art tracking systems used to capture the kinematics of the limbs, which are then represented in the virtual workspace, while yet other sensors can be employed to capture the dynamics of the actions, such as forces and torques.

1.5.1. Benefits of Virtual Reality rehabilitation

Several aspects support the effectiveness of VR-based rehabilitation. Firstly, the recent advances in VR and serious gaming technologies, especially from the entertaining industry, provide the great potential of increasing users' participation to the rehabilitation exercises, thus encouraging more repetitions

of goal-oriented tasks [36, 66, 117], which are paramount in neurological rehabilitation [65]. Increasing visual quality and immersion of virtual environments results in larger recruitment of visuomotor networks, which may benefit motor performance and learning [36]. Furthermore, VR-based training produced evidence of provoking neuroplasticity, increasing ipsilesional representation and larger activation of the primary motor cortex [66]. The effectiveness of VR practice on motor learning depends on task complexity, where complex tasks lead to marked positive effects, while the concurrent visual feedback brought by simple virtual motor tasks proved rather unfavorable, possibly due to the guidance hypothesis - i.e., permanent feedback acquired during learning leads to a dependency on the feedback [109].

1.5.2. General features of a Virtual Reality setup

In the following paragraphs, clinical studies reporting the use of augmented visual feedback in the form of virtual reality training are reported. A stereotypical example of a virtual reality scenario is represented in Figure 1.3. In some studies, the movement of the whole body is captured by motion tracking systems [111]. This information is used to reproduce the movements in space, usually projected in real-time on a large screen. The representation of the biomechanical system of the end effector can resemble human aspects, assuming the form of an avatar [111] or appear through more abstract shapes. Examples of such abstract representations are arrows depicting the direction of motion in a 3D space [77] or bars varying in color and height according to the arm's movement [42]. Even in case of a more realistic and complete representation of the environment, feedback related aspects are usually enhanced to avoid distractions, for a clear understanding from the user. Another important characteristic of VR systems is the involvement of the subject in the execution of the task, motivation increases when the task pretends to be either useful in a real environment or amusing in a game setting.

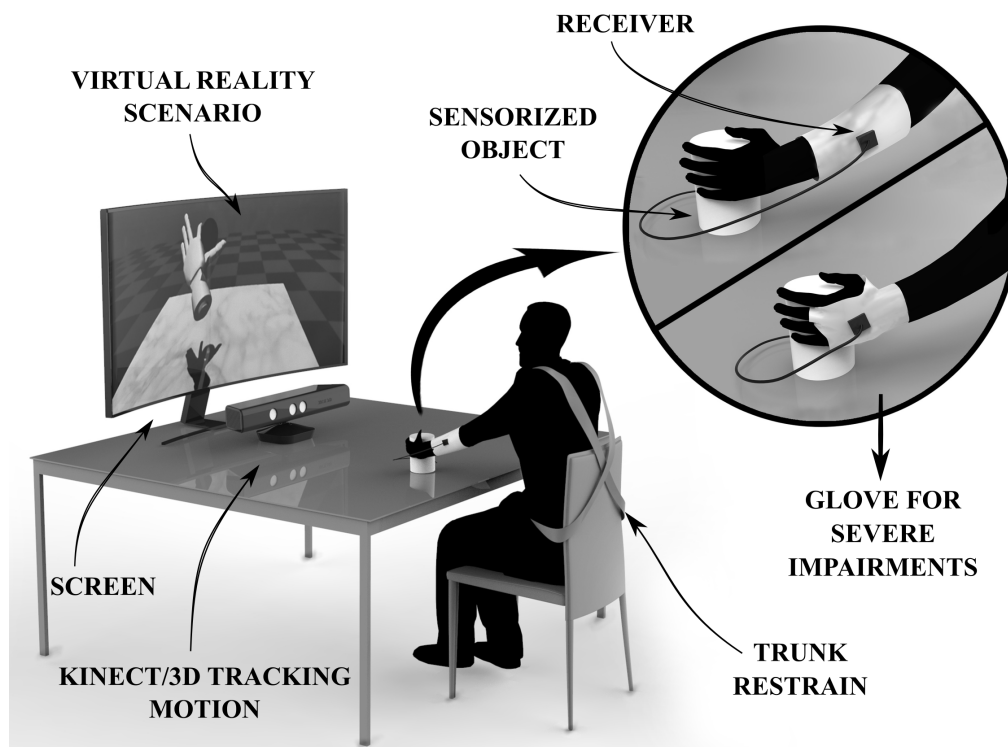


Figure 1.3: Stereotypical example of a VR setup for hand rehabilitation purposes. It features a motion tracking system (e.g., an RGBD sensor) and a screen or a projector to display the VR scenario. The motion of instrumented objects can be coupled with virtual objects by means of a receiver placed on the patient's limb. These objects can be attached to a glove worn by the patients in case of severe motor impairments, which prevent them from grasping the object. Methods to restrain the patients' trunk can be included to avoid compensatory movements.

In these rehabilitation therapies, stroke patients are usually asked to perform both simple and complex tasks. Simple tasks can be achieved by reaching an object, while more complex tasks, such as pouring water from a bottle in a glass, involve the activation of many muscles and can be decomposed

in several sub-movements. In both cases, it is common to use physical sensorized objects, synchronized with virtual objects in the virtual environment [60]. The virtual objects should resemble in shape the real ones as much as possible and follow their displacements in real time thanks to electromagnetic, piezoelectric, capacitive or resistive tracking sensors placed on the sensorized objects. In case the patient presents severe grasping deficits, sensorized gloves are often used and real objects can be forcedly attached to them [59, 60, 67, 90]. The same motor task can be performed with increased complexity by adding extra virtual elements which do not have a correspondence in the real environment [60, 90].

The kinematic features extracted by the VR experimental setups can be beneficial both for the clinicians to evaluate the motor performance and for the patients to increase their awareness on the sensory events while executing the movements. These features consist of several kinematic variables recorded by the tracking systems, e.g. mean velocity of end effector, time to complete the task or number of sub-movements executed to complete a complex task (peaks) [12, 59, 60, 90]. The representation of more complex features such as the torque or force applied by the patient's upper limb, the joint range of motion, trunk compensation or movement trajectory is often employed [23, 67, 77, 111]. Additional information on the error and error rate can be provided as knowledge of results feedback [111].

1.5.3. Studies in Virtual Reality for rehabilitation purposes

Studies using VR systems that provide solely visual feedback compared the effects of *Reinforced Feedback in Virtual Environment* (RFVE) to standard rehabilitative protocols. Significantly larger improvements in the motor function assessment measures were seen in the RFVE groups compared to the control group receiving the same amount of personalized or standard traditional therapy [60, 90]. The virtual reality scenarios in these two studies consisted of a motion tracking system, a large screen and sensorized objects. These objects were coupled with an electromagnetic sensor on the dorsal part of the hand or on a glove worn by the patient in case of severe motor impairments. Improvements in Fugl-Meyer Upper Extremity scale for the RFVE group resulted from these studies. Moreover, Kiper et al. reported an increase in Functional Independence Measure with respect to the control group. These works demonstrated that motor functions improved after VR-based rehabilitation exercises in addition to regular therapy.

Another advantage of VR-based exercises is the possibility of delivering several types of augmented sensory feedback through the use of sensorized objects. Studies employing multimodal sensory integration through virtual reality systems will be described in the dedicated section.

1.5.4. Other visual feedback delivery methods

In addition to VR, augmented visual feedback can be added to traditional rehabilitation to provide information on the level of the force applied during grasping, as studied by Quaney et al. [94]. In their study, augmented visuomotor training was administered to patients performing a lifting task by providing information on the target and the current magnitude of the grip force (GF), continuously during object manipulation. After the visuomotor training session, the patients were able to pick and lift with higher GF accuracy, and the improvements remained stable after the removal of feedback. In fact, the authors hypothesize that stroke patients appropriately used predictive GF by recalling the prior knowledge on motor commands. Another example of providing augmented visual feedback is the display of information on direction and intensity of normal and tangential forces applied by stroke subjects during a manipulation task, where the participants were asked to reach and maintain target levels of normal and shear forces [101]. The training resulted in increased scores of Box and Block Test and Action Research Arm Test between pre- to post-test measurements. The tangential to normal force ratio decreased after training, indicating a higher level of hand motor performance. Notably, the improvements persisted even after the visual feedback was removed.

1.5.5. Conclusions on visual feedback

Visual feedback has been thoroughly investigated for neuromotor rehabilitation, and the level of evidence of its effectiveness is significant. Both VR and visual cues have been demonstrated to provide neurological patients with valuable information that they can leverage to improve their motor performance. In particular, VR-based approaches are particularly promising, increasing the level of performance, also thanks to the continuous advances in this field promoted by the entertainment industry, and allowing for a higher level of engagement. Similarly to auditory feedback, vision-based approaches

are often coupled with other types of augmented information in a multimodal fashion, further extending the potential of this method.

1.6. Haptic Feedback

Haptic feedback, meaning information relayed by the sense of touch, enables us to interact bidirectionally with the environment, i.e., to act on it and contemporarily perceive these actions [109]. The study of haptic feedback attracted many researchers worldwide and the impact of haptics on motor learning and rehabilitation have been widely investigated. These studies contributed to our understanding of how we use touch to explore the environment and how they impact on our motor function [26]. It was discovered that motor performance can be improved through haptic stimulation, which increases corticospinal excitability and expands the cortical representation of the body part that is stimulated [10]. Moreover, it was found that substantial processing of somatosensory afferent stimuli occurs in the motor cortex, demonstrating the great interconnection between motion and sensation [19, 109]. Notably, haptic feedback does not require visual attention during exercise [117] and indeed it is used to reduce the workload of visual and auditory system [109]. Haptic feedback can be broadly divided into two different categories: kinesthetic and tactile feedback [26]. The former is used by the CNS to infer the position and motion of the body parts (referred as kinesthetic awareness or proprioception), and the latter consists of information from the external environment. Muscle spindles, golgi tendon organs and mechanoreceptors (quick adaptive Pacinian corpuscles FAII and slow adaptive Ruffini endings SAII) in the joint capsules, ligaments, and skin surrounding the joints collect kinesthetic stimuli, while four types of mechanoreceptors, thermal receptors and nociceptors provide tactile information [26]. The mechanoreceptors are divided in fast adapting (FA) and slow adapting (SA) types, in particular: Meissner corpuscles (FA I), Pacinian corpuscles (FA II), Merkel Cell Neurite Complexes (SA I) and Ruffini endings (SA II).

1.6.1. Movement-based (implicit) and sensory-based (explicit) haptic feedback

In haptic research it is possible to differentiate between devices that primarily target the sensory function, which therefore provide only references for the completion of a specified movement, from devices that instead guide the user through the movement, which do not provide haptic feedback as a primary goal but nevertheless provide sensory feedback by promoting motor activity [26].

In fact, robotic therapists, such as exoskeletons or wall-mounted systems, guide the limb motion providing assistive or resistive actions. Notably, they do not only promote rehabilitation due to the implicit improvements in muscle strength or joint range of motion but purposely facilitate motor learning through sensorimotor integration. Despite the increasing adoption of these devices in clinical practice and the proven efficacy in upper limb rehabilitation [81], their intervention cannot be considered as primarily sensory and will not be extensively treated in this chapter.

On the other hand, the devices that primarily target sensory function and do not impose motion can either be based on kinesthetic feedback or tactile feedback. Kinesthetic feedback can be delivered through an electromechanical or pneumatic apparatus, such as a force feedback joystick or mouse. Alternatively, other devices that primarily target the sensory function consist of vibrotactile displays and pressure displays, namely *tactors*. Vibrotactile systems represent the most common way of providing haptic feedback, as testified by their pervasive adoption on technological devices such as phones or wearable gadgets. These devices have been widely used to support motor learning [109] and rehabilitation [117]. Notably, several parameters can be tuned in a vibrotactile display, similarly to auditory displays, such as vibration frequency, intensity, duration, polarity (i.e., the vibration can pull toward the signal or push away from it [109]) and application site, although it is not yet possible to draw conclusions on how to properly tune these parameters. Tactile afferent information has been proven to be central in object manipulation, which are used by the CNS to mark the task' phases and link them to sub-goals [52]. The fast adaptive nerve endings in human skin are very sensitive to vibrations, with a peak in sensitivity in the range of 200 – 300Hz for Pacinian corpuscles and 40 – 50Hz for Meissner endings [52]. The delivery of discrete vibrotactile cues demonstrated successful in restoring important tactile information in the field of prosthetics, where vibrotactile feedback was delivered to a sensitive part of the patient's body, i.e., the arm, simultaneously with tactile events at the fingertips, and they were quickly and seamlessly integrated in the user's motor control [20].

1.6.2. Feedback for kinesthetic illusion

Proprioceptive feedback provides conscious information on the position and movement of one's own body parts to the CNS, which uses it to refine balance and motor control [107]. Joint capsule receptors, Golgi tendon organs and muscle spindles respectively provide information on joint position, muscle force and muscle contraction velocity. Golgi tendon organs are located in series with muscle fibers in the tendons and are activated when the tendon attached to the active muscle is stretched. On the other hand, muscle spindles are located in intrafusal fibers, parallel to the regular ones. There are two types of muscle spindle sensory endings: the faster primary endings respond to both changes in length and velocity while the slower secondary endings are only sensitive to length and therefore provide information on the position [55]. Damages to the anterior primary motor cortex area caused by strokes also affect the function of muscle spindles, generating excessive or absent reflexes to proprioceptive stimuli leading to severe losses in motor control and in particular, in fine manipulation skills [10].

It has been demonstrated that vibrations in the range of 70–110Hz delivered to musculotendinous regions can induce an illusory limb movement, namely kinesthetic illusion [40, 74, 99]. The rehabilitative potential of the kinesthetic illusion is suggested by the fact that it can elicit proprioceptive sensations in patients regardless of their motor abilities and without requiring actual limb motion. Its efficacy in clinical practice has not been thoroughly assessed [99], but a recent effort to define a standardized approach may change this in the future.

For the aim of this study, we will not focus on the branch of haptic feedback augmenting proprioception, as they do not provide an extrinsic information while performing a task, we are instead more interested in the tactile sensation.

1.6.3. Devices for haptics

A variety of technologies can be instead employed to devise tactors, ranging from motors constricting bands worn around the limbs and skin indentation or stretching mechanisms, to more exotic solutions employing ultrasounds, magnetorheological fluids and shape-memory alloys, however their efficacy in rehabilitation practice is limited by the reduced sensitivity of individuals affected by somatosensory neuropathies [26]. In the remaining part of this section, we describe the clinical studies that focused on delivering haptic feedback as a primary intervention for rehabilitation.

Tactile stimuli can be delivered through many types of motors and devices on the skin, even though the most common technique is to use vibrations generated by eccentric mass, voice coil, piezoelectric or servo motors [5, 31, 64, 70]. Other methods consist of applying mechanical pressure or a stretch to the patient's skin [5, 85], or exerting a resistive force through the handle of a haptic device proportional to the information to be augmented [1, 12]. The information provided through haptic extrinsic feedback can be of the same type of the feedback, i.e. tactile, [15, 70] or can represent other physical quantities that differ from the modality of delivery [31].

When applying a vibrational stimulus to substitute fingertips' tactile sensation, particular attention should be given to the location and the duration of the vibration: in fact, if the actuator is placed directly on the fingertips it can interfere with object manipulation, and the subjects feel like touching a vibrating object instead of holding it with their fingers [82]. Moreover, exposing the participants to prolonged stimulation could cause adaptation of the receptors to the stimulus or even tissue damage [26]. Adaptation to a stimulus can be prevented if the stimulation is interrupted intermittently [76, 105]. Additionally, concurrent feedback could be detrimental for motor learning. In a study where participants had to learn six different movements, concurrent vibrotactile feedback distracted the participants and led to poorer outcomes [6].

Vibrotactile feedback can be employed to effectively provide proprioceptive information. In a study by Elangovan and colleagues [31], the patients controlled a wrist robot to complete a virtual task that was simultaneously displayed on a screen and haptically rendered by the robot. Beyond the visual and the haptic feedback, they received vibrational cues on their forearm regarding the position of the virtual target. The robotic rehabilitation session resulted in a significant reduction of the *Just Noticeable Difference* (JND) threshold of the wrist joint angles, demonstrating that impaired proprioception can benefit from augmented haptic feedback.

Information on dynamic interactions can be conveyed by means of haptic displays with rehabilitation purposes. In a study by Cameirão and collaborators [15], the force applied by the patients to virtual objects was fed back through the handle of robotic device in a rehabilitation task, which led to better clinical outcomes with respect to other procedures without haptic stimulation. In a study by Broeren

and collaborators [12], the reaction force generated by the interaction with objects in virtual environments was rendered to chronic stroke patients through a haptic stylus, resulting in improved clinical outcomes after the treatment. Haptic feedback can also provide information about the Knowledge of Performance of the ongoing motor action: the force applied by a haptic device was proportional to the trajectory error in target-reaching tasks [1], which resulted in improvements in clinical scales similar to conventional therapy. or it can be triggered when a distance threshold is overcome during a reaching task (named outcome-triggered feedback by the authors) [42]. Haptic feedback is a powerful modality for delivering augmented feedback and is often used in combination with other types of feedback for greater effectiveness through a multimodal sensory feedback integration.

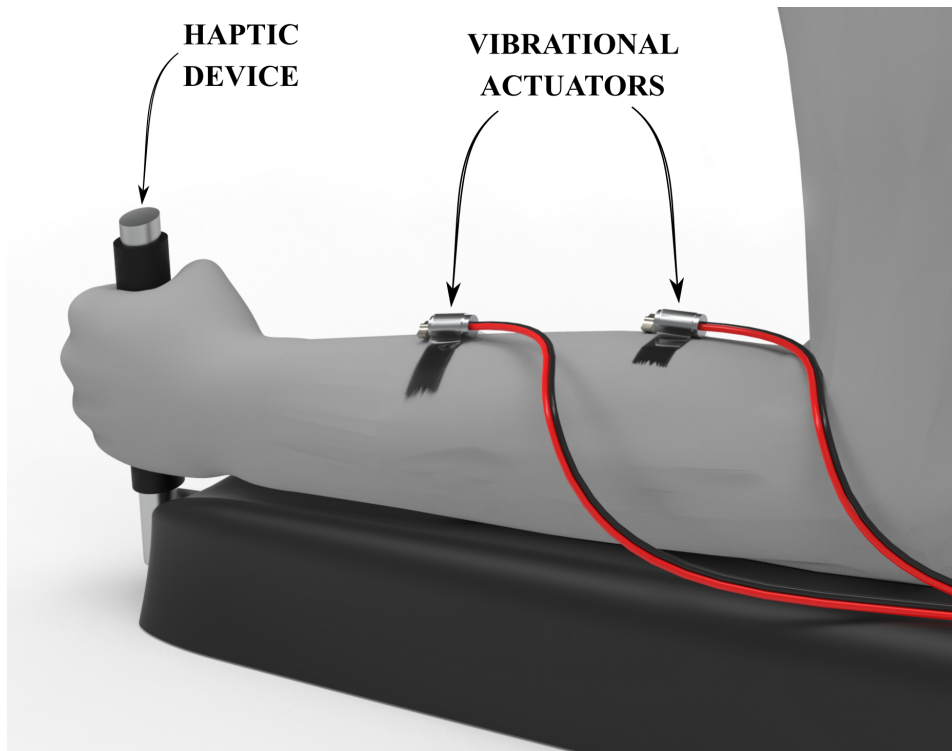


Figure 1.4: Example of a setup for delivering augmented haptic feedback. Tactile information can be delivered through vibrational actuators or tactors placed on the patients' skin, while kinesthetic information can be delivered through forces or torques applied by a haptic device.

1.6.4. Conclusions on haptic feedback

The tactile sense is a fundamental channel for neuromotor rehabilitation. We reported on several studies that leveraged different types of augmented haptic stimulation to promote recovery after stroke. The haptic modality is often combined with other types of feedback, especially with vision in VR-based scenarios, which makes particularly difficult to draw conclusions on the effectiveness of this sensory channel. However, we can argue that adding haptic stimulation to the sensorimotor rehabilitative training generally leads to beneficial effects.

1.7. Multimodal Feedback

The CNS can integrate information coming from different sensory modalities with prior knowledge on the task, minimizing the uncertainty on sensory signals [7, 35]. These signals are often inaccurate and noisy, especially in post-stroke convalescence, when afferent pathways are corrupted. Bays and Wolpert suggested that the brain normally integrates the information coming from distinct sensory modalities through the use of weights, modulated according to the accuracy of the sensory signals [7]. The lower the variance of the signal coming from a specific sensory modality, the higher the weight used by the CNS when integrating this information (Fig. 1.5). The same concept applies to the integration of prior knowledge the subject has on the task, which is weighted more if the intrinsic feedback is degraded. Hence, in humans, multisensory integration facilitates the processing of sensory informa-

tion, ultimately improving motor functions.

Many examples of multimodal augmented feedback in rehabilitation tasks can be found in the literature. In fact, visual feedback and VR systems are very often combined with other types of feedback to increase realism and immersion.

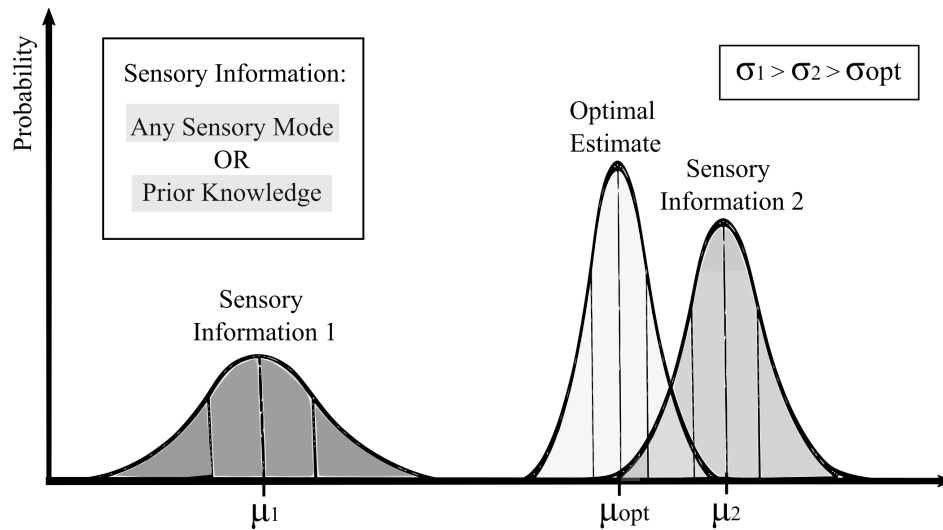


Figure 1.5: Integration of the information coming from multiple sensory modalities (i.e., intrinsic feedback) and prior knowledge. Higher importance is given to the sensory information with lower variance resulting in an optimal estimate with lower variance than the two original distributions processed and integrated.

1.7.1. Virtual reality and haptic feedback

The combination of haptic devices and virtual reality for rehabilitation proved to be effective in a study by Broeren et al., increasing the mean velocity at which the task is performed and decreasing the hand path ratio compared to the baseline, i.e., the ratio between the length of a path hand-drawn by the participant and a perfect linear movement [12]. Furthermore, the experiment performed by Cameirão and colleagues, showed how merging VR and haptic feedback is more convenient than VR alone or combined with a bimanual exoskeleton by comparing the three setups in the same rehabilitation procedure. Coupling the haptic device and a VR scenario demonstrated significantly better outcomes on upper limb Fugl-Meyer assessment, Box and Block test scores and on the ability of performing Activities of Daily Living (ADLs) [15].

1.7.2. Robotic rehabilitation: visual and haptic feedback

The field of rehabilitation robotics represents an important example of the beneficial integration of haptic and visual feedback: robotic trainers outperform other therapeutic tools lacking sensory feedback. Furthermore, Sensory-Enhanced Robot-aided Motor Training (SERMT), proved to be more effective than robotic training alone in increasing Motor Status score [70]. In this study a vibratory stimulus was delivered on the subject's hand according to the location and direction of the pushing/pulling force applied to the handle of a robot during hand movements. The subjects that underwent this condition outperformed the group that performed the reaching task with the robotic assistance alone.

A similar procedure, performed in a bimanual modality, was used to compare robotic rehabilitation to the combination of robot-aided therapy and error augmentation techniques immersed in a VR environment [1]. In this experiment, an upper limb robotic tool for bimanual practice where the location of the non-affected wrist was recorded and displayed together with the affected wrist position as a visual feedback on a screen. The robot delivered haptic feedback based on error augmentation, which significantly increased upper extremity Fugl-Meyer Assessment score with respect to the control group, whereas it did not show significant changes in Motor Activity Log and Wolf Motor Function Test.

In contrast, a study by Hayward and colleagues showed that outcome-triggered haptic feedback added to a rehabilitation training supported by a passive device with adjustable inclination, did not improve the level of performance [42]. The impaired arm was placed on the device, which constrained the motion with a linear slide to assist reaching movement while the position of the arm and the target

of the reaching movement were represented on a screen to entail the patient. In the group receiving outcome-triggered robotic training, an additional electrical stimulation was displayed to indicate that the patients surpassed their own best personal distance. Both rehabilitation strategies led to significant increases in Motor Assessment Scale compared to a control group receiving usual care, with no significant difference between the two.

Cordo et al. used a robotic device for providing hand assisted movement therapy combined with tendon vibrators to five patients [23]. Training with this setup led to improvements in ADLs, hand strength and function, observed both in post-test measurements and in the six-months follow-up, demonstrating the benefits of assisted movement therapy combined with sensory augmentation in motor recovery with effects in the long term. In another study, visual information regarding the passive force exerted by a grounded end effector robot on the subject's limb was provided during the performance of repetitive movements [77]. This rehabilitation therapy led to statistically significant improvements in Fugl-Meyer and Functional Independence Measurements scores in the experimental group with respect to a control group receiving the same treatment to the unaffected limb. The improvements were retained in a follow-up after three months.

1.7.3. Visual and auditory feedback

Reinforced Feedback in Virtual Environment (RFVE) was proven to be more effective than conventional one-to-one therapy when combined with auditory feedback providing information on the correctness of movement performance [59]. In this large study, Kiper and colleagues compared functional and kinematics outcome measures before and after the performance of simple and complex tasks both in a VR environment and in a 1-to-1 traditional hospital treatment setting. The VR setup was similar to previous studies [60] although it featured additional feedback modalities. A score, provided through acoustic signals and a digital voice, informed the participants on their spatial error while performing the tasks. Moreover, additional visual feedback was provided in the form of a virtual teacher on the screen. This multisensory environment for rehabilitation led to significant improvements in the Functional Independence Measurements and Upper Extremity Fugl Meyer scores with respect to traditional therapy, as well as in kinematics variables performance parameters.

1.7.4. Visual, haptic and auditory feedback

An illustrative example of multisensory stimulation consists of *Adaptive Mixed Reality Rehabilitation* (AMRR) [67]. It featured a VR environment where abstract feedback was delivered through visual, auditory and haptic modalities to promote independent movements during reaching and grasping tasks. Each sensory modality was used to provide information on a specific set of variables: space-related measures were represented by visual feedback, time-related variables by auditory signals, and grasp-related parameters by haptic feedback. A combination of auditory and visual feedback was also displayed to provide proprioceptive information, such as joint positions and compensatory movements of the trunk. Specifically, these feedback stimuli, adaptable according to the needs of each participants, were selectively activated to indicate an inefficient movement and provided information on the direction and magnitude of movement errors. The results of this pilot study, performed on 3 stroke participants, stressed the potential benefits of multisensory stimulation in post-stroke rehabilitation: Wolf Motor Function Test score increased in all subjects following the AMRR treatment. Possibly, information on the performance fed back through an integrated multimodal stimulation could have had a central role. The authors underlined the importance of avoiding dependence on the feedback, delivering it only when the patient needed it, instead of using a constant concurrent feedback.

1.7.5. Conclusions on multimodal feedback

Despite the large number of studies reporting beneficial effects of multisensory stimulation, many authors agree that valid conclusions on their efficacy cannot be drawn. This uncertainty can be attributed to the extremely wide variety of combinations of feedback modalities that have been tested so far [10, 29, 84, 109, 114]. For the same reason, we cannot conclude whether multisensory rehabilitation strategies can outperform interventions that target a single sensory modality, and further investigations are needed.

1.8. Sensory information enhancement

Along with the delivery of additional sensory feedback stimuli, another way of augmenting intrinsic information on sensory events in post-stroke patients is to strengthen the action of the intact afferent pathways. To date, we identified two non-invasive methods that aim at increasing sensitivity by enhancing intrinsic feedback mechanisms and brain plasticity: vagus nerve stimulation and stochastic resonance.

1.8.1. Vagus-nerve stimulation

Non-invasive *transcutaneous Vagus Nerve Stimulation* (tVNS) consists of electrically stimulating the inner side of the tragus in the ear (as shown in Fig. 1.6), as reported in a representative study [16], where the stimulation was delivered through two Ag-CI surface electrodes. After this stimulation period, the patients participated in a robotic therapy session. The results obtained after 10 days of tVNS and robotic therapy showed a significant improvement in Fugl-Meyer score. The authors hypothesized that tVNS stimulation induced neuroplasticity and therefore promoted motor functions recovery, as supported by previous studies that showed an increase in brain derived neurotrophic factor and neurotransmitters such as noradrenaline, associated with neuroplasticity and recovery after brain lesions after VNS therapy [34].



Figure 1.6: Illustrative example of transcutaneous vagus nerve stimulation. The tragus is electrically stimulated through a pin electrode, while sham stimulation can be done by moving the pin to the auricle, the outer part of the ear.

1.8.2. Stochastic resonance

Another approach to increase sensitivity consists in applying sub-threshold vibrational noise. Low intensity noise was found to enhance the afferent tactile signals due to a physical process named stochastic resonance [33, 71, 102, 103]. According to this process, when noise is infused into a non-linear system characterized by an activation threshold (akin many biological and physical systems) it can improve the detection of weak input signals. It is common to consider noise as an adverse factor in signal processing, which corrupts the signal depriving it from its informative content. Conversely, according to the aforementioned process, random energetic fluctuations injected in a system can improve the quality of its output [43]). However, this happens only for optimal amplitudes of the injected noise: the output performance is in fact a reversed U-shape function of the noise amplitude: it increases towards a maximum corresponding to the resonance peak, i.e. the optimum level of noise, and decreases for larger noise intensities (Fig. 1.7). When optimum noise is injected the system can detect subthreshold inputs, therefore it increases the signal-to-noise ratio and it lowers the detection threshold. An interesting feature of stochastic resonance is the possibility of applying any type of noise (random, periodic, aperiodic, etc.), regardless of the input signal [71, 80].

Most of the neural processes taking place in the human body, such as sensation, require the stimulus to supersede a threshold. It is suggested that subthreshold noise promotes tactile sensitivity by increasing cortical sensorimotor activity and neural synchronization between cortical regions [64]. Con-

sequently, the use of low-intensity noise started to gain attention in the biomedical field and in particular for rehabilitation techniques, given the crucial importance of sensory information in motor learning. In fact, subthreshold noise applied in several locations of the hand were tested and produced comparable results in fingertips sensitivity enhancement [33, 63]. The benefits obtained exploiting stochastic resonance did not depend on the distance between application area of the subthreshold stimulus and the target site where to enhance sensory sensitivity, as long as they pertain to the same body district and they present interneuronal connections at a spinal or subspinal level [63].

In practice, subthreshold noise areis commonly delivered via voice coil actuators, which allow decoupling frequency and amplitude of the stimulus signal and therefore modulating the amplitude of the vibration according to each patient sensory threshold.

Some studies explored the use stochastic resonance in stroke patients to enhance their tactile sensitivity and improve their motor functions. Liu et al. reported a significant decrease in the vibrational threshold following the application of mechanical noise randomly superimposed on a vibrational stimulus during an experimental protocol [71]. Another study reported changes in motor function and responsiveness to sensory stimulation after brief applications (20 minutes) of mechanical noise, which led to significant improvements in motor functions and upper limb skin sensation, measured through *somatosensory evoked potentials* [89].

Enders and collaborators reported that light touch sensation of the fingertips increased after the application of subthreshold white noise in four locations of the upper limb [33]. Monofilament Test score significantly increased, i.e. the sensitivity threshold decreased, while the Two-Point discrimination test remained unaltered, i.e. the spatial resolution was not affected. Conversely, Seo et al. found the Monofilament Test score was unaltered by the application of subthreshold noise but it led to improvements in hand dexterity, increased movement coordination and grip force during manipulation [102]. Lakshiminarayanan and colleagues recently prototyped and tested a wearable device to deliver subthreshold vibration for rehabilitation purposes and tested it on stroke survivors [103]. The treatment group significantly improved their hand motor function score in Box and Block Test and Wolf Motor Function Test compared to baseline, and retained these improvements in the 19-day follow up. Interestingly, the control group did not present significant improvements compared to baseline, probably because of the limited therapy dose provided during the trial.

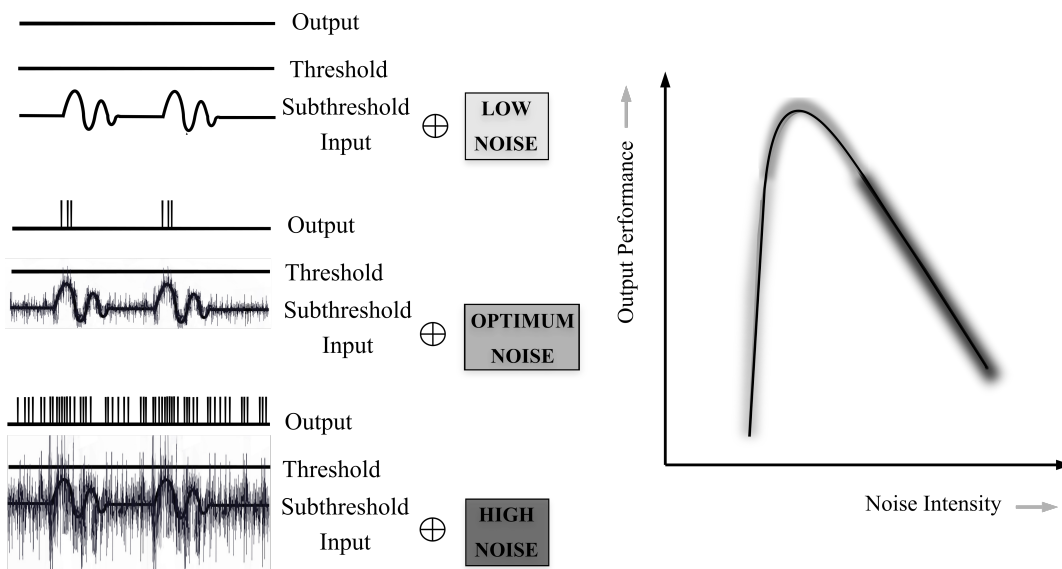


Figure 1.7: *The mechanism of stochastic resonance. a) If the amplitude of noise is too low, the output is still below threshold. B) When the noise intensity is optimal, the SNR increases, the output activated by the peaks of the input signal (resonance peak on the graph). C) When the noise amplitude is too large, the quality of the output degrades. On the right, the intensity of the noise is plotted with respect to the output performance.*

Curiously, some authors employed subthreshold stimuli as a sham baseline feedback to test the efficacy of other experimental techniques. The effects of stochastic resonance stimuli certainly reflected in the baseline group, and possibly hindered the outcomes of the experimental procedures. For example,

Johansson and colleagues tested the effects of acupuncture and transcutaneous electrical stimulation compared to a control group, to whom they delivered a low intensity stimulation at 80Hz through surface electrodes. No significant difference was found in ADLs measurements between groups, which all improved their motor performance after the test conditions and kept improving in the 3-months and 12-months follow-ups [48]. This result, instead of pointing to the ineffective outcomes of the proposed interventions may suggest that subthreshold stimulation can produce long-term beneficial effects. However, this hypothesis cannot be validated due to the lack of conclusive evidence and further studies on stroke patients with follow-ups are needed.

1.8.3. Conclusions on sensory enhancement

To conclude, according to the guidance hypothesis, augmented feedback can in some cases be distracting and hinder motor learning. This may happen because of the possible dependency on the extrinsic feedback, which leads to ignoring the intact intrinsic feedback. This effect might be prevented by amplifying the intrinsic feedback stimuli using stochastic resonance or vagus nerve stimulation.

1.9. Future directions for augmented feedback

Many devices have been designed with the aim of delivering augmented feedback, throughout the years. They were not included in the above sections since that they were not validated in rehabilitative scenarios and their effectiveness was tested only on healthy subjects. These alternative approaches, however, could serve as an inspiration for future research and might be used in the near future for stroke rehabilitation therapies.

In a study, Stepp et al. delivered vibrotactile stimuli to the upper arm of healthy participants to inform them of the force they applied during a virtual transfer task. They were instructed to transfer a virtual object across a horizontal barrier and place it in a target without breaking it, by acting on a sensorized splint. The amplitude of the vibration was linearly proportional to the normal force applied by the index finger, and it led to a significant increase in object manipulation performance [110]. Clinical trials should be performed to assess the effectiveness of this technique with impaired participants, as well as retention tests to evaluate its therapeutic effects after the removal of the concurrent feedback.

Vibrotactile feedback could be beneficial to improve the effect of robotic trainers, as suggested by Cuppone et al. [25]. In their work, vibrations were delivered to the arm of participants to provide information on the deviation from the ideal path during the performance of discrete, goal-directed reaching movements while using a wrist robot. Interestingly, this preliminary study found no difference if the stimulation was applied to the same or the opposite arm with respect to the one receiving proprioceptive training. In fact, regardless if the stimuli were applied on the treated arm or in the resting one, the participants who received additional vibrotactile feedback on movement error, significantly reduced their need of guidance from the haptic device, in contrast with the group receiving robot assisted therapy only.

Qualitative studies have been performed on other innovative devices to provide augmented feedback in stroke rehabilitation. Merret and colleagues designed and tested three different haptic devices to be worn on the dorsum or ventrum of thumb and fingers [82]. The tactile device aimed to augment the sense of touch through vibrations originated from a miniature cylindrical motor attached to the fingertips. This configuration, however, did not give the perception of holding something in the hand, instead participants stated that it felt like touching a vibrating object. This result could suggest the unsuitability of providing tactile feedback directly at the fingertips, compared to the other two devices described above in which the stimulus was delivered on the arm.

In a study by Norman et al. with healthy participants, haptic skin stretch feedback resulted effective in improving the motor performance in planar movements [85]. They applied haptic feedback through a tactor placed on the fingertips, which could deliver directional cues by stretching the skin in up to eight directions. Thanks to the information provided by haptic cues, the users were able to match their movements with the stimulus direction.

An interesting approach for delivering augmented vibrotactile feedback is to deliver short-lasting stimuli corresponding to relevant mechanical events that delimit the manipulation phases, akin how humans naturally organize motor tasks according to the *Discrete Event-driven Sensory feedback Control* (DESC) model [51]. Our group previously showed that healthy subjects can temporally integrate DESC vibrotactile feedback in their sensorimotor control during manipulation tasks using an artificial hand [2, 20, 21]. DESC feedback could be integrated in upper limb rehabilitation procedures to guide

the patients through the performance of manipulation motor tasks.

Novel developments in telehealth technology could potentially translate supervised upper limb stroke rehabilitation therapies to the home setting with low-cost devices. An example is the *Mechanical Muscle Activity with Real-time Kinematics* (M-MARK (Mechanical Muscle Activity with Real-time Kinematics)), a wearable device comprising two elasticized garments equipped with sensors worn by stroke patients while practicing ADLs such as reaching, grasping and manipulating objects [14]. The data recorded by the sensors is used to provide feedback about movements and muscle activity on a screen in the form of an avatar. The M-MARK system also provides auditory feedback on the correctness of movement strategies and muscle activation timing. An advantageous characteristic of this device is the possibility to be used by the therapists as a system to diagnose movement deficits. Current studies are being carried to identify the best choice of sensors to be integrated in this device, such as a combination of IMUs and mechanomyographic (MMG) sensors to measure quality and quantity of movement. Clinical studies on stroke patients are still needed to evaluate the effectiveness of this promising wearable device.

Several other techniques and devices have been devised with the aim of delivering augmented feedback for rehabilitation, however, only preliminary studies are available, and their effectiveness still needs to be thoroughly assessed. Despite their preliminary status, they can certainly be of inspiration for future research in post-stroke rehabilitation and demonstrate the increasing interest in the field of sensory-enhanced rehabilitation.

1.10. Goals of the project

For the aim of the thesis project, I will focus on haptic feedback delivery through a wearable device: the DESC glove. DESC stands for Discrete Event-driven Sensory Control, according to which sensory events are detected as discrete stimuli and used to define the beginning and the end of action phases related to task subgoals.

The goal of this project is to complement the current rehabilitation exercises for the upper limb with perceptual rehabilitation, consisting of delivering augmented sensory feedback. The hypothesis is that including sensory information in motor rehabilitation promotes neuroplasticity, increases motor function and ultimately facilitates motor learning. With this aim, I will prototype a device consisting in a soft wearable glove instrumented with thin and sensitive sensors at the fingertips to detect tactile events while not interfering with the natural hand movements. This device will be named DESC-glove from the type of feedback that we will use, described in the next section (1.11). For the purpose of the DESC-glove project, it is important that the improvements in motor functions provided by the device and measured during the preliminary experimental procedures are retained in time. In fact, this is paramount to support the use of the proposed device for therapeutic purposes. Moreover it is necessary that the device does not activate when moving the hand in space (e.g. opening and closing of the fist or bending fingers movements) but only in correspondence of actual contact of the hands with objects.

The device will be preliminarily tested on healthy participants to provide baseline data while waiting for Ethical Committee approval to experimentation with stroke participants. Subsequently, we will conduct an experimentation with stroke patients to evaluate the effectiveness of the device. This will be done by comparing the motor improvements after a therapeutic session, where motor therapy will be administered together with tactile feedback augmentation provided by the glove, with a control group receiving the same amount of motor therapy without sensory augmentation in order to obtain an unbiased evaluation of the benefits given by the device.

1.11. Idea: DESC Glove - Restoring tactile feedback at the fingertips to improve hand dexterity

As explained in section 1.1 of the introduction, the sensory information plays a crucial role in hand motor control. According to the Discrete Event-driven Sensory Control (DESC), the CNS encodes signals coming from the afferent pathways concurrently with discrete mechanical events such as contact with an object or its release. According to the DESC feedback augmentation, a discrete vibrotactile stimulus is delivered in an arbitrary sensitive part of the body, e.g. the arm, only in the moment of contact, slippage or release of the grasped object. Discrete contact events are recorded during the performance of movements, through the use of sensors placed at the fingertips of the wearable glove.

After an initial investigation on the sensors used in literature for detecting tactile stimuli, we hypothesised that the lack of effectiveness of other feedback augmentation techniques could be due to the use of inappropriate, noisy and not fittingly sensitive sensors. We focused on unconventional sensors, which have a response signal similar to the physiological way of detecting sensory information: piezoelectric PolyVinylidene Fluoride (PVDF) sensors. These sensors are composed by two conductive layers (made of silver) with a dielectric separating them (a thin layer of piezoelectric polymer). The peculiarity of this sensing technology is that its response is linearly proportional to the derivative of the force applied, i.e. the derivative of the acceleration. They respond with a positive spike when a pressure is applied and then immediately return to the neutral condition, a negative spike is then sent when the pressure is released. In this way, PVDF sensors placed on the fingertips can transduce information on the discrete contact events while manipulating an object. The response signal from the sensors is directly used to control vibration actuators placed on the arm which activate in concurrence with the electric spikes generated by the PVDF, corresponding to the tactile events.

The use of time-discrete feedback was proven to be advantageous when compared to continuous feedback in prosthetics applications [21]. The DESC policy implies the application of short-lasting sensory information, which can provide the additional advantage of saving battery life, since the activation time of the vibration motors is shorter than the activation of a continuous pressure. More importantly, as explained in section 1.3, when delivering continuous concurrent feedback during the performance of the task, a dependency on the extrinsic feedback can be developed, which leads the subject to ignore his residual intrinsic feedback mechanisms. According to this concept, namely guidance hypothesis, all the improvements on motor performance noticed during the experimental procedure are lost in retention

tests. Motor learning does not occur and the benefits are not visible in absence of extrinsic feedback, therefore the procedure cannot be used for therapeutic purposes. The aim of our project is to design a device that provides benefits that persist in the long term instead of generating improvements only during its usage. Dependency on feedback should not occur in our setup, since it is delivered in a discrete fashion, providing information only on the beginning and the end of the action phases. The DESC type feedback simplifies the familiarization process with feedback, as the subjects only need to associate specific mechanical events with temporally synchronous discrete sensory stimuli.

Through the repetitive use of the glove, we expect stroke patients to quickly learn to associate the vibrotactile stimuli delivered in a sensitive part of the body, e.g. the arm or the shoulder, with contact sensory events at the fingertips. This mechanism is due to the associative memory, which *tricks* the brain into thinking that the sensory stimuli perceived on the arm are actually coming from the fingertips.

2

PVDF sensors prototyping and manufacturing

The hardware prototyping and manufacturing of the DESC-glove requires many steps, thoroughly described in the following three chapters. In section 2.1 I reported a brief outline of the manufacturing process. In this chapter the process to manufacture the piezoelectric sensors to be placed on the glove is described.

2.1. Hardware prototyping outline

- Sensors fabrication, silicone and glove sewing (Chapter 2)
- Characterization of the sensors (Chapter 3)
- Design of the printed circuit board to acquire sensors' signals (Chapter 4)
- Building of the setup for the experiments (Chapter 6)

2.2. Sensors design

The first main decision to be taken in order to begin prototyping was the number of sensors to use and their position on the glove. By looking at the distribution of mechanoreceptors on the hand, shown in Figure 1.2, we noticed that index, thumb and middle fingertips are the regions with highest density of tactile receptors. These are in fact the most utilized fingers while manipulating objects and their tactile sensitivity is crucial during grasping. Therefore we decided to place three sensors on the glove to detect touch at the thumb, index and middle fingertips. A higher number of sensors was considered redundant and not necessary as the other fingers are rarely used when performing the rehabilitative movements, in case of necessity they will be introduced in a further stage of the study when designing a second version of the device. One important aspect to take into consideration when designing the shape of the sensors is their possible unsolicited activation in case they bend during certain movements. For this reason, triangular cuts were made around the semicircular shape of the fingertips to be able to adapt the PVDF sheet to a curved surface without generating wrinkles (Fig. 2.1). In order to avoid solicitation given by the folding of sensors, it was important to reduce their size and keep them on the distal phalanges to avoid their crossing of the interphalangeal joints which would cause bending of the sensors during movements. Moreover, we decided to include the sense of touch also coming from the side of the thumb for pinching movements by adding a fourth sensor (Fig. 2.1). However this sensor resulted to be superfluous as the two thumb sensors both activated synchronously, it was later removed in a further design enlarging the one single thumb sensor to cover also stimuli from the lateral pinch (Fig. 2.2). Part of the sensor was needed to connect the cables to the two sheets of the PVDF, therefore a rectangular space was added, at first to the bottom of the sensor (Fig. 2.1). This was later modified and moved to the top of the design (Fig. 2.2) so that, instead of having the cables on the palm, interfering with object manipulation, they could be stacked on the dorsum of the hand. In a later version of the

design, the number of rectangular incisions to prevent the inappropriate stimulation of the sensors was reduced (Fig. 2.2), as we noticed that by inserting the sensor in between two silicone sheets the risk of generating a signal from sensor folding was lower. In the latest design, a small rectangular part was added to the index finger sensor in order to provide tactile sensation in the internal lateral part of the fingertip to increase the sensitivity during pinch grip (Fig. 2.2). In both designs the sensors were made to bend around the top of the fingertips without generating wrinkles that would cause electric signals to be inappropriately sent.

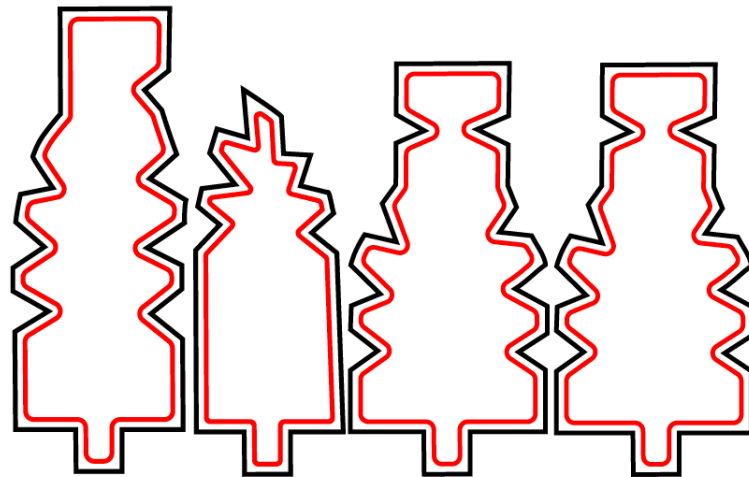


Figure 2.1: First design of the PVDF sensors on Inkscape, from left to right: Thumb central, Thumb lateral, Index, Middle finger. The edges were covered with small triangular cuts to prevent from self activation of the sensors when bent on the fingertip shape. The cable connection rectangle was firstly placed in the bottom part of the sensor.

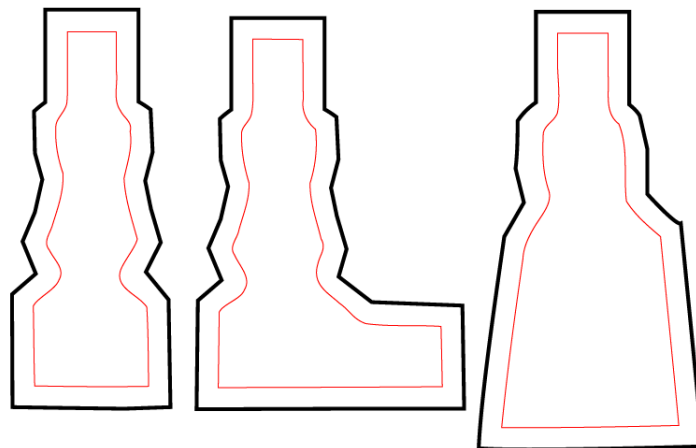


Figure 2.2: Last design of the PVDF sensors on Inkscape, from left to right: Middle finger, Index, Thumb. The cuts were reduced in size and number as they were seen not to be essential after the placing of the silicone. The thumb sensor became a larger single one, as they were seen to be activated concurrently and therefore one of them was redundant. The cable connection rectangle was moved to the top part of the sensor and a rectangle for lateral index sensitivity was added.

2.3. PVDF sheet laser cutting

After designing the PVDF sensors on Inkscape, I used the laser cutting machine to cut the shape of the sensors starting from a A5 PVDF sheet. When making piezoelectric sensors it is very important to make sure the two conductive layers are not in short circuit. This would happen by normally cutting the sensor's shape with the laser and the producers suggest to leave a 2mm offset on one side of the sensor free of conductive layer, to avoid short circuit risk. Steps for laser cut:

- Cover PVDF sheet with paper tape on both side, to allow for offset cutting and protection during the next phase of cleaning
- Give different colors to the external border (black) and the offset (red) in order to be able to cut them differently
- Laser cut machine settings: red - *Power* = 6, *Speed* = 100, *Thickness* = 0.2. Cut only the top layer of paper tape.
black - *Power* = 60, *Speed* = 90 *Thickness* = 0.2. Cut all layers of tape and PVDF.
- Run the laser cut machine and wait for the process to be terminated, then remove PVDF sheet from machine.

2.4. Offset cleaning for short circuit prevention

After removing the top layer of tape from the 2mm offset, the goal was to remove the silver conductive layer from the offset on one side of the sensor in order to prevent conduction between the two silver layers that compose the PVDF. In order to do this I used acetone (C_3H_6O) with some cotton and gently removed all the silver until there was no connection between the two electrode plates as shown in Fig. 2.3. The multimeter was repetitively used to check for short circuits until all the offsets were properly clean. The paper tape was therefore removed from the sensors' surfaces.



Figure 2.3: Setup for cleaning the sensors' offset from the silver layer to prevent short circuit. On the top right a baker with acetone to remove the silver layer using cotton-swabs shown on the left. The sensors covered with paper tape in the central part to protect the rest of the silver from the acetone, get cleaned in the outer edge offset.

After a first attempt, the offset had to be enlarged, as we can see from Fig. 2.4 to Fig. 2.5, since it was very complicated to avoid a connection between the two conductive layers with the thin safety offset of Fig. 2.4.

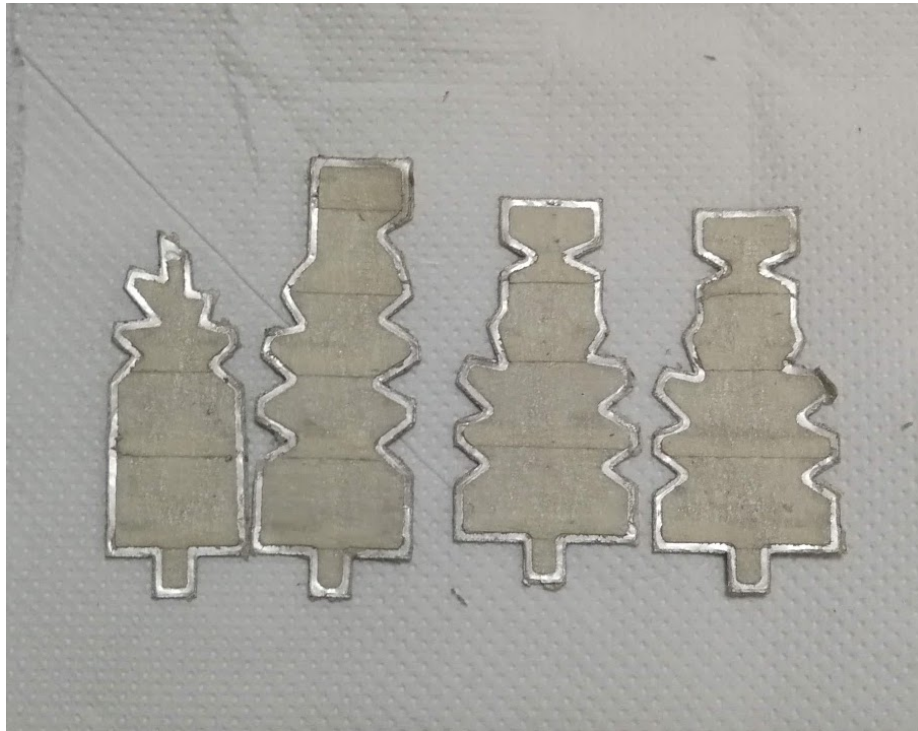


Figure 2.4: Sensors with outer edge cleaned from silver layer to avoid short circuit. Version 1, thinner offset of 1.5mm shown in the figure. This offset was not enough to prevent short circuit and was therefore enlarged in the following versions of the sensors.



Figure 2.5: Sensors with edge cleaned from silver layer. Version 2, larger offset of 2mm shown in figure. This offset width was enough to clean the sensor edge properly and therefore prevent short circuit. The simpler shape of the second version of the sensor also helped in the edge cleaning.

2.5. Cables connection

To be able to record a signal when mechanical stimuli are applied, cables must be attached to both of the conductive sensor surfaces. This was firstly done using a conductive paste, and secondly improved using a conductive tape which was seen to be more resistant and a better conductor. I utilized the conductive tape (ECG7033H) from 3M Electronics (USA) with 0.32mm thickness. The cleaned sensors connected to the cables are shown in Fig. 2.6.

The sensors were then tested using an oscilloscope to check their response to pressure and the cable connections, before inserting them in the silicone. The analog signal in response to the application of pressure was analyzed from the output of the oscilloscope. I concluded that the sensors were working correctly, sending a positive response following the application pressure and a negative one after the pressure was released. In order to properly fix the connection between the cables and the conductive layers of the sensors, a drop of super glue was added on each connection.

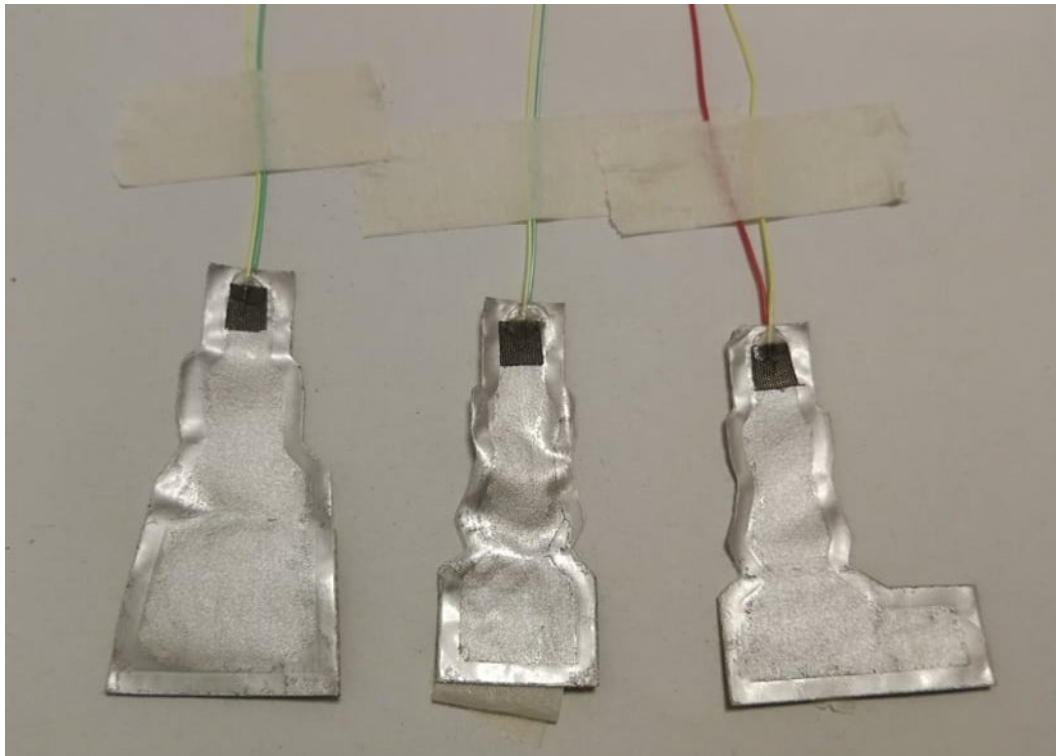


Figure 2.6: Sensors connected to the cables with conductive tape. From left to right: Thumb, Middle and Index finger. The conductive tape attached a cable on each side of the sensor and allowed for contact between the cables and the silver layers on the sensor. To properly fix the connection between cables and sensor, a drop of super glue was added on the top of the conductive tape before the insertion in the silicone layers.

2.6. Silicone layers around sensors

For a higher resistance to stress and a better homogeneity in the stimulation, PVDF sensors are usually inserted in between silicone layers. After some attempts, I decided to make these layers as thin as possible in order to avoid interference with movements and increase the level of comfort of the glove. For this reason, I picked a soft silicone, Ecoflex 30 (Smooth-on, inc.). The spreading of the silicone into a thin layer needed a rolling cylinder to be done precisely and homogeneously. Therefore I cut plexiglass with the laser machine and created a base for silicone spreading and two tracks for the cylinder to roll on at a height of 0.5mm from the base (Fig. 2.7). By pouring the liquid silicone on the base and then using the cylinder to spread it, a very thin layer of silicone was obtained. After the curing time, the sensor was glued to the first layer using the specific silicone glue, and then another layer of silicone was poured on it and spread in the same way, with 0.5mm thickness. After the curing time of this second layer of silicone, we cut these layers around the shape of the sensors, leaving an edge of silicone around them that will be used to sew the sensors on the glove (Fig. 2.8).

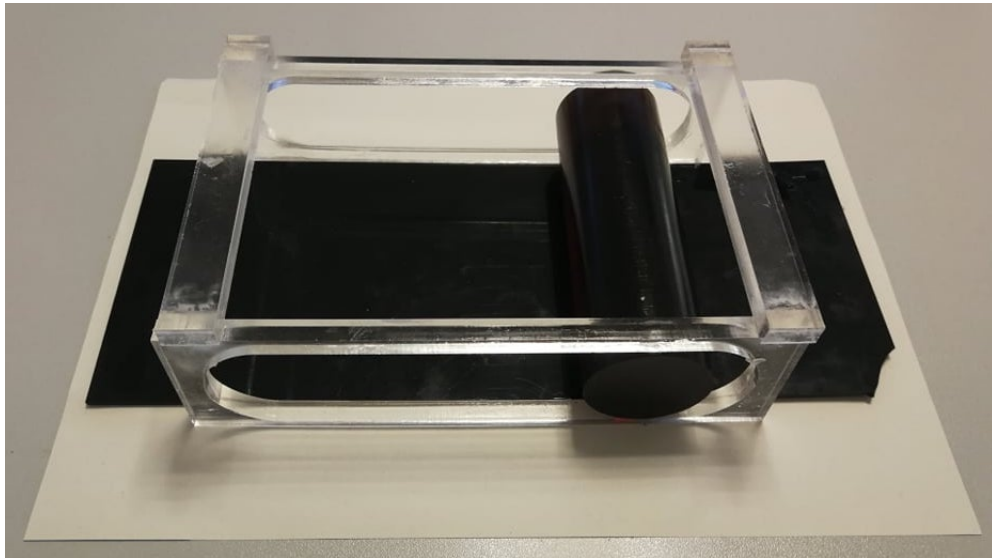


Figure 2.7: Mechanism to spread the silicone into a thin layer. A black thin layer of plexiglass was placed as a base, two thicker transparent pieces of plexiglass were cut with the laser to obtain two tracks for the cylinder to slide inside. The two tracks were then glued at a fixed distance using other two pieces of plexiglass, and the cylinder was inserted inside the tracks. The cylinder rolled from right to left on the plexiglass base, at a height of 0.5mm, spreading the silicone on the black base in a very thin layer.

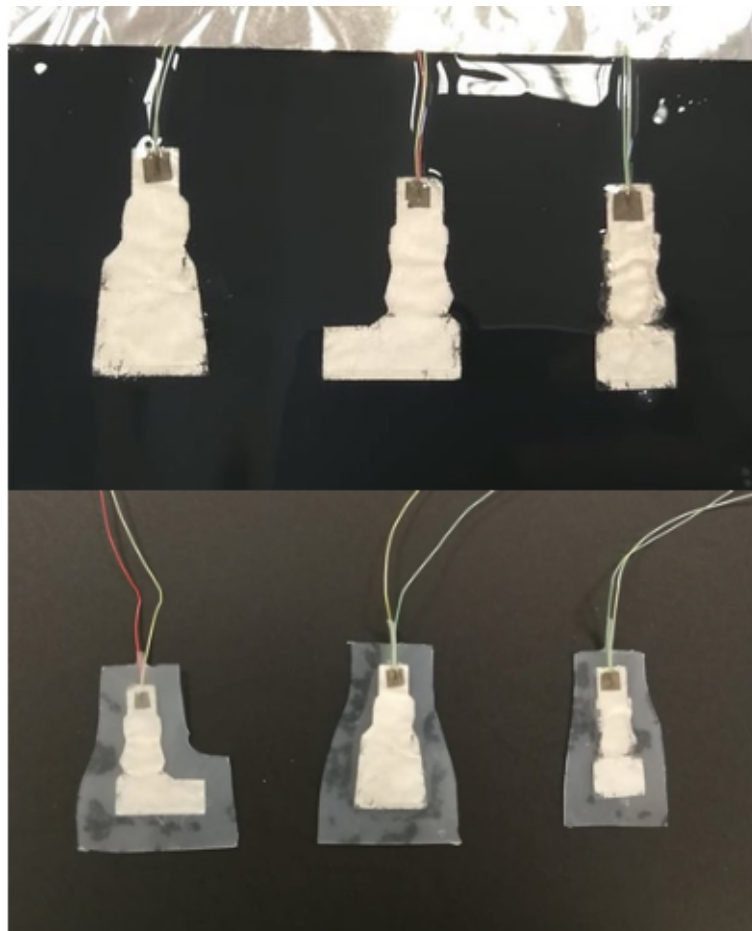


Figure 2.8: On the top: final version of the sensors inserted in between two thin layers of silicone. The sensors were glued on a layer of silicone and then covered with another layer using the mechanism showed in Fig. 2.7. On the bottom: Final shape of the sensors with silicone cut around them. Once the top silicone layer cured, the sensors were cut following their shape leaving a silicone offset to be sewed on the glove.

2.7. Sensors placing on the glove

The sensors shown in Fig. 2.8 were tested with an oscilloscope to check whether they were still working after the fabrication process. Since they were all functioning they were then incorporated on the fingertips of an elastic fabric glove by sewing the silicone edges (Fig. 2.9).



Figure 2.9: DESC glove, three sensors sewed at the fingertips one on the thumb, one on the index and one on the middle finger. The sensors were sewed using the silicone layer offset to the fabric of the glove. They were then covered with another layer of fabric, as shown in 2.10.

The sensors were then covered with another layer of elastic fabric sewed on top of of them in order to create a pocket in which the sensor could be steadily positioned inside. A membrane was also created with the fabric to contain the cables on the fingers. Fig. 2.10 and Fig. 2.11 show the final prototype of the glove with the sensors sewed on it and covered with fabric.

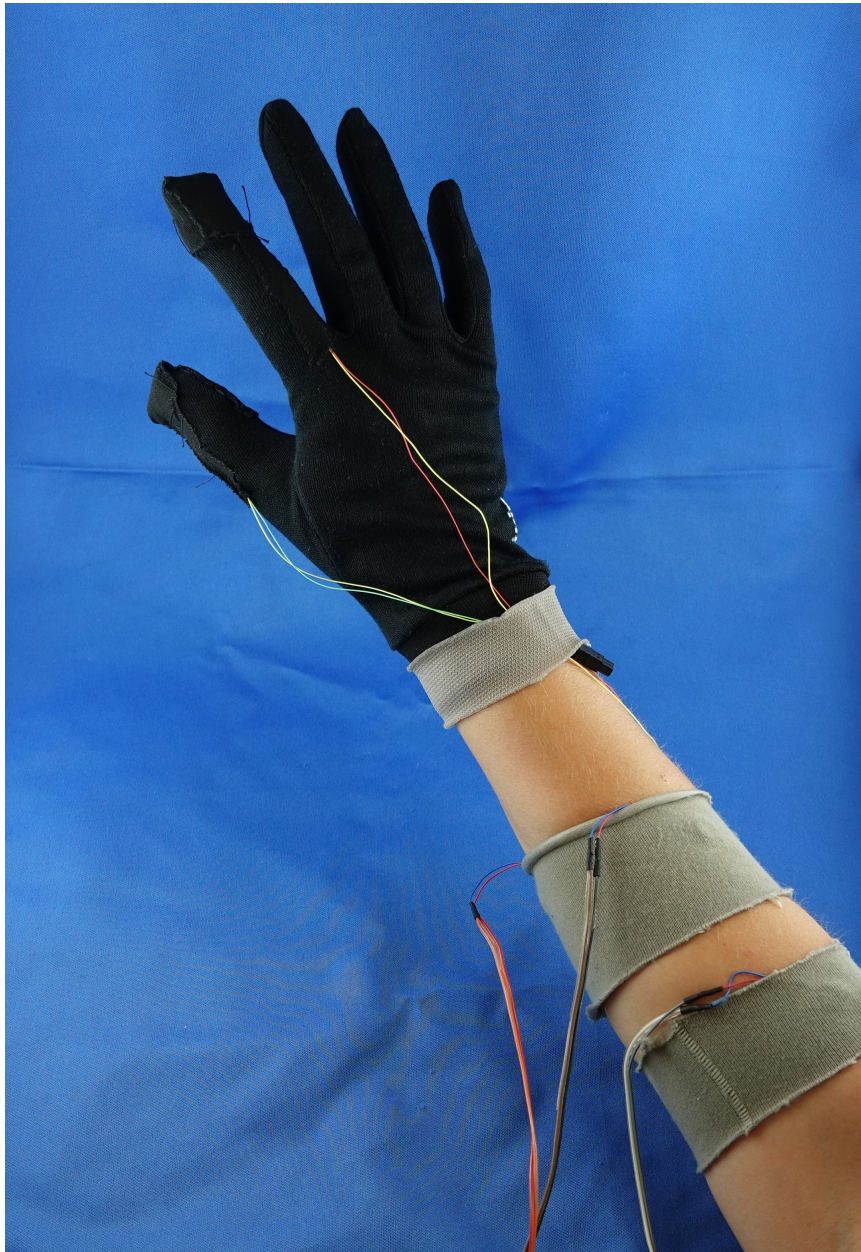


Figure 2.10: *Final prototype of the DESC glove. The sensors are covered with another layer of elastic fabric sewed on them and a membrane is made to contain the cables on the fingers. The actuators that will be placed on the forearm to provide feedback are also shown in the picture.*

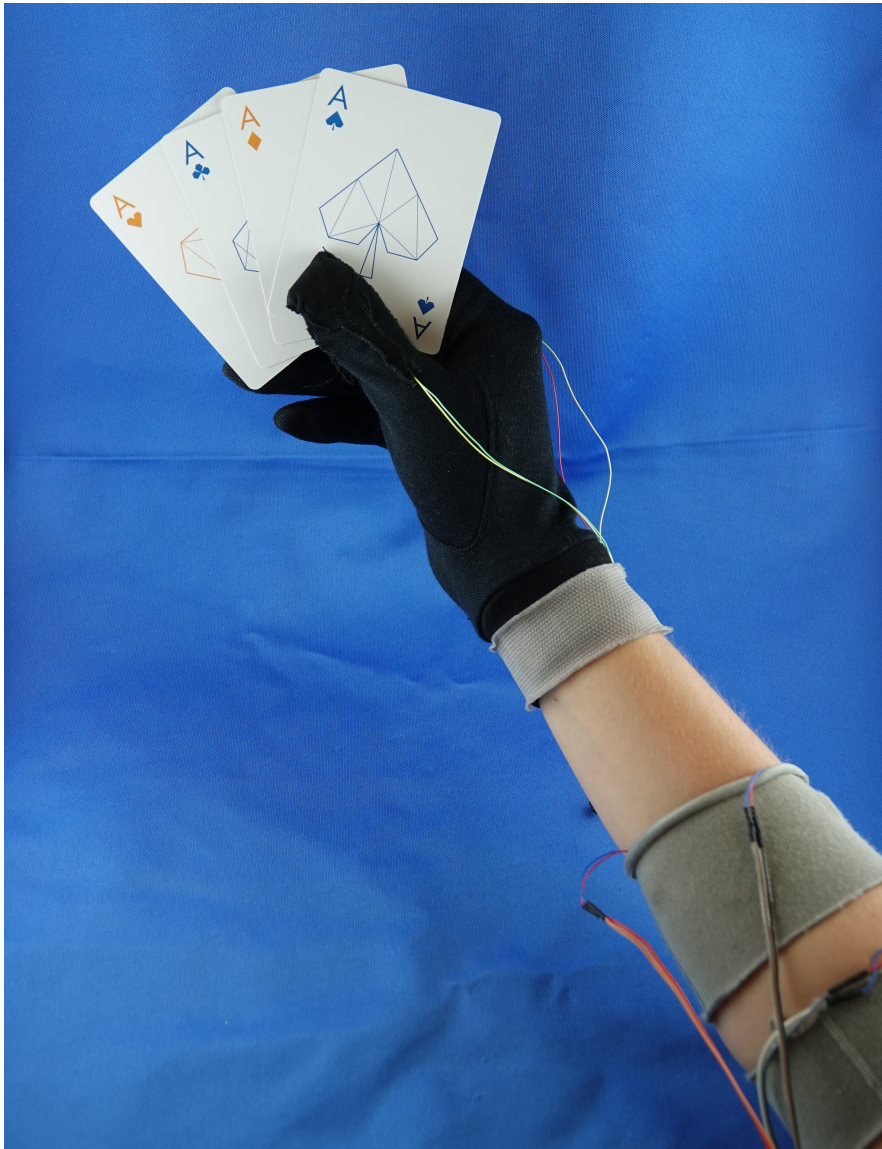


Figure 2.11: Final prototype of the DESC glove while holding playing cards and providing tactile feedback at the forearm.

3

Sensors characterization

In this chapter the setup, the experimental procedure and the analysed results of the characterization of our PVDF sensors are described.

3.1. Set up: 3D moving platform, load cell and sensors

The characterization of sensors was done using a three-dimensional moving platform to apply several forces on the sensor with increasing velocities. I used a SI 25-025 triaxial load cell to precisely measure the force applied during the experiment (Fig. 3.2), connecting it to the end point of the platform through a crown in order to reduce the surface in contact with the sensor and increase the pressure. The load cell was connected to a DAQ for the acquisition of data on the three forces and three torques recorded during the experiment in vectors sampled at $f_s = 1kHz$. These vectors were represented in a graph in real time on a LabView program, and saved in a matrix of six columns. The signal coming from the sensor was acquired simultaneously using a second DAQ with the same sample rate of $f_s = 1kHz$. In order to do this, the sensors were connected to a board, powered at $3.3V$, used to to amplify their signal (Fig 3.1). The analog output of this board was connected to the DAQ which sent it to the LabView program. The amplitude of the signal was plotted in real time in a separate graph and saved in a vector at the end of the experimental session. The sensor was tightened on a support, placed at a fixed distance from the starting position of the moving platform, as seen in Fig. 3.2.

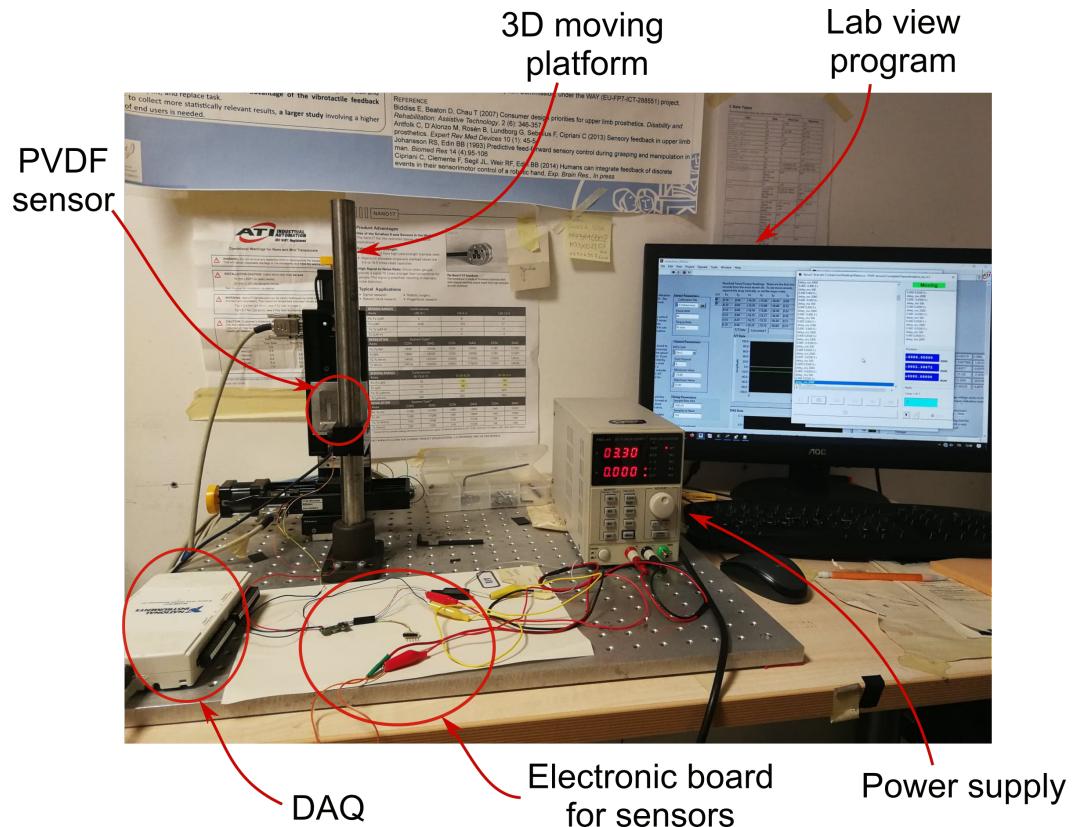


Figure 3.1: Set up for the characterization of the sensors. Three-dimensional moving platform on the left with the triaxial load cell attached to it. DAQ on the bottom left used to acquire the signal from the sensors. The PVDF sensor signal acquisition and amplification board and its power supply are shown in the front. LabView program on the PC on the right used to concurrently acquire the data from the load cell and the sensor and save it into matrices.

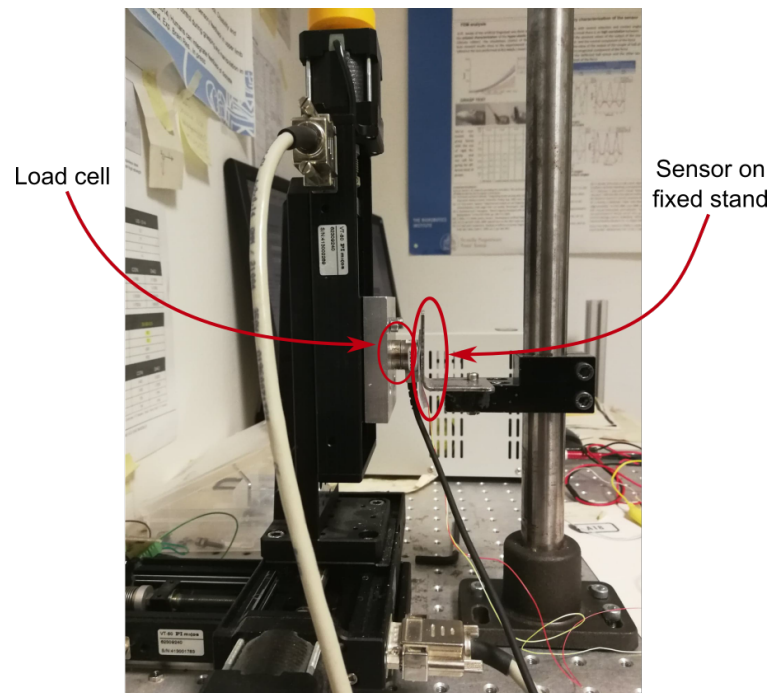


Figure 3.2: 3D Moving platform with attached the triaxial load cell on the left. The fixed support on which the sensor is placed during the whole experiment is positioned in front of the load cell and showed on the right.

3.2. Experimental procedure parameters

In order to characterize the manufactured PVDF sensors we decided to use five different forces, each one applied at five velocities. The platform was moved towards the sensor in order to detect the minimum force that generated a response, which in our case resulted to be $0.2N$. We were interested for our sensors to detect forces above $0.3N$, which is the common sensory threshold to pressure in human hands, and therefore it resulted to be an appropriate starting point. This value of the force corresponded to a displacement of the moving platform of $\Delta x = 0.03mm$ from the imposed initial position towards the sensor, and we increased it to $\Delta x = 0.05$, $\Delta x = 0.07$, $\Delta x = 0.1$ and $\Delta x = 0.15mm$ for the next trials. For each of these displacements five different velocities of the platform were tested: $v = 1, 3, 5, 7, 10mm/s$. The velocities were chosen based on physiology, in fact the maximum velocity to be felt should be $8Hz$ and therefore $8mm/s$ for $1mm$ displacement. For each combination of displacement and velocity, five repetitions were done for data acquisition. During each repetition the load cell was moved by the platform of the desired displacement towards the sensor, held in that position for $2.5s$ and then returned to the initial rest position. A pause of $5s$ was introduced in between separate trials. A script was written to control the moving platform to perform these movements in repetition. The data from the sensors and the load cell was saved at the end of the acquisition session and transferred to MATLAB 2019b (MathWorks, Inc.).

3.3. Sensor characterization results

In order to analyse the behavior of the sensors with respect to variations in displacement and velocity, the analog response of the sensor was plotted in the following characterization plots. The response in voltage was plotted first with respect to velocity five times, one plot for each different force applied by the platform. The sensor response in voltage was then plotted with respect to force five times, one for each value of the velocity at which the force was applied. The values of force represented in the plots are the values of the maximum force reached during each condition, averaged across the five repetitions.

3.3.1. Sensor response behavior

Fig. 3.3 shows an example of the force recorded by the load cell when a displacement of $0.07mm$ was made by the platform and the corresponding sensor response in voltage.

The maximum force applied by the platform was calculated from the load cell signal for each repetition at every velocity and displacement. The sensor response was analysed using as metrics the maximum of the positive peak (for the contact event) and the minimum of the negative peak (for the release event) (Fig. 3.3). The reference value of the sensor's signal in voltage, to which the signal returns in absence of any change in force, was found computing the mode within each trial. The positive peak ($A_{positive}$ in Eq. 3.1) was calculated as the difference between the maximum value of amplitude (A_{max}) reached during the trial and the mode (A_{mode}) of the signal in that trial.

$$A_{positive} = A_{max} - A_{mode} \quad (3.1)$$

The negative peak ($A_{negative}$ in Eq. 3.2) was calculated as the difference between the mode of the signal during trial and the minimum value of amplitude (A_{min}) reached in that trial, and therefore also had a positive value.

$$A_{negative} = A_{mode} - A_{min} \quad (3.2)$$

The mean and the standard deviation of all the values across the five repetitions for each condition of force and velocity were then calculated and used in the characterization plots.

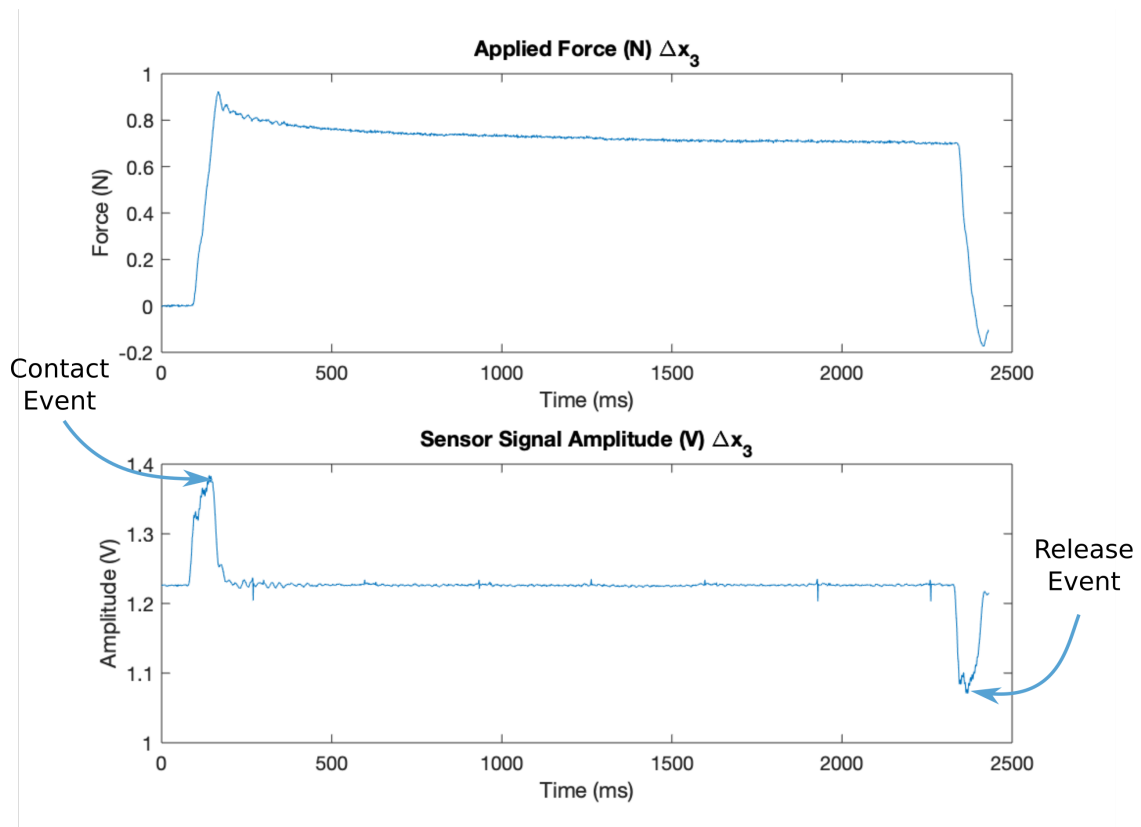


Figure 3.3: Upper plot: Force applied by the 3D platform on the sensor and held for 2.5s. This plot reports an example 0.8N of force, which was generated by a displacement of 0.07mm towards the sensor. Lower Plot: Amplitude of the sensor response to the application of a force of 0.8N. The response is evident: a positive spike reaching 1.4V when the pressure is first applied (contact event) and a negative one of about the same amplitude when the pressure is released (release event).

3.3.2. Sensors response to velocity

The sensors seemed to have a constant response to increasing velocity, as we notice from Fig. 3.4 where the five plots are shown, one for each value of tested force. For too low values of velocity ($v < 3\text{mm/s}$) the amplitude of the response of the sensor is very low, almost imperceptible. After surpassing this velocity the response of the sensor remained constant for increasing velocities, independently of the value of the constant force that was being applied by the platform. The results shown in these plots suggest that the response of our sensor does not depend on the velocity at which the force is applied.

Hysteresis

We can notice that the negative peak of the sensor signal, in response to the pressure release, had a slightly larger amplitude than the positive one, except for the lowest value of the force for which the application and removal of pressure generated almost identical responses. This phenomenon is called hysteresis and is defined as the difference between two separate measurements taken while applying the same level of maximum force, the first is taken while first applying the force and the second taken while removing it. From the plots in Fig. 3.4 we see a variable hysteresis according to the maximum force applied to the sensor, while it remain about constant for different velocities. The lowest hysteresis range emerged from the application of the smallest displacement $\Delta x = 0.03$. The difference in the contact and release sensor response peaks reached a value of 0.05V for $\Delta x = 0.07, 0.1, 0.15\text{mm}$ displacements for velocities higher than $v = 4\text{mm/s}$. In any case, this value is very low compared to the overall response of the sensor and will be therefore neglected for the purpose of our study. Moreover, we are not interested in the amplitude of the response of our sensor, whilst in the instances of the activation peaks.

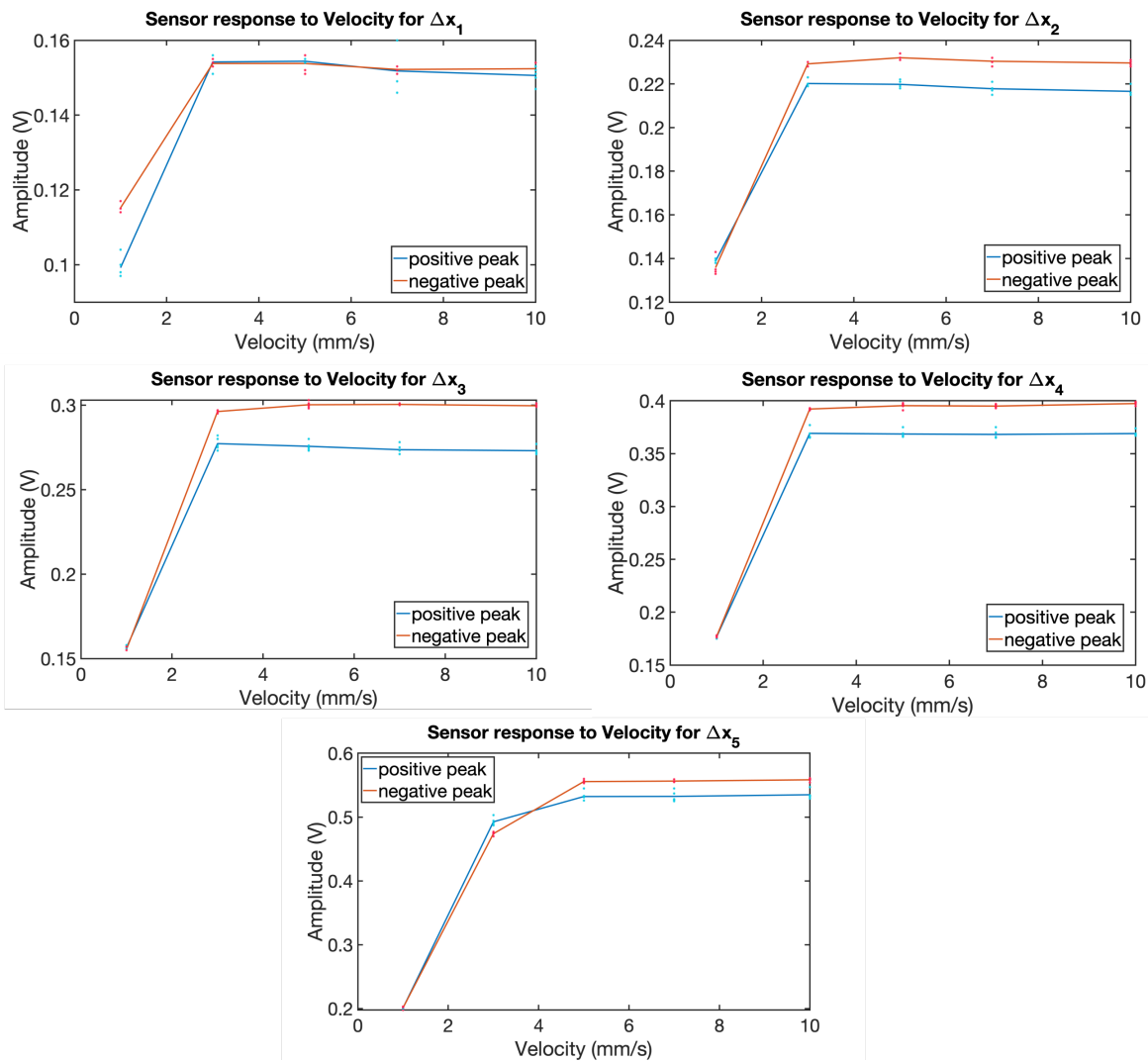


Figure 3.4: Sensors response to the velocity for all five forces applied, increasing values of force going from the top left graph (smallest F) to the bottom one (largest F). The blue lines indicate the response of the sensor when the force was first applied (contact event) while the red lines indicate the response of the sensor when the force was removed (release event). We can notice a difference between these two measurements of maximum $0.05V$, indicating the hysteresis of the sensor.

3.3.3. Sensors response to force

The plots in Fig. 3.5 represent the amplitude of the response of the sensor with respect to increasing force applied at five different velocities. The forces reported on the x-axis are the maximum forces detected by the load cell for each condition, averaged across the five repetitions. Each plot represents a different velocity at which the force was applied during the experiment. The amplitude of the signal from the PVDF sensor seemed to increase almost linearly with the increasing force. The larger was the velocity, the more evident was this linear trend in the sensor response to force. The lower the force and the lower is the voltage response from the sensor. For example for the lowest force applied (about $0.3N$), the sensor response is only around $0.1V$, which is still distinguishable from noise. We notice that the highest sensor response, $0.6V$, corresponds to the highest value of the force applied, of about $2.3N$.

Hysteresis

The hysteresis was also evident in the analysis of the sensor response to force evaluated at different velocities reported in Fig. 3.5. We notice the same behavior as the one found in the plots in Fig. 3.4. For the lowest value of velocity $v = 1mm/s$ the sensor responses to application and removal of pressure have the same values, as we can see from the top left graph in Fig. 3.5 in which the red and blue line are overlapping. For higher values of velocity, $v \geq 3mm/s$, the hysteresis phenomenon is

clearly visible with the red line representing the release of the force laying above the blue line in which the force was firstly applied. The hysteresis remains almost constant for increasing forces, being at its minimum for the lowest values of force of $0.3N$. In any case, the hysteresis resulted to be very low compared to the overall response of the sensor and will be therefore neglected for the purpose of our study, as mentioned in the section above.

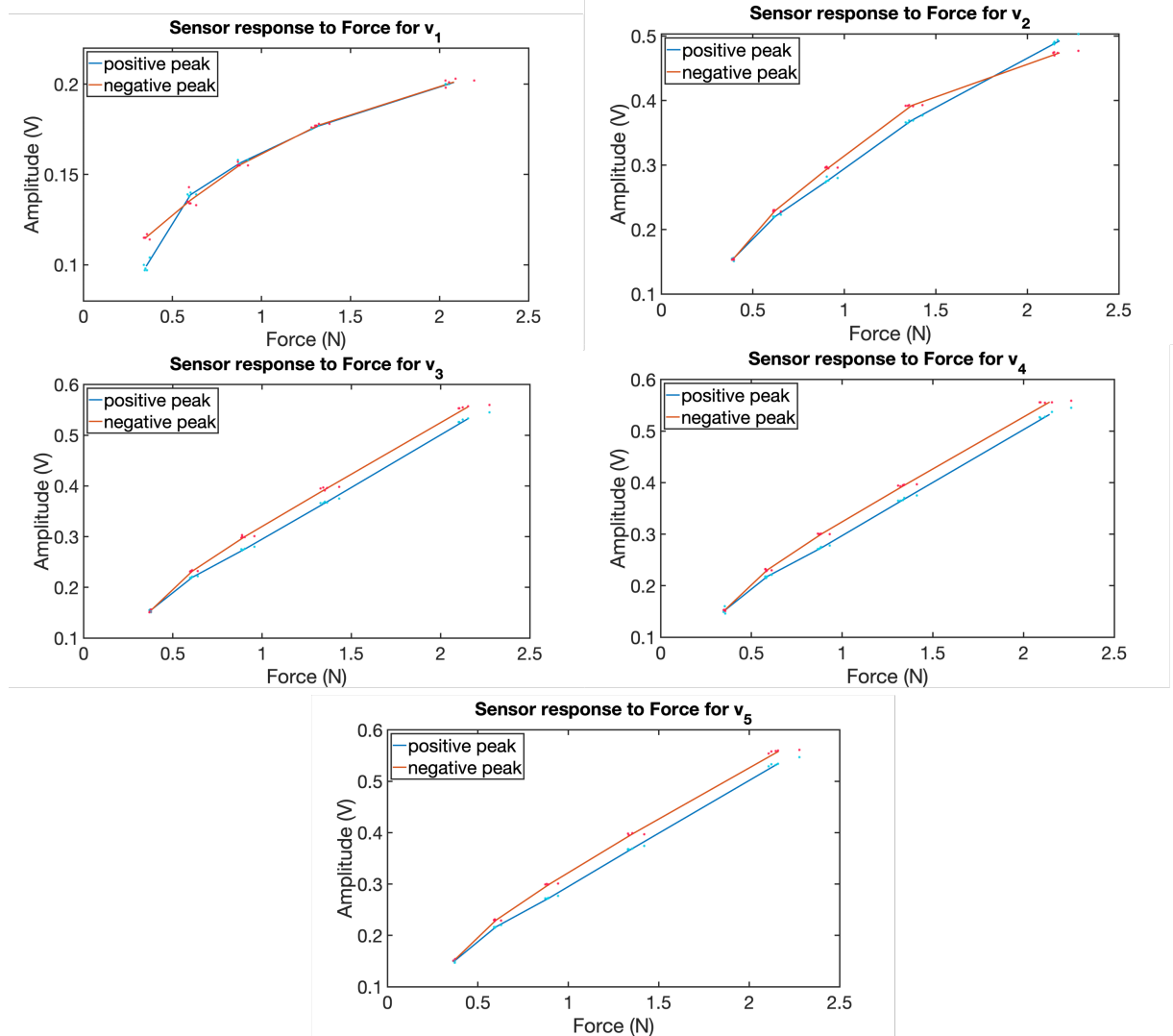


Figure 3.5: Sensors response to the force applied at all five velocities, increasing values of velocity going from the top left graph (smallest v) to the bottom one (largest v). The blue lines indicate the response of the sensor when the force was first applied (contact event) while the red lines indicate the response of the sensor when the force was removed (release event). We can notice a difference between these two measurements indicating the hysteresis of the sensor.

3.3.4. Sensor response delay

The results shown in the previous sections led to the conclusion that the PVDF sensors we produced are appropriate for the detection of tactile stimuli at the fingertips. However, another important aspect to be considered when fabricating sensor is the reaction time to the stimuli.

After setting a Limit of Detection (LoD) shown in Eq. 3.3, the activation points of the load cell force and the sensor signal were compared in time to detect the delay between the two. The activation point of the load cell was saved as the index of the force vector element that surpassed the force LoD the first time. The activation point of the sensor signal response was saved as the index of the signal vector element that surpassed the sensor LoD for the first time. The delay in time between the two activation points was found for each trial by subtracting the activation point of the sensor to one of the force, and

later averaged across the five repetitions performed for each condition of force and velocity.

$$LoD = Mean + 10\sigma \quad (3.3)$$

Where σ is the standard deviation of the signal in the time window we are considering (one repetition) which is multiplied by ten in order to increase the accuracy of the detection. In this way we reduced the probability of detecting a disturbance of the noisy signal as an activation. The *Mean* and the standard deviation of the sensor signal for each trial (in the time window we are considering) were previously calculated.

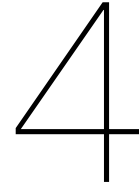
The delay in time between the application of the force, detected by the signal coming from the load cell attached to the moving platform, and the sensor response resulted to be negligible. In fact the values of these delays are so small, or in some cases even negative, that seemed to be generated by the processing time for the data coming from the DAQs or possible delays in data acquisition and can be neglected. Therefore we can conclude that our PVDF sensors don't have any noticeable delays in the activation following a stimulus.

3.4. Feasibility for DESC feedback

The manufactured sensors responded with a single spike to the application or removal of force, suggesting the dependency of the sensor response to the derivative of the force instead of the force applied. We are particularly interested in this aspect of the PVDF sensors, as in human brain tactile events are encoded as discrete mechanical events that define the beginning and the end of action phases related to subgoals. Therefore, sensitive to the rate of change in acceleration, our sensors generate an instantaneous response whenever a force is applied and an opposite response whenever the force is released. This resembles what happens in physiology and justifies the use of these type of sensors for DESC type vibrotactile feedback in rehabilitation. In fact, the principle behind DESC policy (as explained in Section 1.11) is exactly the discrete activation synchronously with contact events.

Moreover, the sensors proved to have a very low reaction time, which resulted to be negligible, and can therefore provide a feedback almost in real time. Of course we need to consider the delays in the processing time of the electronic board that will be amplifying the sensors signal and the one that will be using it to control the vibration motors. These can be compared to the delays occurring in our body for the communication of sensory information to the CNS through afferent pathways. The hysteresis of the PVDF sensors proved to be low and can be therefore neglected for the purpose of our study, as we are not interested to the amount of force applied but instead to the moments of application and release of pressure.

The sensors we produced are very lightweight and appear in a very thin shape which easily adjusts to the hand. This is very important as we want to keep high the level of comfort of the glove and reduce any possible movement hindrance given by the device.



Design of the Printed Circuit Board

This chapter describes the process for prototyping and fabricating the electronic board for the sensors signal acquisition.

4.1. Electronic board prerequisites

In order to process the analog signals coming from the PVDF sensors and utilize them to provide a vibrotactile feedback, I designed a printed circuit board (PCB). The board needed to integrate the following functions:

- Acquire the analog signals from five piezoelectric sensors (five input channels)
- Amplify the analog signals and shift them above zero
- Output pins for amplified analog signals for characterization and sensors testing (five output channels)
- Digitalize the PVDF signals
- External communication of digital outputs through a serial port

4.2. Acquisition and amplification circuits

A moxex connector with five pins was placed on the board to acquire the signal coming from maximum 5 sensors on the glove. Another moxex connector with three pins was used for the battery, with a power supply of 3.3V. The analog signal amplification circuit is reported in Fig. 4.1. I used a Dual 2.9μA, Operational Amplifier (producer code OPA2379AIDCNT, Texas Instruments, USA) operating in a range from 1.8 to 5.5V.

A voltage of 1.2V, generated by a voltage regulator, is also summed to the analog signal in order to shift it above the 0V line. In fact the signal from the PVDF has a positive spike when the pressure is applied and a negative one when the pressure is released. A completely positive signal is needed for the digitalization. The outputs from five of these amplification circuits (from PIEZO1 to PIEZO5) are then sent to the microcontroller in order to be digitalized.

The voltage output of the amplification chain is calculated as reported in Eq. 4.1. In this equation V_{PIEZO} is the amplified analog signal from the sensor, at the end of the amplification chain (PIEZO1 in Fig. 4.1), to be sent to the microcontroller to be digitalized. V_{IN} is the voltage difference between the two electrodes sheets in the PVDF (PVDF31 and PVDF32 in Fig. 4.1). R_1 and R_2 are the two resistors inserted between the operational amplifiers.

$$V_{PIEZO} = 1.2 + V_{IN} \left(1 + \frac{R_1}{R_2}\right) = 1.2 + V_{IN} \left(1 + \frac{100}{47}\right) = 1.2 + 3.12V_{IN} \quad (4.1)$$

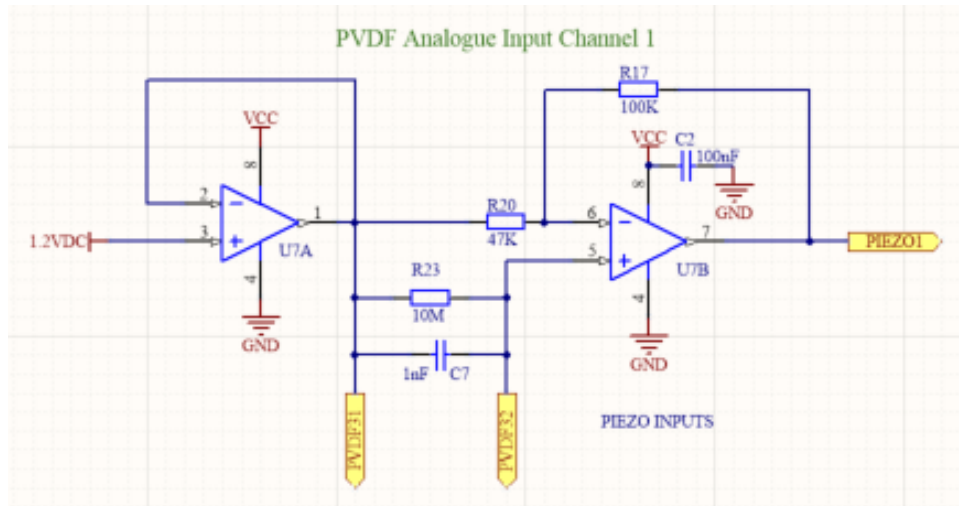


Figure 4.1: Schematic of the amplification circuit. The inputs from the two layers of the PVDF sensor are represented by the two yellow arrows at the bottom of the schematic (PVDF31 and PVDF32). The voltage difference between these two layers is amplified using two operational amplifiers U7A and U7B. A bypass capacitor (C2) of 100nF is added between the power and ground. The output signal of this circuit is the amplified PVDF sensor signal PIEZO1. Five of these circuits are present in the complete schematic of Board 1.

4.3. PIC Microcontroller

The microcontroller utilized in this board is PIC24F16KL401 (Microchip Technology, USA), which is a 16bit Flash microcontroller with 20 pins, powered at 3.3V. This component needed to be programmed in order convert the PVDF amplified inputs into digital outputs using an ADC. In order to do this, a firmware was written on MPLab X IDE (Microchip Technology, USA) and uploaded on the microcontroller using a Pikit3 programming device. The firmware will be described in detail in Chapter 5.

The external communication was planned through the UART register, using a serial port. The sent information will be the input of the board controlling the vibration actuators.

The schematic of the microcontroller with all the connected pins is shown in Fig. 4.2.

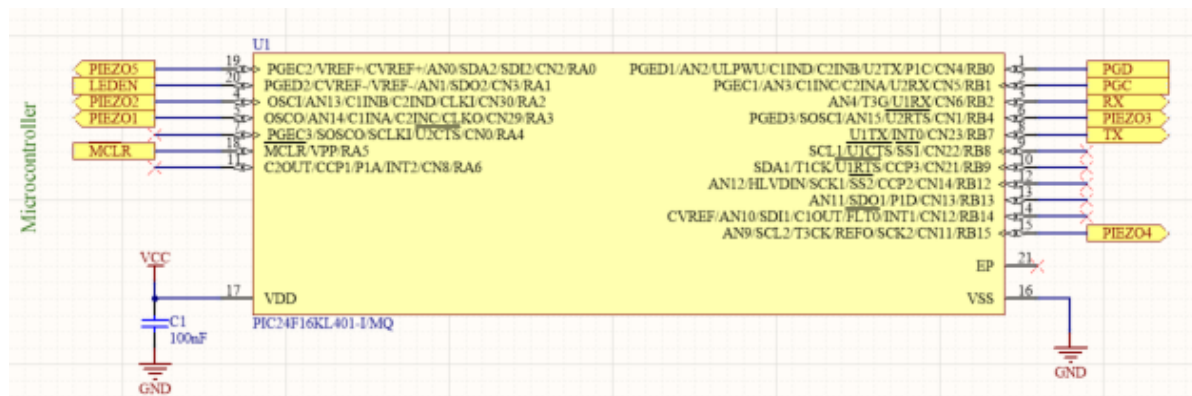


Figure 4.2: Schematic of the microcontroller with all the connected pins. The five amplified PVDF signals are connected to the analog input ports of the microcontroller. The serial port pins for transmitting (TX) and receiving (RX) are also connected to the UART1 ports. A bypass capacitor (C1) of 100nF is included between the power and the ground.

4.4. Final design of the board

The final structure of the board is represented in Fig. 4.3 (two dimensional view) and Fig. 4.4 (three dimensional view).

4.5. List of components

Designator	Description	Quantity
C1, C2, C3, C4, C5, C6, C7, C8, C9, C10, C11, C12, C13, C14, C15, C16	Capacitors $C = 1\mu F$, $C = 100nF$ $C = 1nF$	16
R1, R2, R3, R17, R18, R19, R20, R21, R22, R23, R24, R25, R26, R27, R28, R29, R30, R31, R32	Semiconductor Resistors $R = 100\omega$, $R = 2, 1K\omega$, $R = 10K\omega$, $R = 18K\omega$, $R = 18K\omega$, $R = 100K\omega$, $R = 10M\omega$	19
D1	LED	1
IC1	Voltage regulator 1.2V	1
J1, J2, J4, J5	Molex connectors 2, 3, 5 and 10 pins	4
S1	Switch Button	1
U1	Flash Microcontroller 16bits 3.3V PIC24F16KL401	1
U2	LED Driver and Charge Pump 2.7V to 5.5V LTC3212EDDB#TRMPBF	1
U7, U8, U9, U10, U11	Operational Amplifiers Dual $1.9\mu A$ OPA2379AIDCNT	5

Table 4.1: Table of components used for the PCB. The designators reported in the first column are the ones reported in the schematics and the PCB design in white (Fig. 4.4).

4.6. Hardware block diagram

The block scheme shown in Fig. 4.5 is a complete representation of the hardware used for the functioning of the glove. The touch detection signals coming from the PVDF sensors are amplified and decoded in the PCB that I designed (Board 1), which was thoroughly described in the previous sections. The elaborated digital signal, output of Board 1, is sent to Board 2 in order to control the vibration motors that will be placed on the forearm. The second board was taken from the laboratory and designed by Christian Cipriani in a previous work.

The microcontrollers in the two boards had to be programmed to complete the necessary tasks and the firmware will be described in Chapter 5.

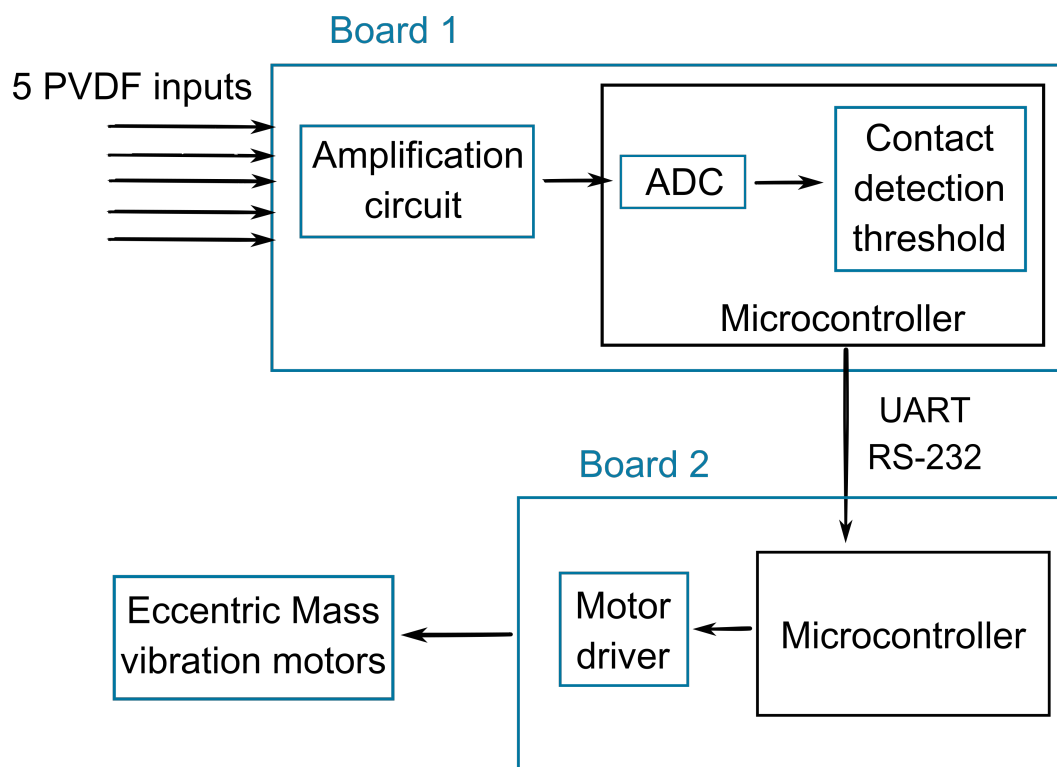


Figure 4.5: Hardware complete block scheme. The inputs from the five PVDF sensors (two inputs for each one) are acquired by the first board and amplified. They are then sent to the microcontroller where they get converted into digital signals and re-elaborated according to the serial communication protocol. Through a serial port the information is sent to the second board which uses this information to control the vibration motors on the forearm.

4.7. Board 1 manufacturing

The electronic components coming from Mouser, USA should have been soldered on the correct pins on the printed circuit board produced by BetaLayout, USA.

Due to problems related to the corona virus situation, the producers could not deliver the material on time. These delays were also related to other technical problems internal to the Institute of Biorobotics. After more than one month of wait, I decided to use a previous version of the electronic board, present in the lab, for the purpose of testing the DESC glove. This board could acquire only the signal coming from one sensor at a time, having one channel for acquisition and amplification. The board also does not have any molex connectors, notably reducing its dimensions, as it was supposed to be included inside the fingers of a prosthesis. A picture of this board is shown in Fig. 5.1.

I used two of these boards one for the sensor on the thumb and one for the index. I soldered the cables and the other missing components to these new boards as visible from Fig. 5.1.

For the purpose of these preliminary study, we decided to neglect the middle finger sensor, as it is the least relevant during a pick and lift task that we will be analysing.

Modifications in the firmware of this older board, moving it closer to the firmware I initially programmed for the board with five channels, were necessary to transmit the correct signal to Board 2 to activate the motors. I included in the firmware the parts already planned for my board, described in Chapter 5, that allow to communicate with the second board through a UART RS-232 protocol.

5

Firmware description

In this chapter, a description of the firmware used to program the microcontrollers is present. The board for the acquisition of the signals from the PVDF sensors (Board 1) and the one that uses these signals to control the vibration actuators (Board 2) communicate through a USART 3.3V serial port. They are both powered at 3.3V and can communicate using two bytes.

5.1. Board 1: Sensors signal acquisition

In this section I will be describing the structure of the firmware for programming the microcontroller in the PVDF sensors acquisition board. A block scheme of the firmware used to control this board is shown in Fig. 5.2. Whenever the hardware is initialized (turned on) a led will be lightened on the board to indicate its functioning. At this point, the microcontroller begins to acquire the analog signals from the PVDF sensors connected to the board, up to five sensors can be connected at the same time.

5.1.1. Analog to digital conversion

The analog to digital converter (ADC) present in the microcontroller (PIC24F16KL401) is a 10 bits ADC meaning that it is able to transform the analog signal into a digital one composed by $2^{10} = 1024$ intervals. The resolution (also called LSB) of the ADC conversion is calculated in Eq. 5.1, taking into account that our input signal goes from 0 to 3.3V. The maximum error ($Error_{MAX}$) that could occur in the converted digital signal corresponds to half of the resolution value (Eq. 5.2).

$$LSB = (3.3 - 0)/2^{(n_{bits})} = 3.3/2^{10} = 0.00322V = 3.22mV \quad (5.1)$$

$$Error_{MAX} = \frac{LSB}{2} = 1.61mV \quad (5.2)$$

These values are very low and acceptable for our purpose as, during the sensors characterization, the amplitude of the signal spikes emerged to be in the range of 100 – 600mV. The ADC sampling frequency is $f_s = 1kHz$ and I decided a time window of $wLength = 10samples$ as a capacity of the buffer to be filled when filtering the data. Since a sample from each channel is acquired every $ts = 1ms$, the buffer for each one of the channels is filled every t_{buffer} , calculated in Eq. 5.3, depending on the number of sensors we will be connecting to the board, i.e. $n_{sensors} = 3$.

$$t_{buffer} = n_{sensors} * ts * wLength = n_{sensors} * 10ms = 30ms \quad (5.3)$$

The ADC present in our board allows to select multiple channels to be scanned and converted to digital signals in series. The five analog inputs were therefore selected for serial input scanning. The number of input channels to be scanned and converted can be selected as a global variable at the beginning of the firmware ($n_{sensors}$), to indicate how many sensors are being used in the glove. For the purpose of this study we will be using maximum 3 sensors but the firmware was programmed to be later modified and used for different applications. The ADC subsequently scans each of these channels and converts the signal contained in the previously defined time window, saving the obtained digital output in a buffer. The conversion result is then low pass filtered to avoid interference and further saved in a new buffer variable. This variable will be analysed through a specific function to detect touch events.

5.1.2. Touch event detection

Whenever the signal is higher than a threshold, set to $iThresholdT = 1.32V$, a counter for the contact events is increased in the time window we are considering ($iCountEventT$). The same happens for the release events, detected when the signal becomes lower than a threshold, set to $iThresholdR = 1.00V$.

In case the counter for contact events is as large as the considered window length, i.e. a touch event is detected for the whole time window, the digital output corresponding to the sensor considered will be set to 1. On the contrary, in case the counter for release events ($iCountEventR$) reaches the value of the window length, the digital output corresponding to the correct sensor will be lowered to 0. Only in the instant of change from 0 to 1 or viceversa of the digital output `TouchEvent`, the contact events variables `ContactEvent` and `ReleaseEvent` are activated. These variables become equal to 1 in the moments in which a DESC feedback should be sent. `ContactEvent` is set to 1 in case there is a change from 0 to 1 of the variable `TouchEvent`, and `ReleaseEvent` is set to 1 in case `TouchEvent` goes from 1 to 0. The code of the function to detect touch events, written in C language, is reported below. The `iPVDDFFilteredBuffer` variable is the result of the ADC conversion, having on each column a vector for each sensor (indicated by the index `p3`), of length equal to the considered time window. `TouchEvent` is the vector of digital variables, one for each sensor and composed only by one bit, it is equal to 1 for as long as the pressure is applied at the sensor and it returns to 0 whenever the pressure is released. The contact event variables instead are equal to 1 only in the exact moment in which the pressure is applied or released and are reset to 0 right after sending the information regarding contact to Board 2.

```
void eventDetection(int p3){
int i;
for (i=0; i<windowLenght; i++){
if (iPVDDFFilteredBuffer[i,p3] >= iThresholdT){
iCountEventT[p3]++;
}
else if (iPVDDFFilteredBuffer[i,p3] <= iThresholdR){
iCountEventR[p3]++;
}
}
if (iCountEventT[p3] == windowLenght) {
if(TouchEvent[p3] == 0){
TouchEvent[p3] = 1;
ContactEvent[p3] = 1;
}
}
else if (iCountEventR == windowLenght){
if (TouchEvent[p3] == 1){
TouchEvent[p3] = 0;
ReleaseEvent[p3] = 1;
} TouchEvent[p3] = 0;
}
if (icheckEvent[p3] == maxEvent){
icheckEvent[p3] = 0;
iShiftBuffer[p3] = 0;
iCountEventT[p3] = 0;
iCountEventR[p3] = 0;
}
else{
icheckEvent[p3]++;
iShiftBuffer[p3] = iShiftBuffer[p3] + windowLenght;
}
}
```

5.1.3. Serial port communication

The variables `ContactEvent` and `ReleaseEvent` contain information on the application and the release of pressure on each of the sensors connected to Board 1. This information needs to be communicated to Board 2 in order to activate the vibration actuators whenever the pressure is applied and when the pressure is released. The communication between the two boards will be done using a UART RS-232 serial port and sending two bytes according to Board 2 protocol, as explained in the next section. The UART transmission protocol is set in the microcontroller of Board1 using UART1TX, the transmission pin for the asynchronous serial port. I used a 8bit asynchronous transmission mode with no parity. The auto baud function was disabled and I used maximum baud rate in fast speed mode. Being the frequency $f = 250kHz$, the formula to calculate the baud rate is shown in Eq. 5.4.

$$BaudRate = \frac{f}{4 * (U1BRG + 1)} \quad (5.4)$$

Where $U1BRG$ is a register to be set during UART initialization. Since we want a baud rate higher than $BR = 57600$, which is the one necessary to communicate with Board2, I used the inverse formula of Eq. 5.4 to calculate the value for $U1BRG$ (Eq. 5.5).

$$U1BRG = \frac{f}{4 * BaudRate} - 1 = \frac{250000}{4 * 57600} - 1 \approx 0 \quad (5.5)$$

By setting $U1BRG = 0$, the baud rate becomes 62500 as shown in Eq. 5.6.

$$BaudRate = \frac{f}{4 * (U1BRG + 1)} = \frac{250000}{4} = 62500 \quad (5.6)$$

Following the changes given by the delays in the production of the board I designed, this part of serial communication was integrated in the firmware of the boards that singularly acquired each sensor's signal. I used two identical boards, one to detect the sense of touch on the thumb and one for the index finger, represented in Fig. 5.1. The firmware on each of the two boards was the same as described in the previous section, except for the index `p3` which referred to the sensor number and was not necessary anymore. Each board acquired and converted the signal coming from one sensor and sent it to the PC through a serial port. The first acquisition board (thumb) sent commands for motor 1 while the second acquisition board (index) sent command for motor 2.

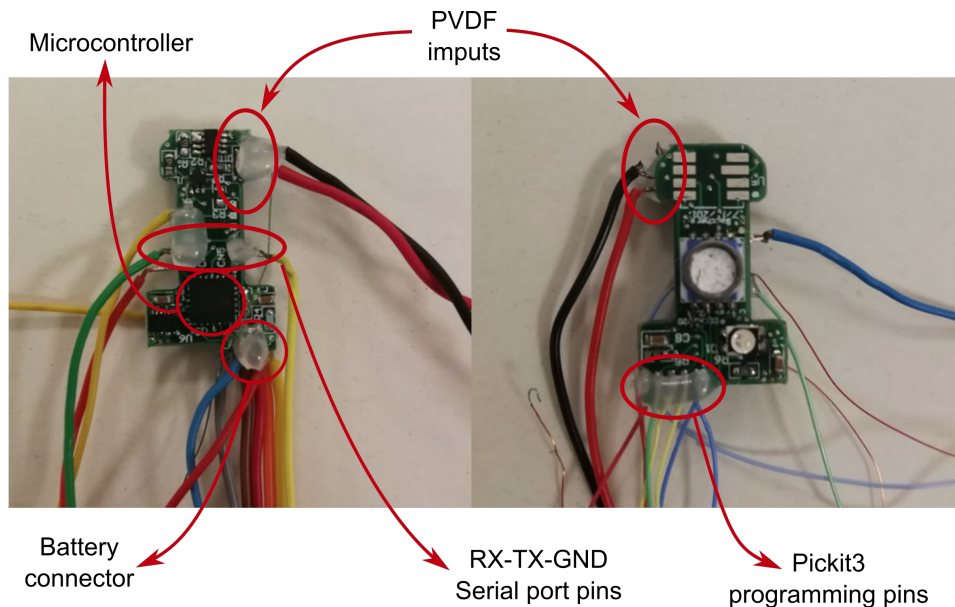


Figure 5.1: On the left: thumb sensor acquisition board (Top view). On the right: index sensor acquisition board (Bottom view). On the top layer there are the connection pins for the sensor inputs, the pins for the serial port communication (TX, RX and ground), the battery connectors and the microcontroller. On the bottom layer there are the pins for programming the microcontroller using a pickit3 device.

Since I used two boards for replacing Board 1, the information from the serial port of thumb and index finger boards had to be transmitted to a computer, elaborated in a Processing 3.5.1 program which read 2 bytes from the serial ports and transmitted the information (as described in section 5.2) for the motors activation to another serial port connected to Board 2. Board 1 communicates with a baud rate of 62500 and the information needs to be sent to Board 2 with a baud rate of 57600, this can be done in Processing by setting the baud rate for each serial port when opening it for reading or writing.

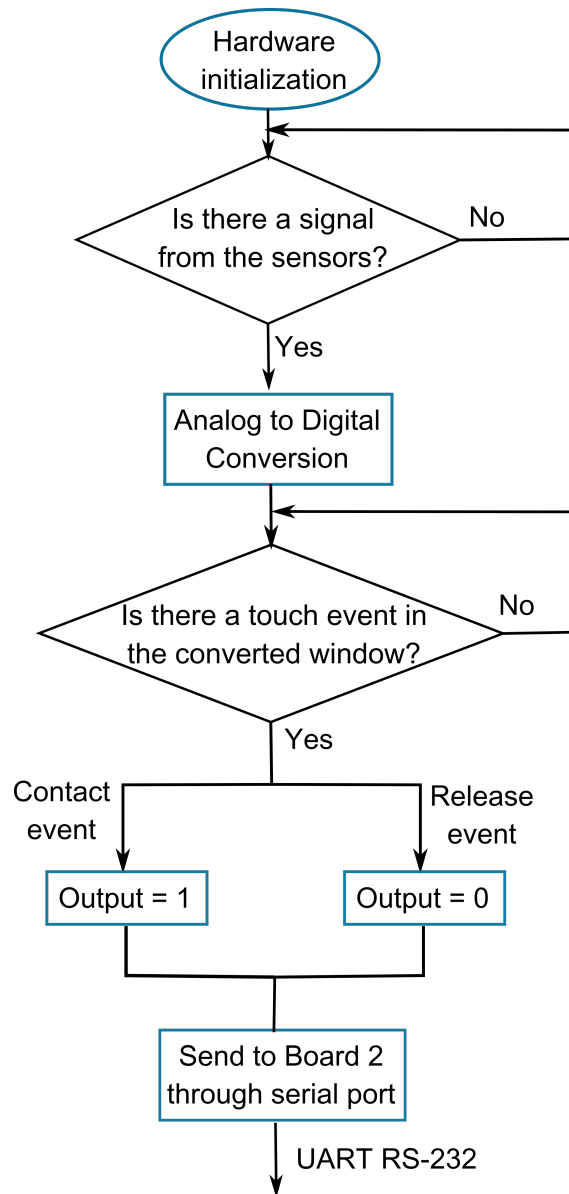


Figure 5.2: Board 1 firmware block scheme. After the initialization of the hardware, the microcontroller checks if there is any signal from the analog input ports corresponding to the amplified sensor signals. In case a signal is detected on an input channel, the microcontroller uses the ADC to convert this signal into a digital output. A function to detect a touch events scans the digital signal to check if it surpasses a threshold. In case a touch event is detected, the information is prepared for being sent to the second board through the UART RS-232 communication port.

5.2. Board 2: Vibration Actuators

In this section I will be describing the firmware used to control the eccentric mass vibration actuators using the signal coming from the sensors. Board 2 is composed by a microcontroller PIC18F4431 (Microchip, USA) and five motor drivers, each one capable of controlling five eccentric mass motors.

The board could control up to 15 motors which is more than enough for us as we need one motor for each sensor, therefore maximum five actuators placed on the forearm. The board can be powered from 3 to 5V and we will be using 3.3V as for Board 1. Board 2 is shown in Fig. 5.3.

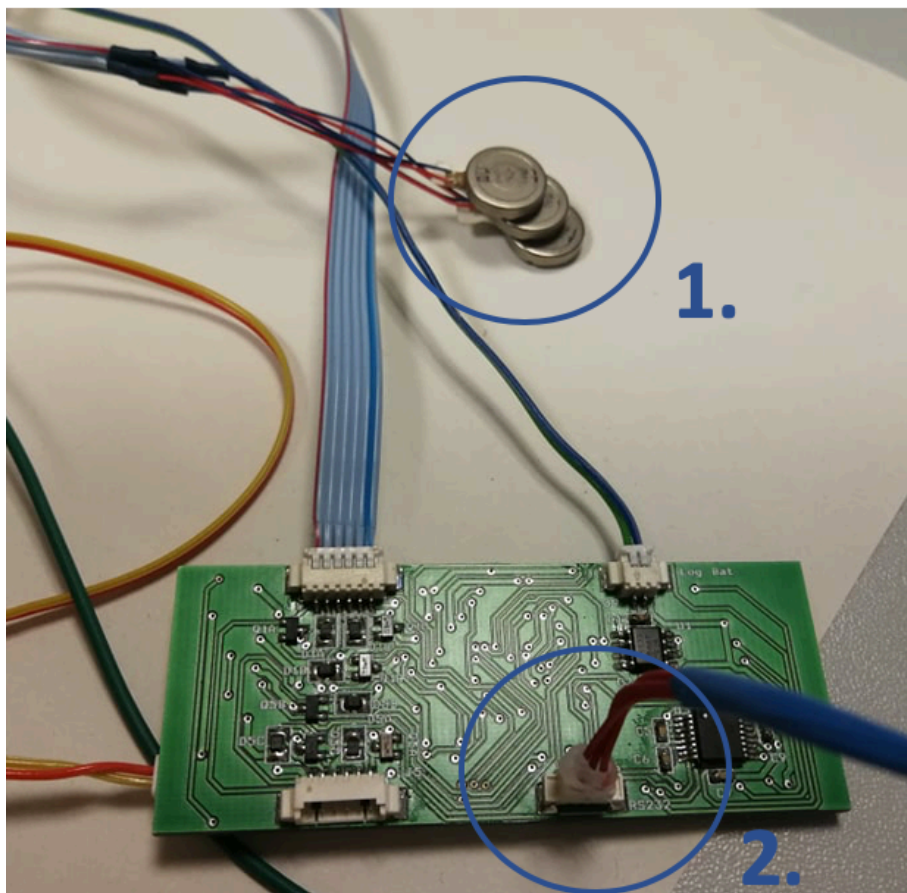


Figure 5.3: Board 2 used to control the eccentric-mass vibration motors (1). The information regarding the contact events is received from this board through a serial port communication protocol having three pins TX, RX and ground (2).

The receiving serial communication protocol was programmed to read 2 bytes (as shown in Fig. 5.4), memorize them in a buffer and use them to satisfy the requests of activation of the corresponding motors. The first byte consists in the 4 bits on the left (most significant bits MSB) indicating the number of motor to be activated (from 1 to 15), and the 4 bits on the right (least significant bits LSB) indicating the duty cycle at which the motor should be vibrating. We decided to use a duty cycle of $DC = 80\%$ constant for every motor and equal for contact and release events.

The second byte carries information of the duration of the vibration, for a total of $2^8 = 256$ possible time intervals spaced out of $10ms$, and the highest value corresponds to an infinite time of vibration. We decided to set the duration of our vibration to $t_{vibr} = 100ms$ for all motors. We want to send a discrete vibration stimulus whenever a contact or release event occurs by activating the motors whenever the pressure is applied or released, according to the DESC policy.

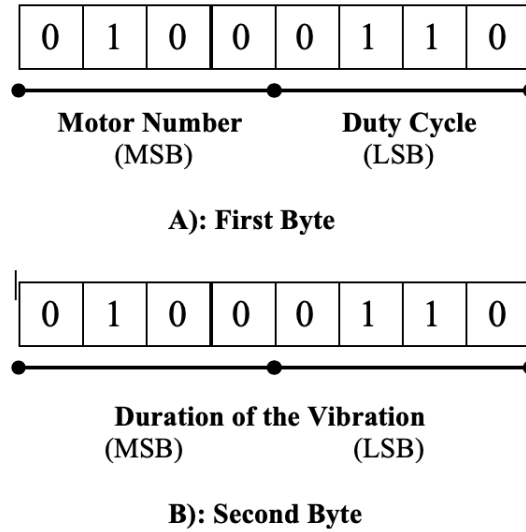


Figure 5.4: Receiving data codification. A) represents the first byte to be sent composed by the number of the motor to be activated and the percentage of duty cycle of the vibration. B) represents the second byte, containing information on the duration of the vibration. MSB is the most significant bit always placed on the left and LSB is the least significant bit placed on the right.

The data is sent from Board 1 to Board 2 using a hexadecimal codification and the codes for the information we are interested in are shown in Table 5.1.

Data	Decimal	Hexadecimal codification (Binary)
Motors	1	1 (0001)
	2	2 (0010)
Duty Cycle	Less than 50% - Turn off	0 (0000)
	80%	9 (1001)
Duration	100 ms	0A (00001010)

Table 5.1: The hexadecimal codification for the controls that I used to program the firmware for the glove. The data has to be sent in hexadecimal to Board 2. Two bytes in total are sent: motor and duty cycle in the first byte and duration of the vibration in the second byte, as described in Fig. 5.4.



Experiments on healthy subjects

In this chapter I will be describing the setup and experimental procedure used for testing the DESC glove. The tests were performed on healthy patients while synchronously performing a cognitive task in order to evaluate the efficacy of the augmented feedback on motor performance. Further trials on stroke survivors will be performed next year as soon as it will be possible.

6.1. Participants

The experiment was performed by 10 right-handed healthy participants, of age between 24 and 33 years old, six females. They were all non-remunerated volunteers working in the Institute of Biorobotics of Scuola Superiore Sant'Anna. They agreed to the terms of the experiment and the treatment of data by signing a study information sheet and an informed consent (both reported in Appendix A). The study was conducted according to the Declaration of Helsinki and was approved by the Ethical Committee of Scuola Superiore Sant'Anna (Approval Number 2/2017).

6.2. Setup for the experiment

The setup for the experimentation was built in the artificial hands laboratory of Scuola Superiore Sant'Anna. It consisted in a first part for the pick and lift task, with the instrumented object and the other elements of the setup, and a second part to deliver augmented tactile feedback.

6.2.1. Pick and lift task setup

The experimental setup consisted in a custom instrumented object (271 g, Fig. 6.1), devised for a previous study [20], that featured three load cells to record grip and load forces, and a red LED to signal object breakage when the grip force overcame a threshold. Two of the load cells were on the lateral surfaces of the object, in order to record the normal forces exerted by index and thumb while lifting up the object. In order to uniform the results, two black dots were added on the object surfaces to indicate the exact points where the two fingers should have been placed. The tangential force, indicating the vertical force applied during the lift to counteract the object weight, was recorded by a third cell placed on the platform on which the object was replaced after each lift. A weight was placed between the object and the platform and it attached magnetically to the object at the beginning of the experiment in order to increase its weight and thus the engagement during the task. Next to the object a large button was placed to detect the beginning and the end of each lift; whenever the button was pressed, the object was ready for the lift indicated through the switching off of the green LED. A vertical bar indicating the height at which the object had to be lifted in each trial (15cm) was placed on the left of the object.

The interaction forces were acquired in real time, through a NI-SCB-68 DAQ board (National Instruments, USA) connected to a PC running Simulink Desktop Real-Time (MathWorks, USA) with sampling rate of $f_s = 1kHz$. Two bench power supplies (TENMA 72-8355, 0 – 36V, 0 – 5A and Aim-TTi Instruments, EX4210R 0 – 42V, 0 – 10A) set at 5V, 0.1A and 10V, 2A were used to power the load cells, the button and the magnet.

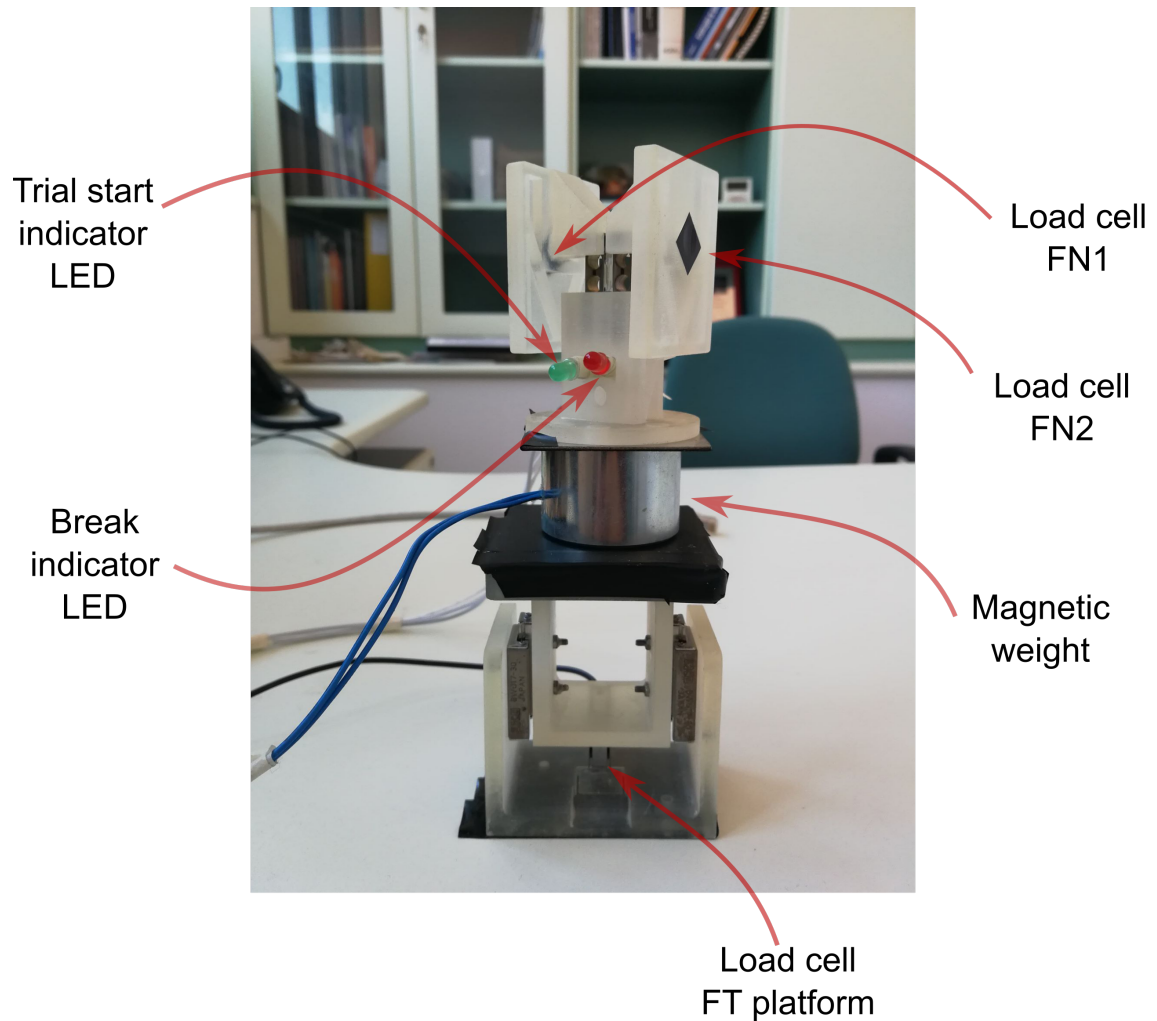


Figure 6.1: Instrumented object recording normal and tangential forces during the pick and lift task. Previously used in [20]. It contains two load cells on its lateral surfaces to record the grip force and one load cell on the platform to record the load force. A magnetic weight was placed in between object and platform to increase the lifted object weight. Two LEDs indicate breakage of the object (red) and the beginning and the end of each trial (green).

Load cells calibration

The three load cells present in the object were calibrated in order to acquire a precise measurement of the forces applied while grasping. For the calibration I used three standard masses of 0.01, 0.1 and 0.2kg and measured the responses generated by the forces applied by these masses on the load cells for three consecutive repetitions. The weights of these masses were 0.0981, 0.981 and 1.962N. Through repeated measures of the voltage response generated by these weights I could relate the force values to each load cell response. Eq. 6.1 shows the relation between the voltage response ($VoltageF_{Platform}$) and the force applied on the load cell placed on the object platform for the measurement of the tangential force ($F_{Platform}$). Eq. 6.2 and Eq. 6.3 show the voltage-force relation for the two load cells placed on the lateral surfaces of the object, that together measure the normal force applied during grasping ($FN = FN_1 + FN_2$). $VoltageFN_1$ is the voltage generated by the first load cell on one side of the object and $VoltageFN_2$ is the voltage response of the second load cell on the lateral surfaces.

$$VoltageF_{Platform} = 2.2356 * F_g + 0.3511 \quad (6.1)$$

$$VoltageFN_1 = 0.1274 * F_g + 0.039 \quad (6.2)$$

$$VoltageFN_2 = 0.125 * F_g + 0.0294 \quad (6.3)$$

6.2.2. Augmented vibrotactile feedback setup

Our prototype of the DESC glove was worn during the whole time of the experiment on the right hand. For the purpose of this experiment, we used only two of the three sensors I manufactured, one on the thumb and one on the index as these two were the fingers used during the pick and lift task. Moreover, as I previously mentioned, I used a precedent version of the electronic board to acquire the signal from the sensors, as the one I designed was not available at the time of the experimentation. One board for the sensor on the thumb and one board for the sensor on the index allowed to detect the sense of touch in real time and deliver the feedback through two vibration actuators. The two eccentric-mass motors were placed in a fixed position on the arm for the whole experiment under two elastic bands (Fig. 6.2) and were activated only in correspondence of a touch or release event. They were placed at a distance of 3cm one another in order to facilitate the discrimination of the vibration stimuli corresponding to tactile events at the two fingertips. The sensors and the motors were powered using a Digimesse BP3002 bench power supply set at 3.3V and 0.1A . Another PC was connected to the serial ports of the acquisition boards (Board 1) and the serial port of the actuators board (Board 2) for the communication between the two. Using a UART RS-232 communication protocol, a script on Processing 3.5.1 ran during the experiment to allow reading and writing of the serial ports. A picture of the complete setup is shown in Fig. 6.3 and the corresponding schematic representation is reported in Fig. 6.4.

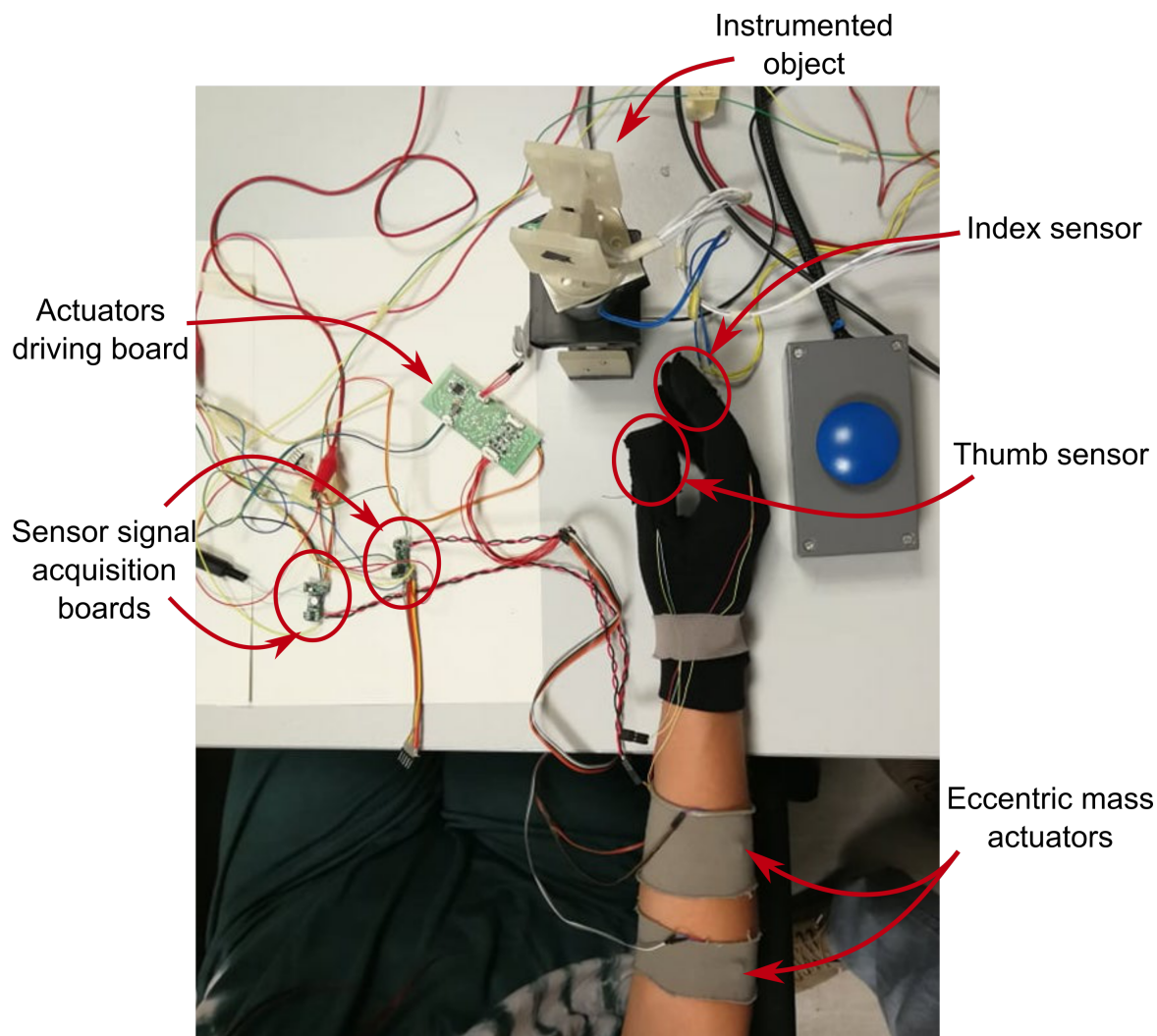


Figure 6.2: Top view of the experimental setup, a participant while wearing the glove with thumb and index sensors. The two eccentric mass vibration actuators were fixed on the forearm with two elastic band (bottom right). The boards for acquiring the sensors signal and the one for controlling the actuators are also shown in the picture. The instrumented object was placed on the table (top).

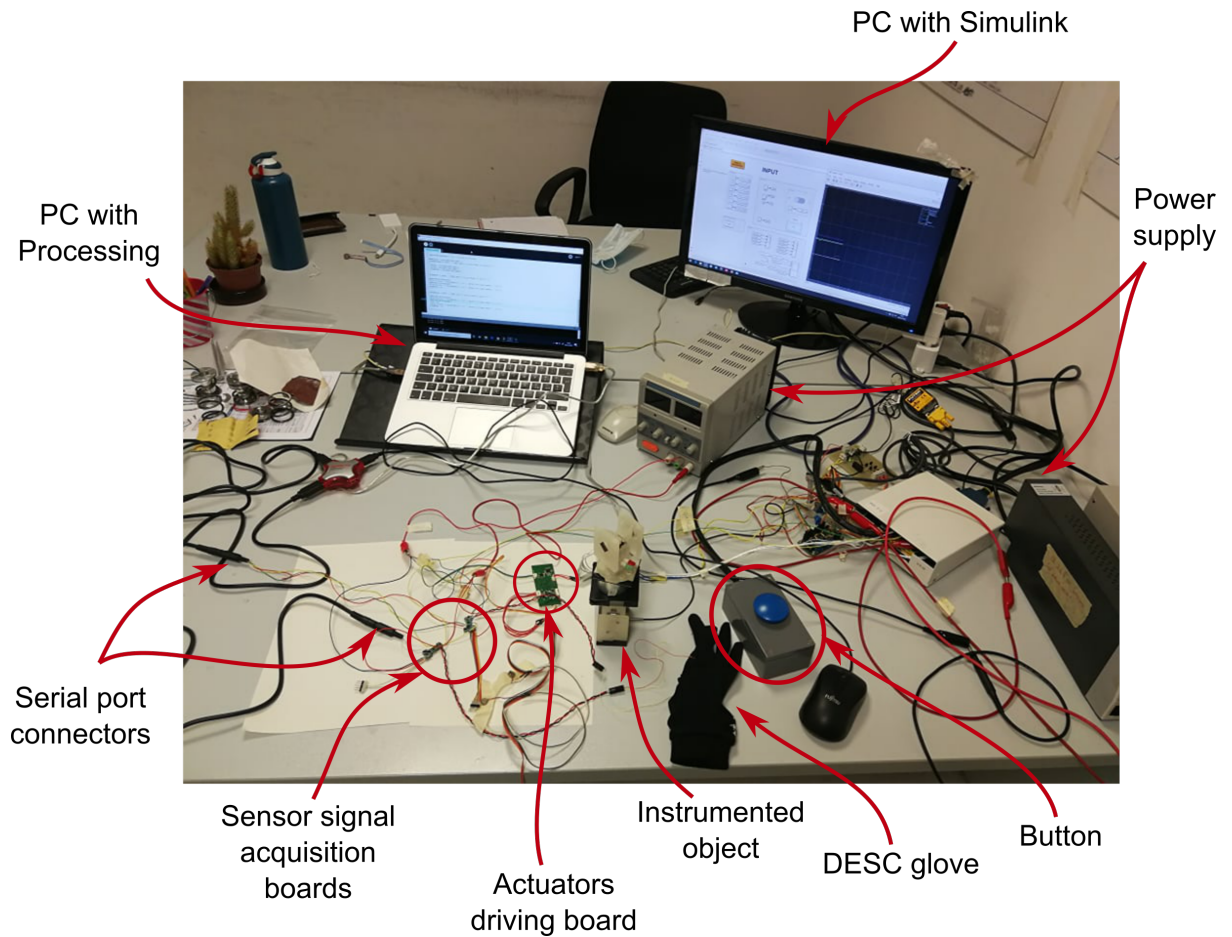


Figure 6.3: Picture of the setup for the DESC glove experimental procedure. The two PCs are shown: the one to acquire the data from the DAQ in real time with Simulink desktop and the one for the serial communication with Processing. The boards for the sensors and the board for the motor were connected through 3.3V serial cables to the PC with the processing script. The instrumented object to be lifted was placed at the center of the desk next to the glove that needs to be worn by the participants. The button to be pressed at the beginning and the end of each lift was placed at the right of the instrumented object. The power supplies were connected to the corresponding boards and load cells.

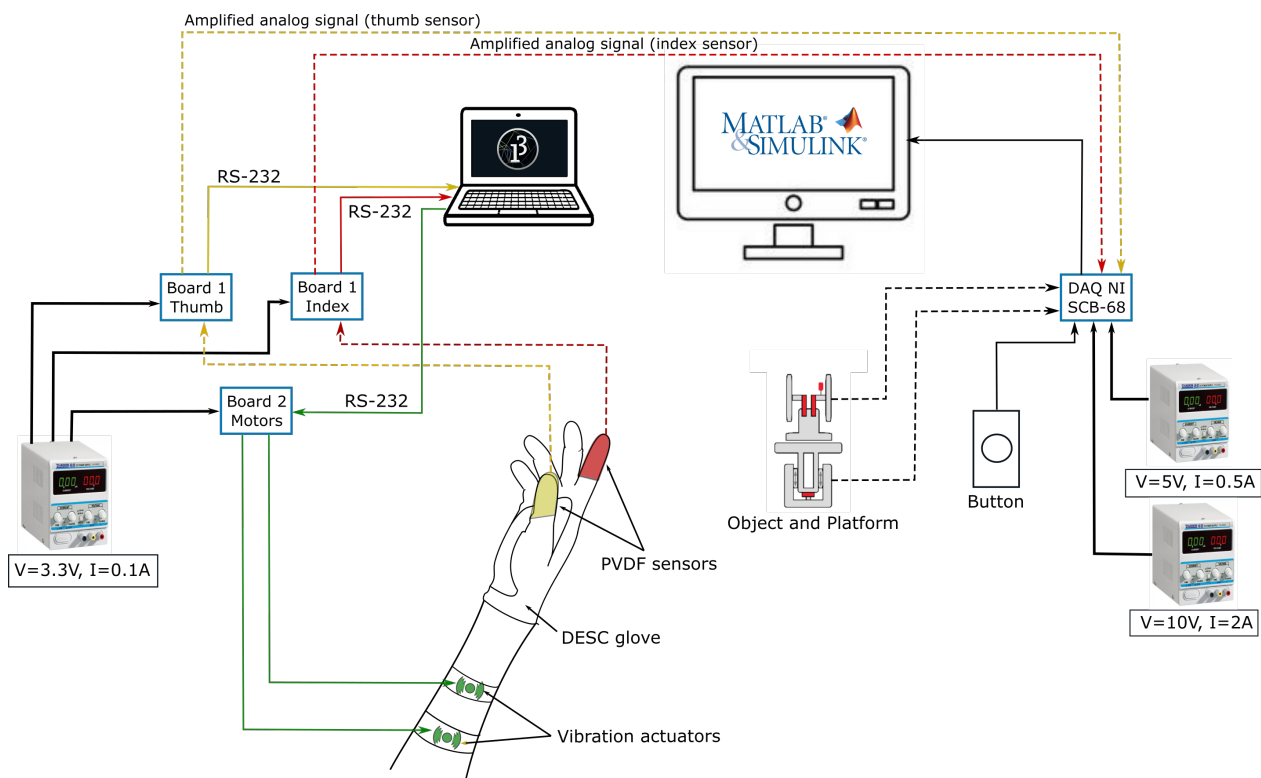


Figure 6.4: Schematic representation of the setup for the DESC glove experimental procedure. All the components present in the picture 6.3 are reported in this block diagram. The dashed lines represent all the analog signals, while the continuous lines the digital ones. Green lines for the actuators, red lines for the index sensor and yellow lines for the thumb sensor. The thicker black lines are the power connections.

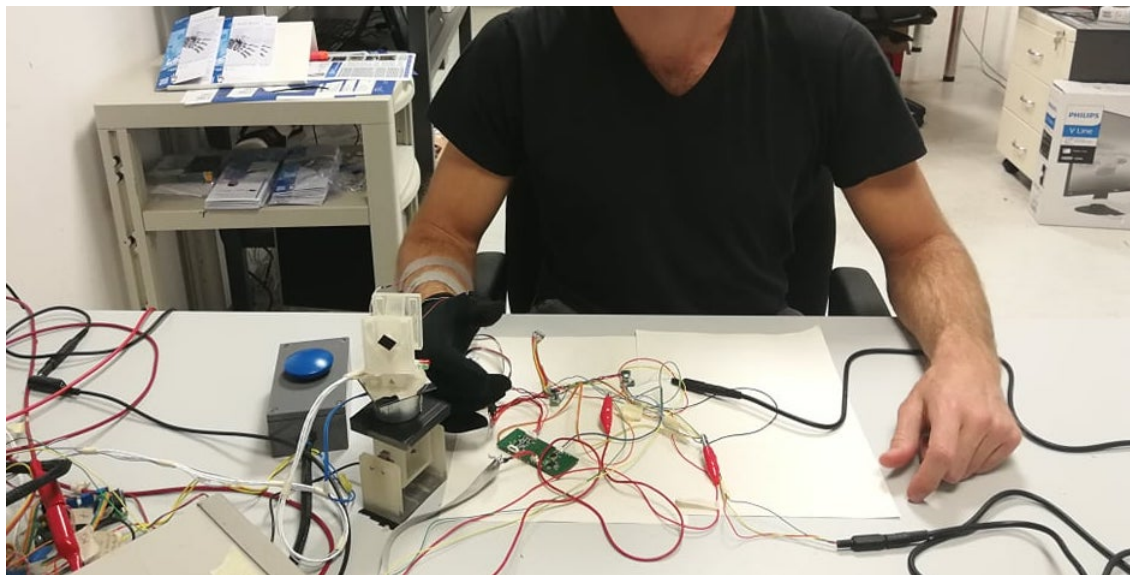


Figure 6.5: Illustration of a subject performing the experiment at the setup table. Starting position for the experimental procedure. The subject was wearing the DESC glove on his right hand and had the actuators on the right forearm. The sensorized object was at the right, next to the button to be pressed for starting the trial.

6.3. Experimental procedure

The first part of the experiment consisted in a brief training in which the participants were asked to perform ten lifts to familiarize with the task and the instrumented object sensitivity. During this part the

subjects were asked to wear the glove but the device was not initialized.

Afterwards, the participants were asked to sit at the table and repeatedly perform a pick and lift task as fast as they could, which consisted of reaching the instrumented object with their right hand, lifting it above a target height (15cm above the table surface, marked with tape) and replacing it stably on the table, as shown in the example in Fig. 6.6. Immediately before and after lifting the object the participants had to press the button, in order to facilitate the detection of separate trials.

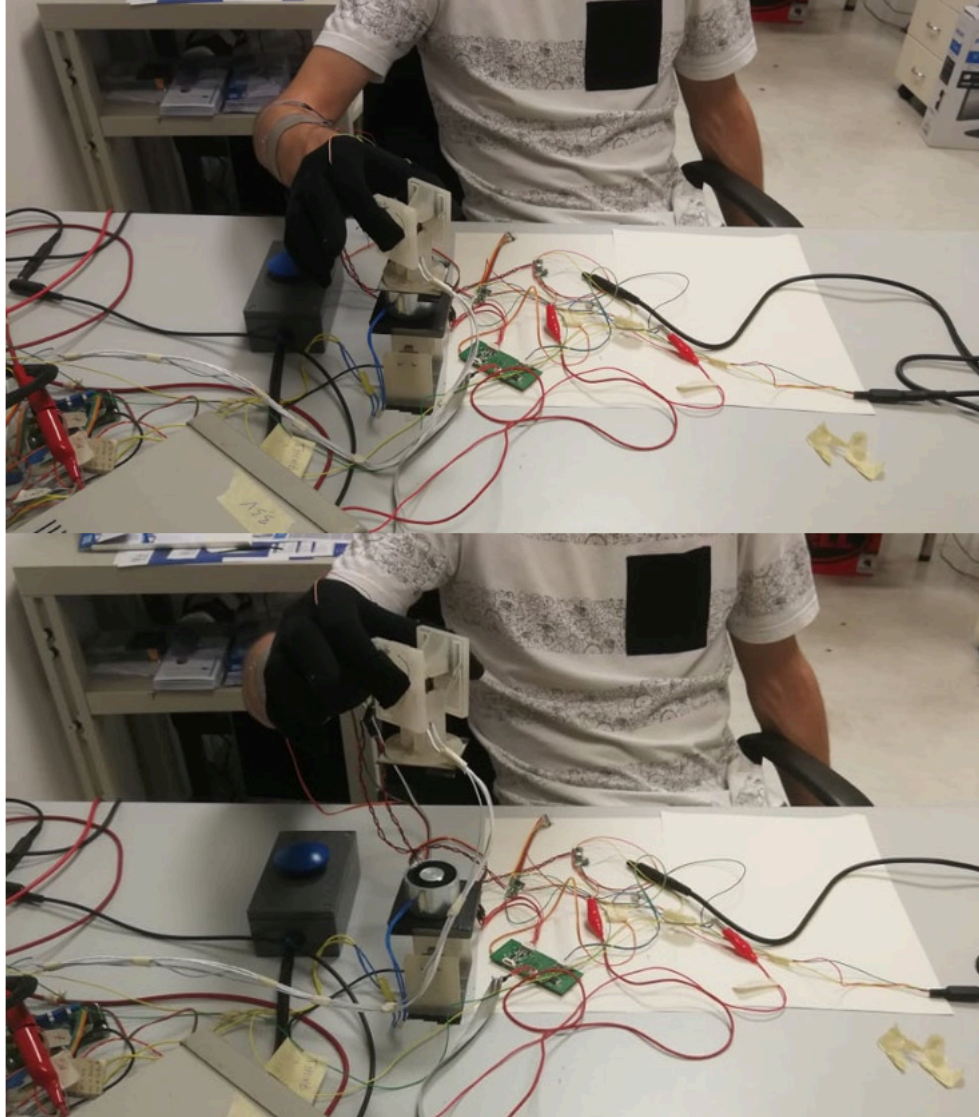


Figure 6.6: Illustration of a subject performing one trial of the pick and lift task. Top: the subject grasps the object using thumb and index fingers, the moment of contact between the fingers and the object was captured. Bottom: the object is lifted at the maximum height. The object will be then replaced on the platform, and the whole task will be repeated again.

To force the participants to employ tactile feedback to successfully complete the task, which would be otherwise completed only with a feedforward control [119], the object was set to virtually break in case the participants applied a grip force larger than a threshold (Th_{break} in Eq. 6.4), which proved to be challenging during a preliminary test. Breakage was signaled with the red LED.

$$Th_{break} = 8N \quad (6.4)$$

The aforementioned task was completed in two conditions, each consisting of 100 repetitions, with a short break in between. In condition A (baseline) the glove was unpowered, while in condition B (intervention) a DESC type feedback was sent in correspondence of tactile stimuli at the fingertips.

The order of the two conditions was randomized for each participant. Concurrently with the pick and lift motor task, the participants were asked to perform a cognitive serial subtraction task (SST) [100]. In this task, the subjects were required to count backward in threes as quickly and as accurately as possible, starting from a different starting point for each condition to avoid task familiarization. A schematic representation of the experimental procedure is shown in Fig. 6.7. A videoclip illustrating a participant performing the experiment was attached in the supplementary material.

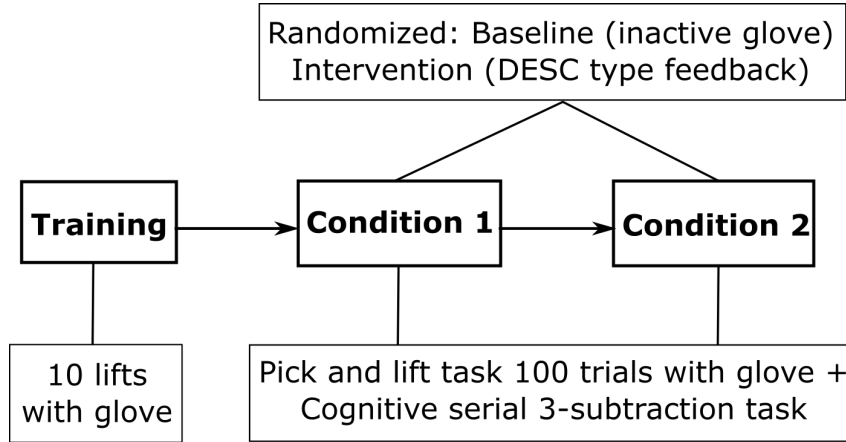


Figure 6.7: Schematic representation of the experimental procedure for the DESC glove testing. During the whole experiment the participants were wearing the glove. After a brief training for familiarization with the instrumented object, the pick and lift task (100 lifts) was repeated in two conditions, whose order was randomized, synchronously with a cognitive task.

6.4. Data acquisition and analysis

The data were acquired using Simulink Real Time Desktop (MathWorks, Inc.) and analyzed using MATLAB 2019b (MathWorks, Inc.). The list of variables acquired during the experiment in real time is: Time, Subject number, Condition, Trial (lift number), Button press, Slippage indicator, FN_1 (normal force on sensed plate 1) both raw and biased, FN_2 (normal force on sensed plate 2) both raw and biased, $F_{platform}$ (tangential force from the platform) both raw and biased, Contact event indicator and Lift Replace event indicators. The analog signal from the PVDF sensors was also acquired in real time by connecting the amplified analog signal from the two Boards 1 to the DAQ ($SensorThumb$ and $SensorIndex$ variables). All the variables were saved in structures and then elaborated and divided in trials, conditions and subjects.

6.4.1. Motor performance analysis

For each repetition of the task, I measured the biased values of grip force (GF) and load force (LF) through the load cells. From grip force and load force vectors in time (GF_{vect} and LF_{vect}) I produced the coordination plots for each subject and each condition. I also extracted the maximum GF (GF_{max}) within the static phase of the lift as the sum of the maximum biased normal forces recorded by the two load cells on the object surfaces during each trial ($FN_{1(max)}$ and $FN_{2(max)}$ in Eq. 6.5).

$$GF_{max} = FN_{1(max)} + FN_{2(max)} \quad (6.5)$$

The duration of each phase of the lift [52], was then calculated as shown in the equations below. The preload phase ($t_{preload}$) was defined as the time interval between the moment of contact between fingertips and object ($t_{contact}$) and the start of the lifting of the object ($t_{startLifting}$, as shown in Eq. 6.6). The load phase duration (t_{load}) was found as the time between the start of the lifting, i.e. the instant in which the participant begins to apply a grip force, to the moment of liftoff ($t_{liftoff}$) in which the object firstly gets lifted above the resting position (Eq. 6.7). The static phase duration (t_{static}) was calculated as the time interval between the moment of liftoff to the instant in which the object is replaced on the platform ($t_{replacement}$), as shown in Eq. 6.8. During the whole time between these two contact events, defined as the static phase of the lift, the grip force should remain about constant, as there was no variation in the weight of the object. The duration of the postload phase ($t_{postload}$) was found as the time interval between the moment of replacement of the object on the platform and the instant in which

the it is released by the fingers ($t_{Release}$), and therefore the end of application of any GF (Eq. 6.9).

$$t_{Preload} = t_{StartLifting} - t_{Contact} \quad (6.6)$$

$$t_{Load} = t_{Liftoff} - t_{StartLifting} \quad (6.7)$$

$$t_{Static} = t_{Replacement} - t_{Liftoff} \quad (6.8)$$

$$t_{Postload} = t_{Release} - t_{Replacement} \quad (6.9)$$

The total duration of each repetition, defined as the time interval between the first contact with the object and its final release, was then calculated by summing all the phases of the task (Eq. 6.10).

$$t_{Total} = t_{Preload} + t_{Load} + t_{Static} + t_{Postload} \quad (6.10)$$

I also calculated the grip response latency (namely, the GF-LF delay), defined as the time delay from the LF reaching a specific value to the GF successively reaching the same value, expressed as a percentage of the maximum LF (LF_{max}). For each trial the indices at which the load force reached certain values, i.e. 1, 2, 5, 10, 20, 30, 40, 50, 60, 70, 80, 90, 100% of LF_{max} , were saved and the same was done for the indices at which the grip force reached the same values. Then the time delay between the two was calculated for each force value, expressed as $n\%$ of LF_{max} , as reported in Eq. 6.11 by subtracting the vector of time evaluated in the index saved for the LF ($idx_{(LF>n\%LF_{max})}$) and the time at the index saved for the GF ($idx_{(GF>n\%LF_{max})}$).

$$GFLFDelay(n\%) = Time(idx_{(LF>n\%LF_{max})}) - Time(idx_{(GF>n\%LF_{max})}) \quad (6.11)$$

All the variables mentioned above were calculated for each trial within each condition and each subject. Successively, the mean and standard deviation across the 100 trials in each condition were calculated for a better comparison between conditions and represented separately for all subjects. The number of breaks within each condition was also found to compare baseline and intervention.

6.4.2. Characterization of the device

From the data extracted during the experimental procedure, an analysis of the performance of the DESC glove was also performed. The aim of this analysis was to evaluate the accuracy of the apparatus in delivering feedback exactly when contact events occurred. In order to do so, it was necessary to study the activation of the sensors, and therefore of the motors, in relation to the activation of the load cells on the object during condition B in which the device was powered and actively working. For this reason I scanned the analog signal acquired by the DAQ during the experiment for both sensors (*SensorThumb* and *SensorIndex*). This signal resulted to be noisy, as the cables connecting the amplified analog sensor output and the DAQ had to be long because of the setup distances. Therefore, I decided to filter the sensors signals using a moving average filter on MATLAB 2019b. An example of the index sensor signal for one single trial in Subject 7 is shown in Fig. 6.8 before filtering (blue line) and after a moving average filter with a window of 100 samples (orange line).

Following the filtering of the signals, the true positive activations of the sensors were considered as the ones that occurred in a range of $\pm 200ms$ from the moment of contact registered by the load cells. A signal higher (in case of contact) or lower (in case of release) than the chosen threshold (described in 6.12 for the thumb sensor) was needed within this range in order for a true positive to occur.

$$Threshold_{Thumb} = Mean_{SensorThumb} \pm \sigma_{SensorThumb} \quad (6.12)$$

Where $Threshold_{Thumb}$ is also called the Limit of Detection (LoD, previously defined in Eq. 3.3), and was set to be one time the standard deviation of the sensor signal added to the mean of the signal, the same for both sensors. Higher values of the LoD were not practical for this particular signals, as they resulted to be noisy and therefore had a high standard deviation.

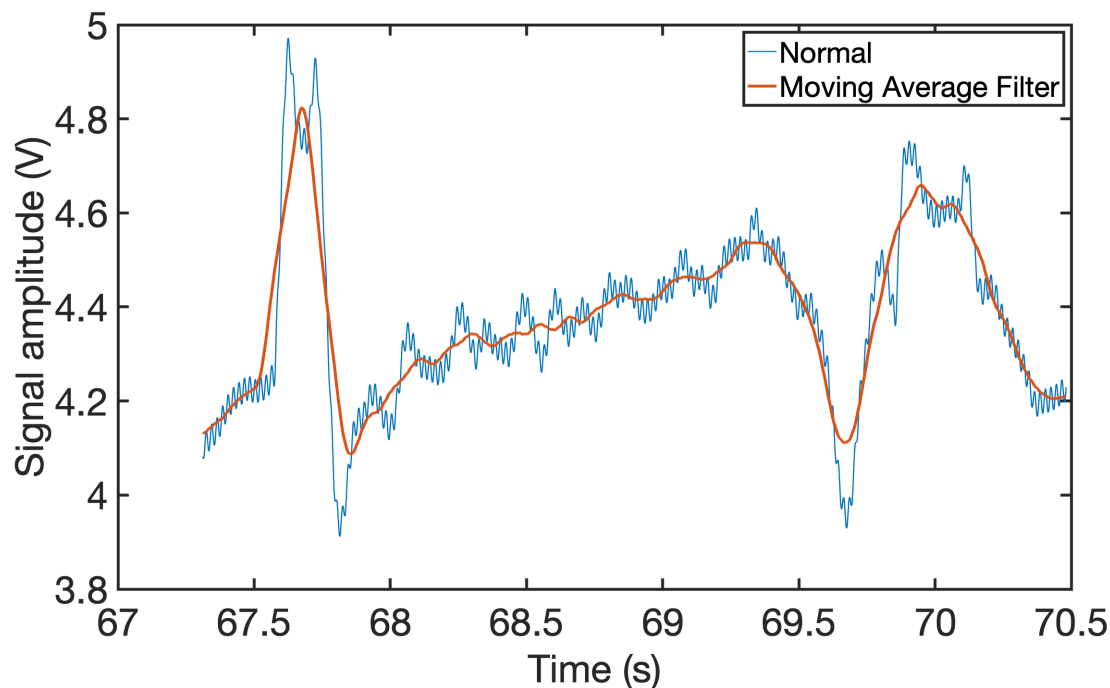


Figure 6.8: Example of the index sensor analog signal acquired from the DAQ during one trial. We can see that this signal is originally very noisy (blue line) and could generate many false positive activations of the motors. After applying a moving average filter on a window of 100 samples the signal becomes smoother (orange line) and it is easier to detect the touch events spikes. There is one positive spike synchronously with contact and one negative spike in concurrence with the release of the object.

In case an activation of the sensors was detected outside the contact and release ranges, it needed to be at least 200ms after the previous detected activation for a false positive to be measured. The interval of 200ms was included to discriminate subsequent peaks in the sensor signal from the real false positive cases, since they would not lead to multiple activations of the motor.

The percentage of true positives (TP) and false positives (FP) was then calculated within each condition for every subject, considering that ideally two true positives should have been present in each trial for both thumb and index sensor.

6.4.3. Statistical Analysis

All data were analysed using the built-in statistics functions of MATLAB2019b (MathWorks, Inc.). Considering the limited number of subjects, the statistical tests were performed only from data within the same subject. The Kolmogorov-Smirnov normality test was performed on all variables in order to understand which type of data we were analysing and consequently choose the most appropriate statistical test to be implemented. Since the grip force and all the durations of the phases of the task resulted to be normally distributed, a t-test was performed on these variables to evaluate the statistical significance of the results. The p-values were calculated relating condition A (baseline) and condition B (intervention with DESC feedback) for each subject.

The GF-LF delays resulted to be not normally distributed variables and, for this reason, I decided to use a Wilcoxon signed-rank test between the two conditions for each subject.

The statistical significance of the differences between baseline and intervention conditions will be reported in the results in Chapter 7 for the variables and subjects in which the p-value resulted to be at least $p < 0.05$.

7

Results and Discussion

In this chapter I will report the results obtained during the experimentation with the DESC glove. The outcomes and their statistical significance will be later discussed.

7.1. Results

The results of the experimentation, described in Chapter 6, are obtained from the data analysis performed with MATLAB 2019b (MathWorks, Inc.) and will be reported in the sections below.

7.1.1. Grip force and Number of breaks

The level of the maximum grip force (GF) applied on the object during the performance of the lift is represented in Fig. 7.1. For each trial, the maximum value of grip force reached during the lift was calculated and saved into a variable GF_{max} , which was a structure containing two fields one for each condition, and matrices with 10 columns (participants) and 100 rows (trials). Fig. 7.1 shows the boxplots of GF_{max} applied by each subject during the performance of the task in the two conditions together with the object breaking threshold (red horizontal line). We can see from this representation that the grip force applied by 3/10 participants increases from baseline to intervention with significant differences for P2 and P8. Contrarily, the grip force applied by 7/10 subjects decreases from baseline to intervention, being statistically significant in all subjects besides P9.

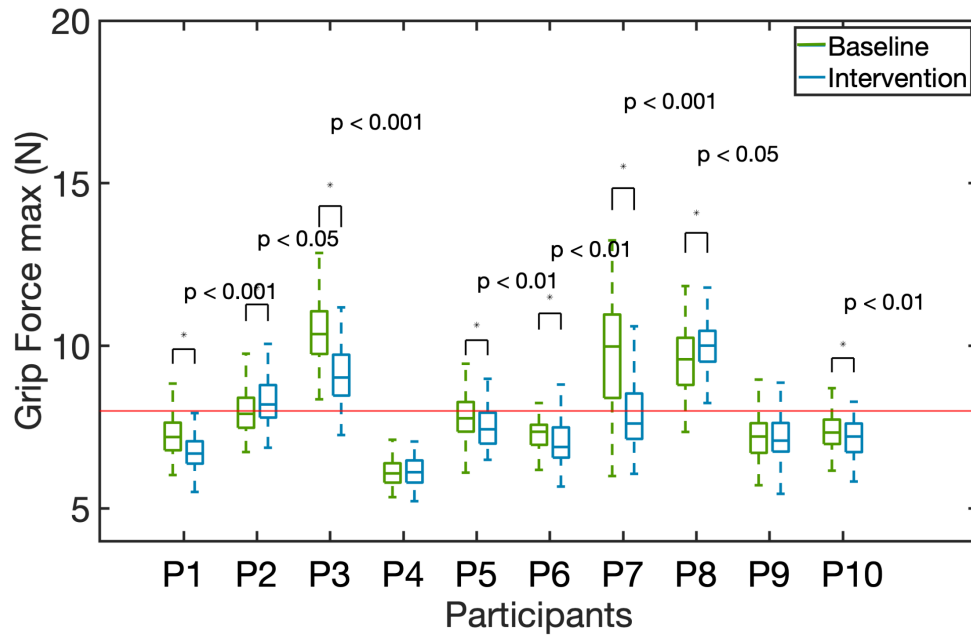


Figure 7.1: Box Plot of the maximum Grip force reached during the trial in baseline (green) and intervention (blue) conditions represented for all subjects. The 10 participants are indicated on the x-axis and the corresponding maximum grip force median and interquartile range are shown on the y-axis in the boxplot. The red horizontal line represents the breaking threshold $Th_{break} = 8N$ of the instrumented object. The p-values are also represented in case of statistically significant differences between the two conditions.

The number of times the instrumented object was broken during each condition was extracted for all subjects, as the number of times the maximum grip force surpassed Th_{break} (Eq. 6.4). Fig. 7.2 shows a bar plot of the number of breaks in baseline (green) and intervention (blue) conditions. There is not a general trend distinguishable from condition A to condition B among all subjects but we can notice that for 7/10 participants the number of times the object was broken is reduced following the application of feedback.

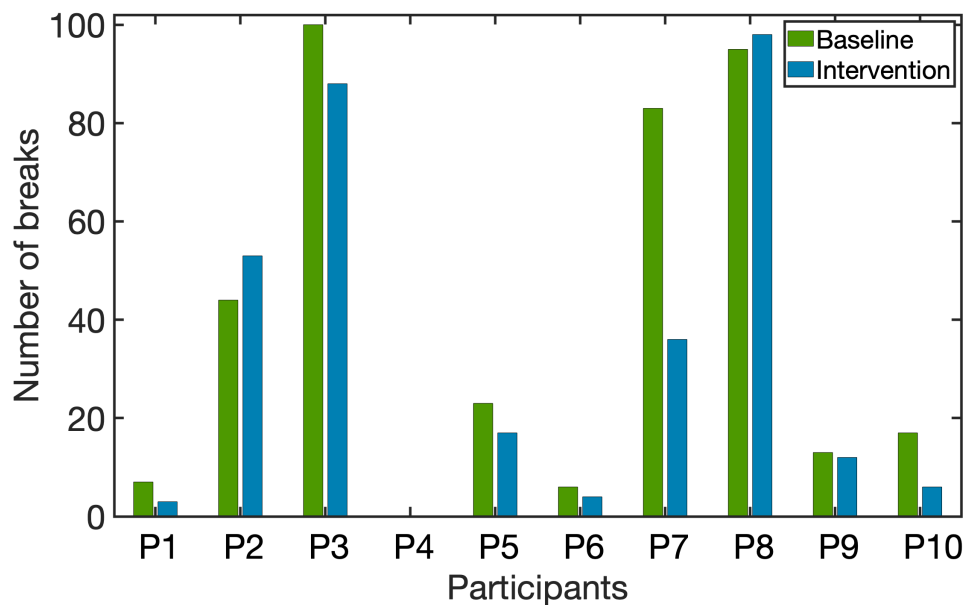


Figure 7.2: Histogram of the number of breaks occurring during the pick and lift task in both baseline and intervention conditions. The object was broken when the grip force applied by the participant on its lateral surfaces overcame a threshold $Th_{break} = 8N$.

7.1.2. Coordination plots

The coordination plots, representing the relationship between grip force (GF) and load force (LF) in every moment of the task, are reported in Fig. 7.3. The vectors of the grip force recorded by the two load cells on the object lateral surfaces and acquired by the DAQ in real time during each trial, are plotted with respect to the corresponding vectors of the load force recorded by the load cell on the platform. This is done for each of the 100 trials all plotted together for both conditions, independently for every subject. The darker central blue and green lines in the plots in Fig. 7.3 indicate the trend of the mean value across all trials, while the lighter color represents the standard error (SE) range around the mean (Eq. 7.1).

7.1.3. Grip force to load force delay

The grip response latency, also named GF-LF delay, is defined as the delay in time from instant in which the load force reaches a specific value to the moment in which the grip force successively reaches the same value. The level of force taken into consideration is usually expressed as a percentage of the maximum LF reached during the trial, and it is therefore dimensionless.

Fig. 7.4 represents the delays calculated using the vectors of grip force and load force recorded during the whole experimental procedure, the same as reported Fig. 7.3. The GF-LF delays were calculated, from the GF and LF vectors for each trial, at 1, 2, 5, 10, 20, 30, 40, 50, 60, 70, 80, 90, 100% LF_{max} and saved in the corresponding variables collecting the delays at the corresponding level of force for all trials and all subjects. The plots in Fig. 7.4 report the amounts of time delays for all trials in each condition in seconds, where the darker lines in these graphs represent the mean values and the lighter colored patch around them represents the standard error range described in Eq. 7.1, same as for the coordination plots.

Each subplot represents the delay across the lift task for each subject in the baseline condition (unpowered device, indicated in green color) and the intervention condition (feedback delivery, indicated in blue color). It is noticeable that the blue line, representing the GF-LF delay following the application of DESC-type feedback through vibrations at the forearm, is located below the green baseline line for most of the subjects. An exception is shown in the subplot for P9 in which the intervention condition has higher delay values with respect to the baseline. The delay in P2 is very noisy and therefore difficult to discriminate whether the intervention line lays above or below the baseline. Participant 1 shows almost the same values of delay between grip force and load force for both conditions.

The significant results in these plots are the ones in central area, as in the beginning (around 0% LF_{max}) and the end (around 100% LF_{max}), a lot of noise is present and the delays are not accurate. For this reason, the delay at 50% LF_{max} is normally analysed to investigate an improvement in the control strategy. The mean and the standard error of the delay at 50% are shown in Fig. 7.5, represented in milliseconds in an histogram plot for each participant. This figure basically represent a zoom of each GF-LF delay plot, considering the mean value (darker continuous line in 7.4) as the top part of the bars of the histogram and the standard error (lighter colored patch in Fig. 7.4) as the range indicated by the black lines on each bar. Through this representation it is easier to notice a decreasing trend from the baseline condition (green) to the intervention with DESC feedback applied (blue) for all subjects except for P1, P2 and P9. Most of the differences between the two conditions result to be statistically significant, except for P1 and P8, with a p-value lower than $p = 0.05$ and in some cases even lower than $p = 0.001$.

$$Range = Mean \pm SE = Mean \pm \frac{STD}{\sqrt{Mean}} \quad (7.1)$$

Where $Mean$ and STD indicate respectively the mean and the standard deviation of the forces across the 100 trials, and SE is the standard error defined as the standard deviation divided by the square root of the samples mean.

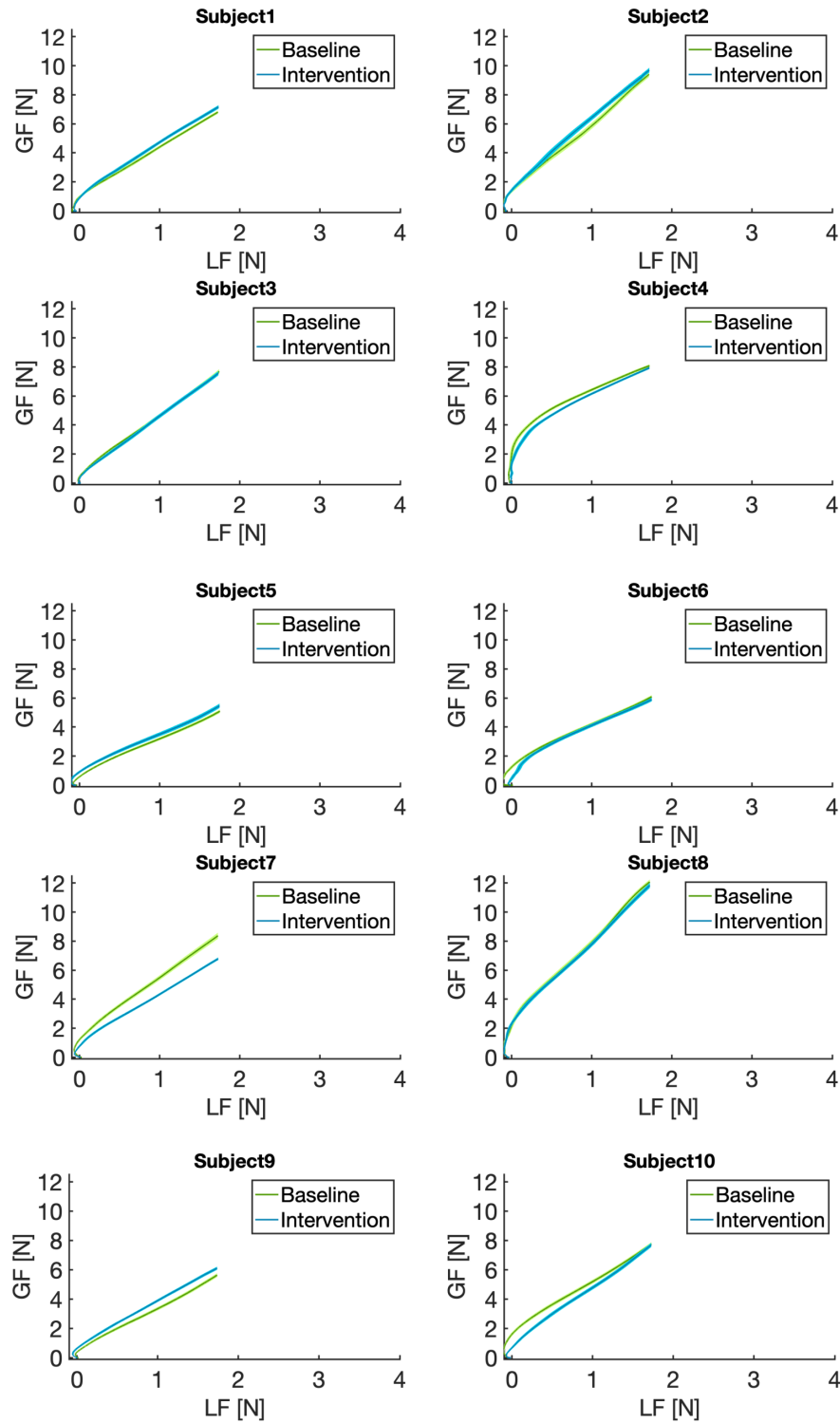


Figure 7.3: Coordination plot (grip force-load force) for all subjects represented in separate subplots. The plots show the relation between the grip force (normal to the object) and the load force (tangential to the object) during the whole duration of the lift, for each trial in the two conditions. The relation between grip force and load force while wearing the unpowered glove is showed in green and the coordination plot with the application of DESC-type feedback is shown in blue.

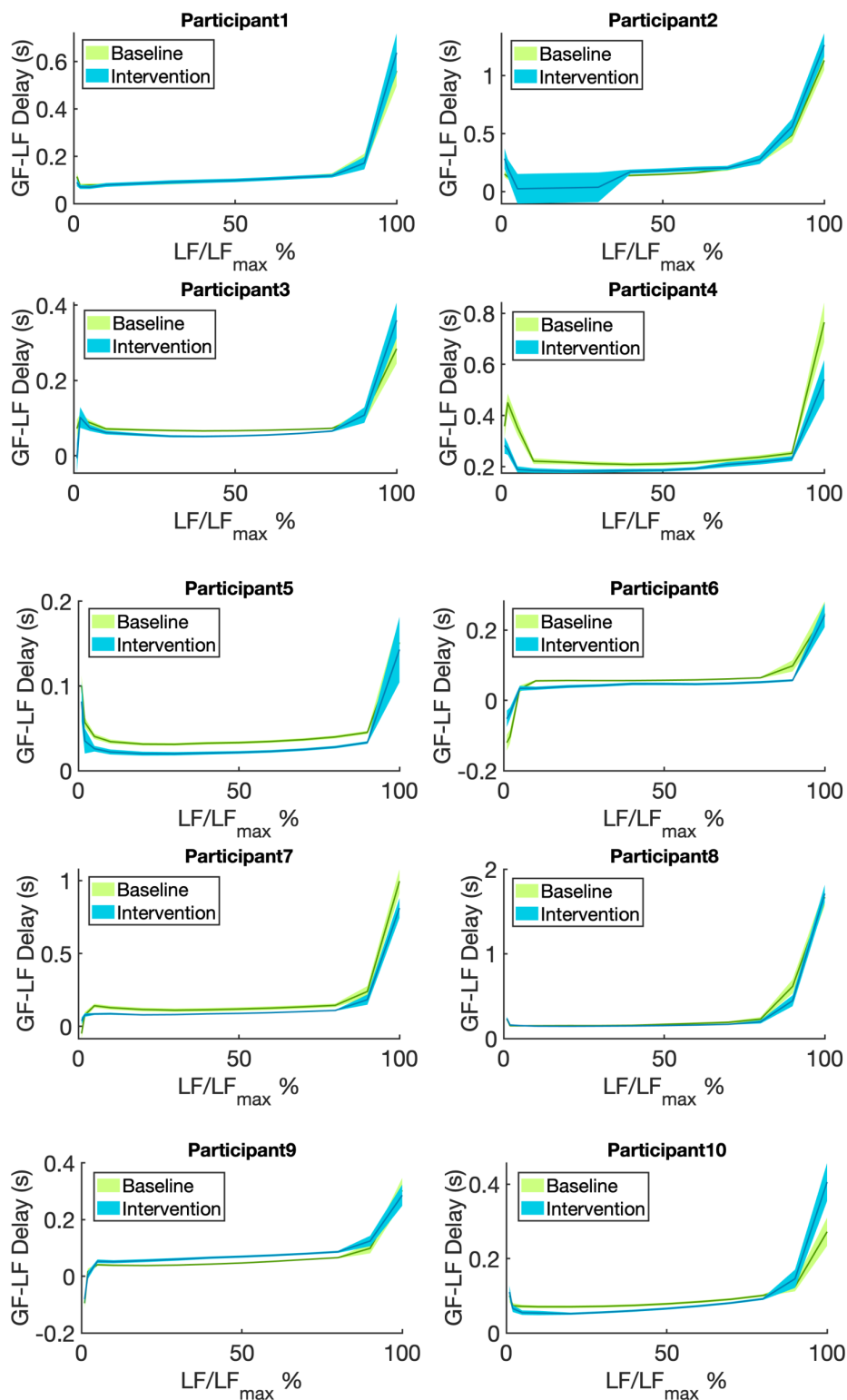


Figure 7.4: Plots of GF-LF delay for each value of the load force, expressed on the x-axis as a percentage of the maximum load force represented in separate subplots for each subject. The time delay between the load force activation and the grip force reaching the same value is shown on the y-axis in seconds. Significant values of GF-LF delay are the ones in the central part of plots.

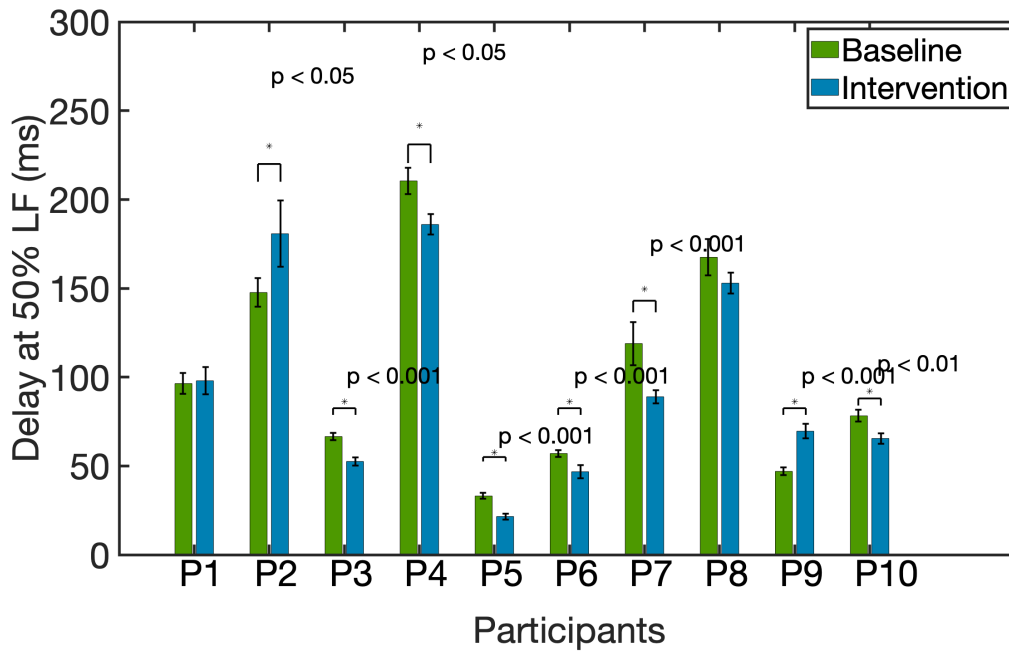


Figure 7.5: Mean and standard deviation of the time delay between load force and grip force activation when the load force is at 50% of its maximum LF_{max} . The delay is represented on the y-axis in milliseconds for each of the 10 participants (x-axis) in both conditions baseline (green) and intervention (blue). The p-values are also reported in case of statistically significant differences between the two conditions.

7.1.4. Duration of the task

The duration of the lift is calculated as described in the previous chapter in Eq. 6.10. It is defined as the time interval between the start of the lifting and the replacement instants. The time spent to perform a motor task is often used as an indicator of the motor performance. Usually, while maintaining the same level of task performance, a reduction in the time used to complete a task indicates a higher level of hand dexterity, and therefore hand motor function.

The boxplot of the total duration of the task for all subjects in the two conditions is represented in Fig. 7.6. The duration of the task is reported in seconds and the statistical significance of the differences between baseline and intervention conditions is also shown in the plot.

The total duration of the lift decreases from baseline to intervention for all subjects besides P5. Moreover, the decrease resulted to be statistically significant in all cases except for P1 and P2.

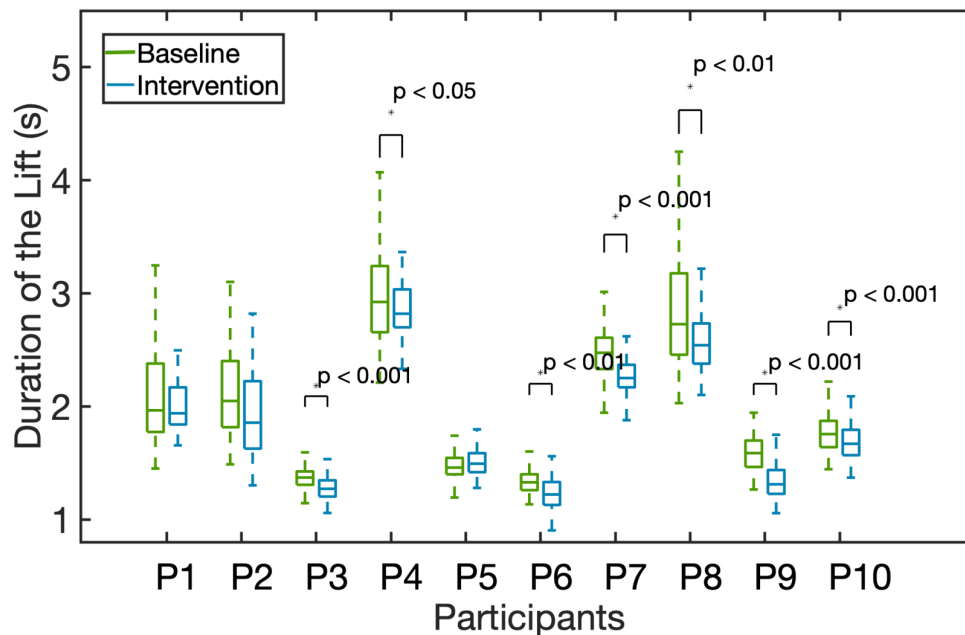


Figure 7.6: Box Plot of the total duration of the lift in baseline (green) and intervention (blue) conditions represented for all subjects in seconds. The 10 participants are indicated on the x-axis and the corresponding task duration median and interquartile range are shown on the y-axis in the boxplots. The p-values are also represented in case of statistically significant differences between the two conditions.

7.1.5. Characterization of the device results

The percentages of true positives (TP) and false positives (FP) among all trials in the intervention condition for thumb and index sensors are reported in the table below for each subject (Table 7.1). As we can see from the values in the table there were no misplaced activations (false positives) for the index nor for the thumb.

Subject	TP Thumb	TP Index	FP Thumb	FP Index
1	99%	98.5%	0%	0%
2	97.15%	98.2%	0%	0%
3	65%	55%	0%	0%
4	70.5%	64.5%	0%	0%
5	100%	100%	0%	0%
6	91.3%	91.3%	0%	0%
7	100%	100%	0%	0%
8	99.5%	59.5%	0%	0%
9	98.5%	100%	0%	0%
10	99.5%	98.5%	0%	0%

Table 7.1: The percentages of true positives (TP) and false positives (FP) that occurred during the pick and lift task experiment for both thumb and index sensors.

The values from Table 7.1 were averaged across all subjects and $TP_{Thumb}Mean$ and $TP_{Index}Mean$

were obtained as reported in the following equations.

$$TP_{Thumb}Mean = 92.05\% \quad (7.2)$$

$$TP_{Index}Mean = 86.56\% \quad (7.3)$$

The average of the false positive rates for both sensors resulted to be zero ($FP_{Thumb}Mean = 0\%$ and $FP_{Index}Mean = 0\%$).

7.2. Discussion

The results that emerged from the analysis of the participants' motor performance and the operation of the device are discussed in the next sections.

7.2.1. Grip Force and Number of breaks

The values of the grip force showed in Fig. 7.1 were very high with respect to the weight of the object, represented by the load force recorded by the platform load cell. This phenomenon can be explained by the fact that the glove largely reduced the friction between the hand and the object, forcing the participants to apply a higher level of force to avoid slippage. In fact, the fabric covering the sensors at the thumb and index fingertips resulted to be very slippery and in addition to this, as demonstrated in many studies present in literature, wearing a glove can largely reduce tactile sensitivity [13, 18]. The reduction of tactile sensitivity leads to the application of a higher force on the object surfaces in order to successfully lift it.

There was no evident trend in the difference between the levels of grip force in baseline and intervention conditions. The GF_{max} increased for 3/10 participants and decreased for the rest. We could observe that the grip force significantly decreased from condition A to condition B in 6/10 participants. The lack of uniformity in this result might have been caused by the biases in the setup described in Section 8.2. The same behaviour we noticed in the GF_{max} was present in the number of breaks bar plot shown in Fig. 7.2, extracted during the performance of the task in the two conditions. There was no common trend between subjects, even though for 7/10 subjects the number of breaks decreased, the number of samples was too low to make any statistical considerations. In fact, there was only one number to describe the number of breaks for each subject and each condition instead of having a vector of length number of trials. For this reason a statistical analysis cannot be performed having only 10 subjects and more data would be needed. Lacking statistically significant differences between the two conditions, we cannot draw any conclusion on the reduction of the number of breaks from baseline to DESC feedback condition.

It is interesting to notice the very high variability in object breakage between subjects. There were some participants that almost always broke the object (as P3 and P8), while others basically never surpassed the breaking threshold (P1, P4 and P6). This could have been caused by the different way the one size glove was fitting on the participants' hand. We could hypothesize that a good fitting of the device would improve the sensitivity through the glove and reduce the slipperiness. Instead when the glove was too large for the subject hand size, it could be possible that there was less friction with the object and therefore a higher grip force was needed to lift it.

7.2.2. Coordination plots

The coordination plots represented in Fig. 7.3 for every subject did not show a specific trend from condition A (baseline) to condition B (intervention). A flattened behavior in the intervention condition (blue line) was present in P4, P6, P7 and P10 subplots. The flatness in the first part of the load phase, therefore the area around the origin in the coordination plots, is a indication of an improvement in the feedback motor control. When the $\frac{GF}{LF}$ rate is lower, it indicates a lower safety margin while grasping an object and therefore a higher efficiency in the movement. In ideal grasping, load force and grip force have the same value at every point of the task, leading to a performance with maximum efficiency and no waste of energy. In this case the safety margin would be null, a grip force equal to the load force would correspond in fact to the minimum necessary force to lift the object perpendicularly to the ground. The safety margin is necessarily introduced in order to compensate for the processing delays represented by the grip force latency. An increase in safety margin may be related to the reduced tactile sensitivity at the fingertips used to encode friction information at the skin-object surface [54].

Unfortunately, from these results we were unable to relate a decrease in the safety margin with the application of DESC-type vibrotactile feedback. There were several biasing factors throughout the experiments, thoroughly described in section 8.2.

7.2.3. Grip force to load force delay

The grip response latency, defined as the time delay in the activation of the grip force following the activation of the load force at a specific level, represents a processing delay in the central nervous system and may lead to object slip if too large [41]. Notably, a shorter latency implies a better control performance. When looking at the GF-LF delays at several points of the load phase (Fig. 7.4) we can see by delivering tactile feedback, the delay was evidently reduced in all subjects besides for P9. The time delays in P2 had a high variability and therefore were not be taken into consideration. The blue lines in the plots were notably lower than the green lines indicating the baseline condition.

This decreasing trend was also evident from the bar plot in Fig. 7.5 where the delay at the 50% of the load force was reported. The statistically significant decrease in the grip response latency in 6/10 subjects led to the hypothesis that by delivering vibrotactile feedback, the information on the contact events throughout a lift task were provided successfully and helped during the definition of the action phases related to task subgoals. We hypothesise that the augmented feedback delivered through the DESC glove could compensate the decrease in sensitivity generated by the worn glove on healthy subjects who usually have complete sensitivity at the fingertips.

A decrease GF-LF delay can be interpreted as a factor indicating a higher level of confidence and improved motor control, following the enhancements in the feedback processing mechanisms.

7.2.4. Duration of the task

In this study, we could observe that the time necessary to perform a manipulation task decreased following the application of a DESC-type vibrotactile feedback at the forearm for 8/10 subjects. As we can see from the boxplot reported in Fig. 7.6, out of these 8 participants who performed the task faster in the intervention condition, 7 showed a statistically significant difference in the duration of the lifts in the two conditions. Since the participants were tasked to complete it as fast as possible, we could infer that the better performance induced by the feedback augmentation implied higher hand dexterity. In fact, when performing a timed motor task, a reduced duration of the trials has been attributed to a faster control and facilitated compensatory reactions [78].

Preliminary experiments demonstrated that the familiarization phase during training was sufficient for the participants to master the task. Through this knowledge and randomization of the order of condition A (baseline) and condition B (intervention), we exclude that the improvements could be the result of learning effects.

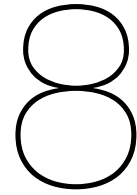
We can therefore hypothesise that the information provided through the vibrations on the arm on the contact and release events while lifting the object allowed for a higher level of confidence during grasping, ultimately reducing the time needed to efficiently lift the object.

7.2.5. Performance of the device analysis

Ideally, we would like to have a device which provides discrete event vibrotactile stimuli in concurrence with contact or release events. By looking at the results of the characterization of the device reported in Table 7.1 we can see that the device had a null percentage of false positive detection of contact. Therefore we can deduce that the DESC glove has a high specificity, being able to avoid the activation of the vibration actuators in absence of discrete contact events. This is an important characteristic of our device, as it was specifically designed to avoid the activation following closing and opening movements of the hand. It is important for future applications that stroke patients wearing the glove during their daily life activities will only receive feedback when their fingers get in contact with objects. At the contrary it would become a problem if a simple bending of the fingers activated the sensors because of the PVDF layer folding on itself.

By looking at the sensitivity, i.e. the probability of detection of contact with external object, we can see from the true positives reported in Table 7.1 that it was above 90% for all subjects besides P3, P4 and P8, ranging from 55% to 100%. The sensitivity of the DESC glove resulted to be very good during the experiments. These values indicate that the device was able for about 92.05% of the times for the thumb sensor and 86.56% of the times for the index sensor to detect the a contact event withing 200ms from the actual contact with the object, detected by the load cells on the instrumented object. The

sensitivity could be further improved in a subsequent version of the prototype. A possibility to increase the sensitivity of the glove would be to modify the acquisition board firmware to be less selective in the activation threshold necessary to send a command to the motors, as largely explained in Section 8.2. However, this could lead to an increase in the false positive rate.



Conclusions and Further Outlooks

In this chapters I will draw the conclusions of my master thesis project. Conclusions on the efficacy of the DESC glove will be deduced, taking into account the level of accuracy of our experimentation and proposing further improvements for future studies.

8.1. Conclusions

The results of this study on a novel wearable device for post stroke hand rehabilitation suggest that the DESC glove might help stroke survivors for a better manipulation of objects in their daily life activities. The prototyped glove resulted to be suitable for the intended application purposes, delivering a discrete event sensory feedback concurrently with touch events and refraining inappropriate activations of the actuators. Moreover, from the tests performed on healthy participants, it emerged that the lack of sensitivity imposed by the layer of fabric of the glove, was compensated following the application of DESC type feedback. This suggests a correct interpretation of the augmented tactile feedback by the subjects' brain, even though they were not familiar with the feedback modality. The encoding of augmented sensory information delivered through the discrete event sensory control resulted to be facilitated, as the sensory inputs from tactile events are processed in the same way in physiology. For this reason, we suggest further investigations on DESC type feedback applications and especially, the performance of clinical trials on sensory impaired subjects using a DESC type feedback augmentation in motor tasks.

8.2. Study limitations and possible improvements

Testing a sensory substitution rehabilitation device on healthy subjects imposes a great limitation on the results that can be obtained. Subjects that don't present any impairments to their upper limbs have maximum level of motor performance possible from physiology. It becomes therefore very hard to notice any significant improvement in hand dexterity following the application of augmented feedback. The fact that the glove partially removed sensitivity to the healthy participants' fingertips might have helped in the detection of some improvements when looking at the level of the maximum grip force and consequently number of breaks, grip response latency and the total duration of the lifts. By subtracting sensitivity, the ability to identify the correct motor commands was also reduced, as proper sensory inputs are not available for correction in the internal models of the cerebellum. The aforementioned limitation affecting our preliminary tests on the device can and will ultimately be overcome through the performance of clinical trials on post-stroke patients. Following the neurological impairments, as explained in the introduction, stroke survivors lack of sensitivity on their hands and show reduced performance in motor control and hand dexterity.

Other limitations to our study were given by the setup chosen to perform the testing of the device. Load cells usually show errors and delays themselves and, even though the three load cells on the instrumented object were calibrated at the beginning of the experimentation, the tests were performed during consecutive days. This might have damaged the calibration settings due to mechanical disturbances or moving of the setup in different days. A solution to this problem could be calibrating the load cells every day before starting the tests.

Another important aspect to be considered is that some subjects were covering the red led indicating breakage of the object with their hand during the performance of the task. The lack of knowledge on the level of force able to break the object might have increased the grip force these subjects applied while lifting, unaware of breaking the object and therefore failing the task. The red led could be moved to the top of the object in future experiments, in order to avoid interference with the lifting movement while remaining always visible during the task.

Moreover, a lot of noise was present in the analog sensors signal acquired from the DAQ making it difficult to analyse the correct activation of the device. As explained in section 6.4.2, the cables connecting the PVDF signal acquisition boards to the DAQ had to be very long because of the setup components position. The solution to this problem could be the direct acquisition of the digital signal sent through the serial port from the board acquiring the PVDF signal to the board controlling the actuators. In this way, we could be certain that the signal we are analysing is the one that the device is using for its activation is therefore the most accurate way to characterize its operation.

As briefly mentioned in section 7.2.5, the sensitivity of the DESC glove (55% – 100% depending on the subject) could be further improved. This value strongly depends on the threshold that we set for the activation of the motors following the detection of the contact event. In this first version of the device prototype, the firmware in the sensors signal acquisition boards was programmed in such way that a contact event was detected after the PVDF signal exceeded (for contact) or went below (for release) two fixed thresholds. A possible improvement to increase the accuracy in the detection of touch events would be to use the derivative of the signal as a regulator for the activation threshold values. In fact, as we could notice from the sensors characterization in Chapter 3, the voltage response of the PVDF sensors following a stimulus, depends on the velocity at which the stimulus is applied. Therefore a variable threshold for different velocities of stimulation could allow for a more precise discrimination of touch events.

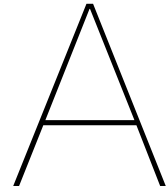
The use of a one sized glove for patients of different genders and age might have reduced the performance during the experiment due to under- or over-fitting of the device. By prototyping at least three different sizes of the glove, small medium and large, we could overcome this limitation promoting comfort and a better object manipulation while wearing the glove.

8.3. Societal and ethical impact

As mentioned in Chapter 1, stroke has a very high incidence worldwide and negatively affects the life of many elderly. Due to the lack of sensitivity on their hands they often present difficulties in manipulating objects, requiring medical assistance to conduct many activities. The aim of this project is to improve stroke patients hand dexterity allowing them to successfully manipulate objects and improving their capability to use their upper limbs in daily life activities. By reducing the sensory and motor deficits that affect these patients, they would gain a higher level of independence which could be also beneficial on a psychological point of view. The lack of independence in conducting domestic (and not) activities often leads to depression and self denigration.

Another aspect to be taken into consideration is the reduction in healthcare expenses that would follow to the higher level of independence obtained by stroke survivors. In case the final prototype of the DESC glove could promote hand dexterity and help in object manipulation as we would wish, this would reduce the patients need of technical assistance in their home setting. This would allow the government to save money and invest them in other applications beneficial for the society.

Appendices



Consent Form and Study Information Sheet



Consent Form

The volunteer must read and answer the following questions:

Have you read all the information about this experiment?	Yes / No
Could you ask questions and clear up any doubts about this study?	Yes / No
Did you receive enough information about this study?	Yes / No
Did you understand that you are free to stop the experiment and leave at any moment and without giving explanations?	Yes / No
Do you agree on taking part in this experiment?	Yes / No
Do you agree on having video/pictures recorded during the experiment? (Your face will be unidentifiable in any recordings.) <i>This is not mandatory to participate!</i>	Yes / No

Taking full responsibility, I declare that:

- According to the Italian law n. 196/03 on privacy and personal data protection, I give my approval to the use of data coming from my experimental session for scientific studies and possible academic publications (anonymously).
- I understand that Scuola Superiore Sant'Anna's public liability insurance covers its employees in the event that they cause any harm to a third party during the execution of their duties.
- I understand that I can revoke consent also at any point after the study by informing the principal investigator, after which my data will be deleted and no longer used for analysis.

Signature _____ Place, Date _____, __/__/_____

Name and Surname in capital letters _____

Investigator _____

In case you would like to ask questions about or to comment on this study in the future, please contact: Christian Cipriani – christian.cipriani@santannapisa.it - Scuola Superiore Sant'Anna – The Biorobotics Institute – Viale R. Piaggio, 34 – Pontedera - Italy

All information obtained during your participation in the experiment will only be published anonymously. All data will be analyzed in group, with no references to personal details.



Subject ID	
Fb group	

Contact Information

E-mail	
Phone	

Commonly required information

Gender	
Age	
Height	
Weight	
Hand-dominance	
Have you smoked a cigarette in the past 2h?	Yes [] How long ago? _____ No []
Have you eaten in the past 2h?	Yes [] No []
Have you taken medications today?	Yes [] Which one? _____ No []

Attention! You are NOT allowed to participate if you have any wounds/impairments on your right hand!

Study information sheet

Dear Participant,

Thank you for taking the time to do this experiment. Please read the following information carefully. You have the right to take your time and ask questions (now and at any point during or after the study).

Participation is voluntary

It is your choice to participate in this study. If you choose to do so, you may change your mind and leave the study at any time. Refusal to participate or stopping your participation will not involve any penalty. Should you stop your participation during the study, you may request that all your data be deleted.

What is the purpose of this research?

The goal of this study is to help test a novel wearable device called DESC glove. The device provides sensory feedback on the arm following the detection of touch from the sensors on the fingertips for people who have lost sensitivity on the hand (as for example stroke patients). The aim of this study is to evaluate the effectiveness of this device for improving hand motor performance.

How many people will take part in this research?

About 5-10 people will be part of this study.

How long will I take part in the study?

This study requires **one session** of up to 60 minutes.

What can I expect if I take part in this research? Please read carefully

If you agree to participate in this study, you will be asked to participate to a brief training (1) and then perform the experiment in different conditions (2).

- 1) The first part of this experiment will consist in training to acquire confidence with the instrumented object (sensorized) and the grasping task while wearing the DESC glove. You will be asked to perform some lifts with both light and heavy weight. You will have to push the blue button in front of you before and after each lift and wait for the green led to go off before starting a lift. The object should be grasped exactly where indicated from the black circles and lifted all the way up to the indicated height. You should hold the object up above the height indicator, trying to avoid breakage (indicated by the red LED). You are asked to performed task as fast as possible, focusing on lifting the object by applying the correct force with the fingertips, to avoid breakage or slippage.
- 2) Once training is complete, you will keep wearing the DESC glove and begin the experiment. You are asked to perform 100 lifts for 2 repetitions with a short break in between. While performing the

experiment you will be asked to synchronously perform a serial-3 subtraction task counting backwards outloud.

Please try to grasp as fluidly as you comfortably can, focusing on avoiding breakage of the object while performing the task as fast as possible.

Should the object slip from your grasp, please indicate this to the experimenters, wait for a sign, and then continue as before.

Photos/Videos

If you agree that photos/videos of you may be taken, the experimenters will ensure that these do not include your face or will censor/blur it. The photo and video files of you will not contain your name or any information that can identify you. The material may be published or shown during presentations. If you agree but change your mind during or after the study, please let us know, and the experimenters will delete any visual material of you.

What are the risks and possible discomforts?

It is possible that you feel an uncomfortable sensation at the hand given by the vibration, this could manifest as a sort of tingling, numbness or hypersensitivity. If this is the case, please inform the experimenters but be aware that it will disappear after a short while that the vibration is not applied anymore.

As with any electrical device, there is a very minimal risk of electrical shock. To reduce this risk all electrical components are sealed in non-conducting plastic boxes and all wires are coated.

You do not have to pay to participate in this research.

Are there any benefits from being in this research study?

There are no direct benefits to participants as a result of participating in this research. However, the results of this research may lead to devices that make grasping easier and/or more pleasant for people with upper extremity amputation or sensory impairments.

You will not be compensated for your participation in this study.

How will my privacy be protected? What happens to the information you collect?

Every effort will be made to ensure that your participation in this study and all records about it remain confidential. All data we collect about you will be labeled with a unique participant number and no other identifying information. Only the PI and study team will have access to the key linking your identity to your participant code. It is possible that we may use the de-identified data we collect (which cannot be used to identify you) with our collaborators, or in publications and presentations. De-identified data may also be made available to other researchers, and sponsors of the study. This does not include your photos/videos.

I have read and understood the information sheet: _____ Date: _____

Bibliography

- [1] Farnaz Abdollahi, Molly Corrigan, Emily D.C. Lazzaro, Robert V. Kenyon, and James L. Patton. Error-augmented bimanual therapy for stroke survivors. *NeuroRehabilitation*, 2018. ISSN 18786448. doi: 10.3233/NRE-182413.
- [2] Mohamed Aboseria, Francesco Clemente, Leonard F. Engels, and Christian Cipriani. Discrete Vibro-Tactile Feedback Prevents Object Slippage in Hand Prostheses More Intuitively Than Other Modalities. *IEEE Transactions on Neural Systems and Rehabilitation Engineering*, 2018. ISSN 15344320. doi: 10.1109/TNSRE.2018.2851617.
- [3] Christian Antfolk, Marco D'alonzo, Birgitta Rosén, Göran Lundborg, Fredrik Sebelius, and Christian Cipriani. Sensory feedback in upper limb prosthetics. *Expert Review of Medical Devices*, 2013. ISSN 17434440. doi: 10.1586/erd.12.68.
- [4] Paul Bach-Y-Rita. Theoretical basis for brain plasticity after a TBI, 2003. ISSN 02699052.
- [5] Karlin Bark, Jason W. Wheeler, Sunthar Premakumar, and Mark R. Cutkosky. Comparison of skin stretch and vibrotactile stimulation for feedback of proprioceptive information. In *Symposium on Haptics Interfaces for Virtual Environment and Teleoperator Systems 2008 - Proceedings, Haptics*, 2008. ISBN 9781424420056. doi: 10.1109/HAPTICS.2008.4479916.
- [6] Karlin Bark, Emily Hyman, Frank Tan, Elizabeth Cha, Steven A. Jax, Laurel J. Buxbaum, and Katherine J. Kuchenbecker. Effects of Vibrotactile Feedback on Human Learning of Arm Motions. *IEEE Transactions on Neural systems and rehabilitation engineering*, 23(1):51–63, 2015.
- [7] Paul M. Bays and Daniel M. Wolpert. Computational principles of sensorimotor control that minimize uncertainty and variability, 2007. ISSN 00223751.
- [8] Jannette M. Blennerhassett, Leeanne M. Carey, and Thomas A. Matyas. Grip force regulation during pinch grip lifts under somatosensory guidance: Comparison between people with stroke and healthy controls. *Archives of Physical Medicine and Rehabilitation*, 2006. ISSN 00039993. doi: 10.1016/j.apmr.2005.11.018.
- [9] Jannette M. Blennerhassett, Thomas A. Matyas, and Leeanne M. Carey. Impaired discrimination of surface friction contributes to pinch grip deficit after stroke. *Neurorehabilitation and Neural Repair*, 2007. ISSN 15459683. doi: 10.1177/1545968306295560.
- [10] Nadia Bolognini, Cristina Russo, and Dylan J. Edwards. The sensory side of post-stroke motor rehabilitation. *Restorative Neurology and Neuroscience*, 2016. ISSN 18783627. doi: 10.3233/RNN-150606.
- [11] Audrey Bowen, Peter Knapp, David Gillespie, Donald J Nicolson, and Andy Vail. Non-pharmacological interventions for perceptual disorders following stroke and other adult-acquired, non-progressive brain injury. *Cochrane Database of Systematic Reviews*, 2011. ISSN 1469493X. doi: 10.1002/14651858.cd007039.pub2.
- [12] Jurgen Broeren, Martin Rydmark, Ann Björkdahl, and Katharina Stibrant Sunnerhagen. Assessment and training in a 3-dimensional virtual environment with haptics: A report on 5 cases of motor rehabilitation in the chronic stage after stroke. *Neurorehabilitation and Neural Repair*, 2007. ISSN 15459683. doi: 10.1177/1545968306290774.
- [13] Dion C. Buhman, Jennifer A. Cherry, Lisa Bronkema-Orr, and Ram Bishu. Effects of glove, orientation, pressure, load, and handle on submaximal grasp force. *International Journal of Industrial Ergonomics*, 2000. ISSN 01698141. doi: 10.1016/S0169-8141(99)00015-3.

- [14] Jane H. Burrige, Alan Chong W. Lee, Ruth Turk, Maria Stokes, Jill Whittall, Ravi Vaidyanathan, Phil Clatworthy, Ann Marie Hughes, Claire Meagher, Enrico Franco, and Lucy Yardley. Telehealth, Wearable Sensors, and the Internet: Will They Improve Stroke Outcomes Through Increased Intensity of Therapy, Motivation, and Adherence to Rehabilitation Programs? In *Journal of Neurologic Physical Therapy*, 2017. doi: 10.1097/NPT.000000000000183.
- [15] Mónica S. Cameirão, Sergi Bermúdez I. Badia, Esther Duarte, Antonio Frisoli, and Paul F.M.J. Verschure. The combined impact of virtual reality neurorehabilitation and its interfaces on upper extremity functional recovery in patients with chronic stroke. *Stroke*, 2012. ISSN 00392499. doi: 10.1161/STROKEAHA.112.653196.
- [16] Fioravante Capone, Sandra Miccinilli, G Pellegrino, Loredana Zollo, and Davide Simonetti. Transcutaneous Vagus Nerve Stimulation Combined with Robotic Rehabilitation Improves Upper Limb Function after Stroke. *Hindawi Neural Plasticity*, 2017:1–6, 2017.
- [17] J R Carey, W K Durfee, E Bhatt, A Nagpal, S A Weinstein, K M Anderson, and S M Lewis. Comparison of finger tracking versus simple movement training via telerehabilitation to alter hand function and cortical reorganization after stroke. *Neurorehabil Neural Repair*, 21:216–232, 2007.
- [18] N. P. CHANDLER and G. P. BLOXHAM. Effect of gloves on tactile discrimination using an endodontic model. *International Endodontic Journal*, 1990. ISSN 13652591. doi: 10.1111/j.1365-2591.1990.tb00846.x.
- [19] Xiaowei Chen, Fuqian Liu, Zhaohong Yan, Shihuan Cheng, Xunchan Liu, He Li, and Zhenlan Li. Therapeutic effects of sensory input training on motor function rehabilitation after stroke. *Medicine (United States)*, 2018. ISSN 15365964. doi: 10.1097/MD.0000000000013387.
- [20] Christian Cipriani, Jacob L. Segil, Francesco Clemente, Richard F. Richard, and Benoni Edin. Humans can integrate feedback of discrete events in their sensorimotor control of a robotic hand. *Experimental Brain Research*, 2014. ISSN 14321106. doi: 10.1007/s00221-014-4024-8.
- [21] F Clemente and others. Non-Invasive, Temporally Discrete Feedback of Object Contact and Release Improves Grasp Control of Closed-Loop Myoelectric Transradial Prostheses. *IEEE Transactions on neural systems and rehabilitation engineering*, 24:12:1314–1322, 2016.
- [22] Louise A. Connell, N. B. Lincoln, and K. A. Radford. Somatosensory impairment after stroke: Frequency of different deficits and their recovery. *Clinical Rehabilitation*, 2008. ISSN 02692155. doi: 10.1177/0269215508090674.
- [23] P Cordo, H Lutsep, L Cordo, WG Wright, T Cacciatore, and R Skoss. Assisted movement with enhanced sensation (AMES): coupling motor and sensory to remediate motor deficits in chronic stroke patients. *Neurorehabil Neural Repair.*, 23(1):67–77, 2009.
- [24] Harrison Philip Crowell and Irene S. Davis. Gait retraining to reduce lower extremity loading in runners. *Clinical Biomechanics*, 2011. ISSN 02680033. doi: 10.1016/j.clinbiomech.2010.09.003.
- [25] A V Cuppone, V Squeri, M Semprini, L Masia, and J Konczak. Robot-Assisted Proprioceptive Training with Added Vibro-Tactile Feedback Enhances Somatosensory and Motor Performance. *PLoS ONE*, 11:1–18, 2016.
- [26] S Demain, C D Metcalf, G V Merrett, D Zheng, and S Cunningham. A narrative review on haptic devices: relating the physiology and psychophysical properties of the hand to devices for rehabilitation in central nervous system disorders. *Disability and Rehabilitation: Assistive Technology*, 8(3):181–189, 2012.
- [27] Bruce H. Dobkin. Neurobiology of rehabilitation. In *Annals of the New York Academy of Sciences*, 2004. doi: 10.1196/annals.1315.024.
- [28] Bruce H. Dobkin. Training and exercise to drive poststroke recovery, 2008. ISSN 1745834X.

- [29] Susan Doyle, Sally Bennett, Susan E Fasoli, and Kryss T McKenna. Interventions for sensory impairment in the upper limb after stroke. *Cochrane Database of Systematic Reviews*, 2010. ISSN 1469-493X. doi: 10.1002/14651858.cd006331.pub2.
- [30] C Duret, A Grosmaire, and H I Krebs. Robot-Assisted Therapy in Upper Extremity Hemiparesis: Overview of an Evidence-Based Approach. *Front. Neurol.*, 10:412:1–8, 2019.
- [31] Naveen Elangovan, I. Ling Yeh, Jessica Holst-Wolf, and Jurgen Konczak. A robot-assisted sensorimotor training program can improve proprioception and motor function in stroke survivors. In *IEEE International Conference on Rehabilitation Robotics*, 2019. ISBN 9781728127552. doi: 10.1109/ICORR.2019.8779409.
- [32] Jeremy L. Emken, Raul Benitez, Athanasios Sideris, James E. Bobrow, and David J. Reinkensmeyer. Motor adaptation as a greedy optimization of error and effort. *Journal of Neurophysiology*, 2007. ISSN 00223077. doi: 10.1152/jn.01095.2006.
- [33] Leah R. Enders, Pilwon Hur, Michelle J. Johnson, and Na Jin Seo. Remote vibrotactile noise improves light touch sensation in stroke survivors' fingertips via stochastic resonance. *Journal of NeuroEngineering and Rehabilitation*, 2013. ISSN 17430003. doi: 10.1186/1743-0003-10-105.
- [34] Paolo Follesa, Francesca Biggio, Giorgio Gorini, Stefania Caria, Giuseppe Talani, Laura Dazzi, Monica Puligheddu, Francesco Marrosu, and Giovanni Biggio. Vagus nerve stimulation increases norepinephrine concentration and the gene expression of BDNF and bFGF in the rat brain. *Brain Research*, 2007. ISSN 00068993. doi: 10.1016/j.brainres.2007.08.045.
- [35] David W Franklin and Daniel M Wolpert. Computational Mechanisms of Sensorimotor Control. *Neuron*, 72:425–442, 2011.
- [36] Michael J. Fu, Jayme S. Knutson, and John Chae. Stroke Rehabilitation Using Virtual Environments, 2015. ISSN 15581381.
- [37] M Gandolfi. Quantification of Upper Limb Motor Recovery and EEG Power Changes after Robot-Assisted Bilateral Arm Training in Chronic Stroke Patients: A Prospective Pilot Study. *Hindawi Neural Plasticity*, 2018:1–15, 2018.
- [38] E P Gardner and J H Martin. *Principles of Neural Science 4/e, Chapter 22: The Bodily Senses*. 2000.
- [39] Oonagh M. Giggins, Ulrik Mc Carthy Persson, and Brian Caulfield. Biofeedback in rehabilitation, 2013. ISSN 17430003.
- [40] G. M. Goodwin, D. I. McCloskey, and P. B.C. Matthews. The contribution of muscle afferents to kinesiesthesia shown by vibration induced illusions of movement and by the effects of paralysing joint afferents. *Brain*, 1972. ISSN 00068950. doi: 10.1093/brain/95.4.705.
- [41] Charlotte Häger-Ross, Kelly J. Cole, and Roland S. Johansson. Grip-force responses to unanticipated object loading: Load direction reveals body- and gravity-referenced intrinsic task variables. *Experimental Brain Research*, 1996. ISSN 00144819. doi: 10.1007/bf00241383.
- [42] Kathryn S. Hayward, Ruth N. Barker, Sandra G. Brauer, David Lloyd, Sally A. Horsley, and Richard G. Carson. SMART arm with outcome-triggered electrical stimulation: A pilot randomized clinical trial. *Topics in Stroke Rehabilitation*, 2013. ISSN 10749357. doi: 10.1310/tsr2004-289.
- [43] Peter Hänggi. Stochastic Resonance in Biology: How Noise Can Enhance Detection of Weak Signals and Help Improve Biological Information Processing. *Chemphyschem*, 3:285–290, 2002.
- [44] Ananda Hochstenbach-Waelen and Henk A.M. Seelen. Embracing change: Practical and theoretical considerations for successful implementation of technology assisting upper limb training in stroke. *Journal of NeuroEngineering and Rehabilitation*, 2012. ISSN 17430003. doi: 10.1186/1743-0003-9-52.

- [45] Susan M. Hunter, Linda Hammett, Sue Ball, Nina Smith, Cheryl Anderson, Allan Clark, Raymond Tallis, Anthony Rudd, and Valerie M. Pomeroy. Dose-response study of mobilisation and tactile stimulation therapy for the upper extremity early after stroke: A phase I trial. *Neurorehabilitation and Neural Repair*, 2011. ISSN 15459683. doi: 10.1177/1545968310390223.
- [46] Hiroshi Imamizu, Satoru Miyauchi, Tomoe Tamada, Yuka Sasaki, Ryouzuke Takino, Benno Pütz, Toshinori Yoshioka, and Mitsuo Kawato. Human cerebellar activity reflecting an acquired internal model of a new tool. *Nature*, 2000. ISSN 00280836. doi: 10.1038/35003194.
- [47] Per Jenmalm, Christina Schmitz, Hans Forssberg, and H. Henrik Ehrsson. Lighter or heavier than predicted: Neural correlates of corrective mechanisms during erroneously programmed lifts. *Journal of Neuroscience*, 2006. ISSN 02706474. doi: 10.1523/JNEUROSCI.5045-05.2006.
- [48] B. B. Johansson, E. Haker, M. Von Arbin, M. Britton, G. Långström, A. Terént, D. Ursing, K. Asplund, A. L. Berggren, E. Degerman, B. Flemström, A. Fondelius, K. Gissen, L. Lindqvist, A. C. Ljunglöf, R. Nylund, C. Sandström, M. Stålhandske, A. Ternér, S. Tuvemo-Johnson, H. Åkerlund, I. Dahlman, B. Mattsson, I. Rorsman, L. Tegård, M. Thornton, J. Bakke, M. Hammar, E. Holmström, R. Jönsson, A. Norevik, B. Tryberg, E. Wahlberg, S. Wendel-Hansen, L. Ytterberg, E. Eek, K. Ekdahl, S. Hermansson, G. Östlund, D. Sommerfeld, K. Gustavsson, A. Olofsson, A. Olofsson, B. O. Olofsson, M. Omgren, K. Westman, P. Kamme, H. Löfqvist, I. Theander, K. Ursing, R. Arespong, C. Åström, A. C. Gramner, B. Henriksson, S. Lennestål, S. Nordqvist, and L. Törne. Acupuncture and transcutaneous nerve stimulation in stroke rehabilitation: A randomized, controlled trial. *Stroke*, 2001. ISSN 00392499. doi: 10.1161/01.STR.32.3.707.
- [49] R. S. Johansson and J. R. Flanagan. Tactile Sensory Control of Object Manipulation in Humans. In *The Senses: A Comprehensive Reference*. 2007. ISBN 9780123708809. doi: 10.1016/B978-012370880-9.00346-7.
- [50] Roland S. Johansson and Ingvars Birznieks. First spikes in ensembles of human tactile afferents code complex spatial fingertip events. *Nature Neuroscience*, 2004. ISSN 10976256. doi: 10.1038/nn1177.
- [51] Roland S. Johansson and Kelly J. Cole. Sensory-motor coordination during grasping and manipulative actions. *Current Opinion in Neurobiology*, 1992. ISSN 09594388. doi: 10.1016/0959-4388(92)90139-C.
- [52] Roland S Johansson and J Randall Flanagan. Coding and use of tactile signals from the fingertips in object manipulation tasks. *Nature Reviews Neuroscience*, 10:345–359, 2009.
- [53] Scott H. Johnson, Paul M. Corballis, and Michael S. Gazzaniga. Within grasp but out of reach: Evidence for a double dissociation between imagined hand and arm movements in the left cerebral hemisphere. *Neuropsychologia*, 2001. ISSN 00283932. doi: 10.1016/S0028-3932(00)00096-8.
- [54] Lynette A. Jones and Susan J. Lederman. *Human Hand Function*. 2007. ISBN 9780199786749. doi: 10.1093/acprof:oso/9780195173154.001.0001.
- [55] Eric R. Kandel, James H. Schwartz, Thomas M. Jessell, Steven A. Siegelbaum, and A. J. Hudspeth. *Principles of Neural Science, Fifth Edition* | Neurology Collection | McGraw-Hill Medical, 2013.
- [56] M Katan and others. Global Burden of Stroke. *Seminars in Neurology*, 38:208–211, 2018.
- [57] Mitsuo Kawato. Internal models for motor control and trajectory planning, 1999. ISSN 09594388.
- [58] Mitsuo Kawato, Tomoe Kuroda, Hiroshi Imamizu, Eri Nakano, Satoru Miyauchi, and Toshinori Yoshioka. Internal forward models in the cerebellum: fMRI study on grip force and load force coupling. In *Progress in Brain Research*, 2003. doi: 10.1016/S0079-6123(03)42013-X.

- [59] Pawel Kiper, Andrzej Szczudlik, Michela Agostini, Jozef Opara, Roman Nowobilski, Laura Ventura, Paolo Tonin, and Andrea Turolla. Virtual Reality for Upper Limb Rehabilitation in Subacute and Chronic Stroke: A Randomized Controlled Trial. *Archives of Physical Medicine and Rehabilitation*, 2018. ISSN 1532821X. doi: 10.1016/j.apmr.2018.01.023.
- [60] Pawel Kiper, Michela Agostini, Carlos Luque-Moreno, Paolo Tonin, and Andrea Turolla. Reinforced feedback in virtual environment for rehabilitation of upper extremity dysfunction after stroke: Preliminary data from a randomized controlled trial. *BioMed Research International*, 2014. ISSN 23146141. doi: 10.1155/2014/752128.
- [61] John W. Krakauer. Motor learning: Its relevance to stroke recovery and neurorehabilitation, 2006. ISSN 13507540.
- [62] I. Laffont, K. Bakhti, F. Coroian, L. van Dokkum, D. Mottet, N. Schweighofer, and J. Froger. Innovative technologies applied to sensorimotor rehabilitation after stroke. *Annals of Physical and Rehabilitation Medicine*, 2014. ISSN 18770657. doi: 10.1016/j.rehab.2014.08.007.
- [63] Kishor Lakshminarayanan, Abigail W. Lauer, Viswanathan Ramakrishnan, John G. Webster, and Na Jin Seo. Application of vibration to wrist and hand skin affects fingertip tactile sensation. *Physiological Reports*, 2015. ISSN 2051817X. doi: 10.14814/phy2.12465.
- [64] Kishor Lakshminarayanan, Fa Wang, John G. Webster, and Na Jin Seo. Feasibility and usability of a wearable orthotic for stroke survivors with hand impairment. *Disability and Rehabilitation: Assistive Technology*, 2017. ISSN 17483115. doi: 10.3109/17483107.2015.1111945.
- [65] Peter Langhorne, Julie Bernhardt, and Gert Kwakkel. Stroke rehabilitation, 2011. ISSN 01406736.
- [66] Kate E. Laver, Belinda Lange, Stacey George, Judith E. Deutsch, Gustavo Saposnik, and Maria Crotty. Virtual reality for stroke rehabilitation, 2017. ISSN 1469493X.
- [67] Nicole Lehrer, Yinpeng Chen, Margaret Duff, Steven L Wolf, and Thanassis Rikakis. Exploring the bases for a mixed reality stroke rehabilitation system, Part II: Design of Interactive Feedback for upper limb rehabilitation. *Journal of NeuroEngineering and Rehabilitation*, 2011. ISSN 17430003. doi: 10.1186/1743-0003-8-54.
- [68] M. Patrice Lindsay, Bo Norrving, Ralph L. Sacco, Michael Brainin, Werner Hacke, Sheila Martins, Jeyaraj Pandian, and Valery Feigin. World Stroke Organization (WSO): Global Stroke Fact Sheet 2019. *International Journal of Stroke*, 2019. ISSN 17474949. doi: 10.1177/1747493019881353.
- [69] Le Yu Liu, Youlin Li, and Anouk Lamontagne. The effects of error-augmentation versus error-reduction paradigms in robotic therapy to enhance upper extremity performance and recovery post-stroke: A systematic review, 2018. ISSN 17430003.
- [70] W. Liu, M. Mukherjee, Y. Tsaur, S. H. Kim, H. Liu, P. Natarajan, and A. Agah. Development and feasibility study of a sensory-enhanced robot-aided motor training in stroke rehabilitation. In *Proceedings of the 31st Annual International Conference of the IEEE Engineering in Medicine and Biology Society: Engineering the Future of Biomedicine, EMBC 2009*, 2009. ISBN 9781424432967. doi: 10.1109/IEMBS.2009.5334526.
- [71] Wen Liu, LA Lipsitz, M Montero-Odasso, J Bean, DC Kerrigan, and JJ. Collins. Noise-enhanced vibrotactile sensitivity in older adults, patients with stroke, and patients with diabetic neuropathy. *Arch Phys Med Rehabil*, 83:171–176, 2002.
- [72] Morrison N. Loh, Louise Kirsch, John C. Rothwell, Roger N. Lemon, and Marco Davare. Information about the weight of grasped objects from vision and internal models interacts within the primary motor cortex. *Journal of Neuroscience*, 2010. ISSN 02706474. doi: 10.1523/JNEUROSCI.6207-09.2010.

- [73] P S Lum, C G Burgar, M der Loos, P C Shor, M Majmundar, and R Yap. MIME robotic device for upper-limb neurorehabilitation in subacute stroke subjects: a follow-up study. *J Rehabil Res Dev.*, 43:631–42, 2006.
- [74] Paul D. Marasco, Dennis J. Bourbeau, Courtney E. Shell, Rafael Granja-Vazquez, and Jason G. Ina. The neural response properties and cortical organization of a rapidly adapting muscle sensory group response that overlaps with the frequencies that elicit the kinesthetic illusion. *PLoS ONE*, 2017. ISSN 19326203. doi: 10.1371/journal.pone.0188559.
- [75] Laura Marchal-Crespo and David J. Reinkensmeyer. Review of control strategies for robotic movement training after neurologic injury, 2009. ISSN 17430003.
- [76] Marko Markovic, Meike A. Schweisfurth, Leonard F. Engels, Tashina Bentz, Daniela Wüstefeld, Dario Farina, and Strahinja Dosen. The clinical relevance of advanced artificial feedback in the control of a multi-functional myoelectric prosthesis. *Journal of NeuroEngineering and Rehabilitation*, 2018. ISSN 17430003. doi: 10.1186/s12984-018-0371-1.
- [77] Stefano Masiero, Andrea Celia, Mario Armani, and Giulio Rosati. A novel robot device in rehabilitation of post-stroke hemiplegic upper limbs. *Aging Clinical and Experimental Research*, 2006. ISSN 15940667. doi: 10.1007/BF03324854.
- [78] Enzo Mastinu, Leonard F. Engels, Francesco Clemente, Mariama Dione, Paolo Sassu, Oscar Aszmann, Rickard Branemark, Bo Hakansson, Marco Controzzi, Johan Wesseberg, Christian Cipriani, and Max Ortiz-Catalan. Neural feedback strategies to improve grasping coordination in neuromusculoskeletal prostheses. *Scientific Reports*, 10(11793), 2020.
- [79] Ruth A. Maulucci and Richard H. Eckhouse. Retraining reaching in chronic stroke with real-time auditory feedback. *NeuroRehabilitation*, 2001. ISSN 10538135. doi: 10.3233/nre-2001-16306.
- [80] Mark D McDonnell and Derek Abbott. What Is Stochastic Resonance? Definitions, Misconceptions, Debates, and Its Relevance to Biology. *PLOS computational biology*, 5:5:1–9, 2009.
- [81] Jan Mehrholz, Simone Thomas, Cordula Werner, Joachim Kugler, Marcus Pohl, and Bernhard Elsner. Electromechanical-assisted training for walking after stroke, 2017. ISSN 1469493X.
- [82] G V Merrett, C. D. Metcalf, D. Zheng, S. Cunningham, S. Barrow, and S. H. Demain. Design and qualitative evaluation of tactile devices for stroke rehabilitation. *IET Seminar on Assisted Living*, -:1–6, 2011.
- [83] Marie H el ene Milot, Laura Marchal-Crespo, Christopher S. Green, Steven C. Cramer, and David J. Reinkensmeyer. Comparison of error-amplification and haptic-guidance training techniques for learning of a timing-based motor task by healthy individuals. *Experimental Brain Research*, 2010. ISSN 00144819. doi: 10.1007/s00221-009-2014-z.
- [84] Birgit I. Molier, Edwin H.F. Van Asseldonk, Hermie J. Hermens, and Michiel J.A. Jannink. Nature, timing, frequency and type of augmented feedback; Does it influence motor relearning of the hemiparetic arm after stroke? A systematic review, 2010. ISSN 09638288.
- [85] Sumner L. Norman, Andrew J. Doxon, Brian T. Gleeson, and William R. Provancher. Planar hand motion guidance using fingertip skin-stretch feedback. *IEEE Transactions on Haptics*, 2014. ISSN 19391412. doi: 10.1109/TOH.2013.2296306.
- [86] L Oujamaaa, I Relavea, J Frogera, D Mottetb, and J Y Pelissiera. Rehabilitation of arm function after stroke. Literature review. *Journal Neurosci Nurs*, 29:179–186, 1997.
- [87] Jack Parker, Gail Mountain, and Jackie Hammerton. A review of the evidence underpinning the use of visual and auditory feedback for computer technology in post-stroke upper-limb rehabilitation. *Disability and Rehabilitation: Assistive Technology*, 2011. ISSN 17483107. doi: 10.3109/17483107.2011.556209.
- [88] Abigail L. Person. Corollary Discharge Signals in the Cerebellum, 2019. ISSN 24519030.

- [89] S. H. Peurala, K. Pitkänen, J. Sivenius, and I. M. Tarkka. Cutaneous electrical stimulation may enhance sensorimotor recovery in chronic stroke. *Clinical Rehabilitation*, 2002. ISSN 02692155. doi: 10.1191/0269215502cr543oa.
- [90] Lamberto Piron, Andrea Turolla, Michela Agostini, Carla Silvana Zucconi, Laura Ventura, Paolo Tonin, and Mauro Dam. Motor learning principles for rehabilitation: A pilot randomized controlled study in poststroke patients. *Neurorehabilitation and Neural Repair*, 2010. ISSN 15459683. doi: 10.1177/1545968310362672.
- [91] Laurentiu S. Popa and Timothy J. Ebner. Cerebellum, predictions and errors, 2019. ISSN 16625102.
- [92] Michael J. Proulx, David J. Brown, Achille Pasqualotto, and Peter Meijer. Multisensory perceptual learning and sensory substitution, 2014. ISSN 18737528.
- [93] Barbara M. Quaney, Subashan Perera, Rebecca Maletsky, Carl W. Luchies, and Randolph J. Nudo. Impaired grip force modulation in the ipsilesional hand after unilateral middle cerebral artery stroke. *Neurorehabilitation and Neural Repair*, 2005. ISSN 15459683. doi: 10.1177/1545968305282269.
- [94] Barbara M. Quaney, He Jianghua, George Timberlake, Kevin Dodd, and Caitlin Carr. Visuomotor Training Improves Stroke-Related Ipsilesional Upper Extremity Impairments. *Neurorehabilitation and Neural Repair*, 2010. ISSN 15459683. doi: 10.1177/1545968309341646.
- [95] Aparna Raghavan and Zahoor A. Shah. Withania somnifera: A pre-clinical study on neuroregenerative therapy for stroke. *Neural Regeneration Research*, 2015. ISSN 18767958. doi: 10.4103/1673-5374.152362.
- [96] P. Ripollés, N. Rojo, J. Grau-Sánchez, J. L. Amengual, E. Càmarà, J. Marco-Pallarés, M. Juncadella, L. Vaquero, F. Rubio, E. Duarte, C. Garrido, E. Altenmüller, T. F. Münte, and A. Rodríguez-Fornells. Music supported therapy promotes motor plasticity in individuals with chronic stroke. *Brain Imaging and Behavior*, 2016. ISSN 19317565. doi: 10.1007/s11682-015-9498-x.
- [97] Vittorio Sanguineti, Maura Casadio, Lorenzo Masia, Valentina Squeri, and Pietro G. Morasso. Robot-Assisted Neurorehabilitation. In *Introduction to Neural Engineering for Motor Rehabilitation*. 2013. ISBN 9781118628522. doi: 10.1002/9781118628522.ch26.
- [98] Siobhan M. Schabrun and S. Hillier. Evidence for the retraining of sensation after stroke: A systematic review, 2009. ISSN 02692155.
- [99] Jonathon S. Schofield, Michael R. Dawson, Jason P. Carey, and Jacqueline S. Hebert. Characterizing the effects of amplitude, frequency and limb position on vibration induced movement illusions: Implications in sensory-motor rehabilitation. *Technology and Health Care*, 2015. ISSN 09287329. doi: 10.3233/THC-140879.
- [100] Nadja Schott and Thomas J. Klotzbier. Profiles of cognitive-motor interference during walking in children: Does the motor or the cognitive task matter? *Frontiers in Psychology*, 2018. ISSN 16641078. doi: 10.3389/fpsyg.2018.00947.
- [101] Na Jin Seo, Heidi W. Fischer, Ross A. Bogey, William Z. Rymer, and Derek G. Kamper. Use of visual force feedback to improve digit force direction during pinch grip in persons with stroke: A pilot study. *Archives of Physical Medicine and Rehabilitation*, 2011. ISSN 00039993. doi: 10.1016/j.apmr.2010.08.016.
- [102] Na Jin Seo, Marcella Lyn Kosmopoulos, Leah R. Enders, and Pilwon Hur. Effect of Remote Sensory Noise on Hand Function Post Stroke. *Frontiers in Human Neuroscience*, 2014. ISSN 1662-5161. doi: 10.3389/fnhum.2014.00934.

- [103] Na Jin Seo, Kishor Lakshminarayanan, Abigail W. Lauer, Viswanathan Ramakrishnan, Brian D. Schmit, Colleen A. Hanlon, Mark S. George, Leonardo Bonilha, Ryan J. Downey, Will DeVries, and Tibor Nagy. Use of imperceptible wrist vibration to modulate sensorimotor cortical activity. *Experimental Brain Research*, 2019. ISSN 14321106. doi: 10.1007/s00221-018-05465-z.
- [104] Reza Shadmehr and Ferdinando A. Mussa-Ivaldi. Adaptive representation of dynamics during learning of a motor task. *Journal of Neuroscience*, 1994. ISSN 02706474. doi: 10.1523/jneurosci.14-05-03208.1994.
- [105] G. F. Shannon. A comparison of alternative means of providing sensory feedback on upper limb prostheses. *Medical & Biological Engineering*, 1976. ISSN 17410444. doi: 10.1007/BF02478123.
- [106] Charles H. Shea, Attila J. Kovacs, and Stefan Panzer. The coding and inter-manual transfer of movement sequences. *Frontiers in Psychology*, 2011. ISSN 16641078. doi: 10.3389/fpsyg.2011.00052.
- [107] Sir Charles Sherrington. The Integrative Action of the Nervous System. Classics in psychology. *The Yale Journal of Biology and Medicine*, 1906. ISSN 0022-3751. doi: 10.1037/13798-001.
- [108] S. Shimojo and L. Shams. Sensory modalities are not separate modalities: Plasticity and interactions, 2001. ISSN 09594388.
- [109] Roland Sigrist, Georg Rauter, Robert Riener, and Peter Wolf. Augmented visual, auditory, haptic, and multimodal feedback in motor learning: A review, 2013. ISSN 10699384.
- [110] Cara E. Stepp, Qi An, and Yoky Matsuoka. Repeated training with augmentative vibrotactile feedback increases object manipulation performance. *PLoS ONE*, 2012. ISSN 19326203. doi: 10.1371/journal.pone.0032743.
- [111] Ho Jang Sung, Sung H. You, Mark Hallett, Woo Cho Yun, Chong Mi Park, Sang Hyun Cho, Hyun Young Lee, and Tae Hoon Kim. Cortical reorganization and associated functional motor recovery after virtual reality in patients with chronic stroke: An experimenter-blind preliminary study. *Archives of Physical Medicine and Rehabilitation*, 2005. ISSN 00039993. doi: 10.1016/j.apmr.2005.04.015.
- [112] Craig D Takahashi and others. Robot-based hand motor therapy after stroke. *Brain*, 131:425–437, 2008.
- [113] Gregory Thielman. Rehabilitation of reaching poststroke: A randomized pilot investigation of tactile versus auditory feedback for trunk control. *Journal of Neurologic Physical Therapy*, 2010. ISSN 15570576. doi: 10.1097/NPT.0b013e3181efa1e8.
- [114] Angelica Maria Tinga, Johanna Maria Augusta Visser-Meily, Maarten Jeroen van der Smagt, Stefan Van der Stigchel, Raymond van Ee, and Tanja Cornelia Wilhelmina Nijboer. Multisensory Stimulation to Improve Low- and Higher-Level Sensory Deficits after Stroke: A Systematic Review, 2016. ISSN 15736660.
- [115] Henk van Dijk, Michiel J.A. Jannink, and Hermie J. Hermens. Effect of augmented feedback on motor function of the affected upper extremity in rehabilitation patients: A systematic review of randomized controlled trials, 2005. ISSN 16501977.
- [116] F. T. Van Vugt, T. Kafczyk, W. Kuhn, J. D. Rollnik, B. Tillmann, and E. Altenmüller. The role of auditory feedback in music-supported stroke rehabilitation: A single-blinded randomised controlled intervention. *Restorative Neurology and Neuroscience*, 2016. ISSN 18783627. doi: 10.3233/RNN-150588.
- [117] Qi Wang, Panos Markopoulos, Bin Yu, Wei Chen, and Annick Timmermans. Interactive wearable systems for upper body rehabilitation: A systematic review, 2017. ISSN 17430003.
- [118] C. J. Winstein. Knowledge of results and motor learning - Implications for physical therapy, 1991. ISSN 00319023.

-
- [119] Daniel M. Wolpert, Jörn Diedrichsen, and J. Randall Flanagan. Principles of sensorimotor learning, 2011. ISSN 1471003X.
- [120] Yingshi Zhang, Jiayi Cai, Yaqiong Zhang, Tianshu Ren, Mingyi Zhao, and Qingchun Zhao. Improvement in Stroke-induced Motor Dysfunction by Music-supported Therapy: A Systematic Review and Meta-Analysis. *Scientific Reports*, 2016. ISSN 20452322. doi: 10.1038/srep38521.